INFORMATION TO USERS

This manuscript has been reproduced from the microfilm master. UMI films the text directly from the original or copy submitted. Thus, some thesis and dissertation copies are in typewriter face, while others may be from any type of computer printer.

The quality of this reproduction is dependent upon the quality of the copy submitted. Broken or indistinct print, colored or poor quality illustrations and photographs, print bleedthrough, substandard margins, and improper alignment can adversely affect reproduction.

In the unlikely event that the author did not send UMI a complete manuscript and there are missing pages, these will be noted. Also, if unauthorized copyright material had to be removed, a note will indicate the deletion.

Oversize materials (e.g., maps, drawings, charts) are reproduced by sectioning the original, beginning at the upper left-hand corner and continuing from left to right in equal sections with small overlaps.

Photographs included in the original manuscript have been reproduced xerographically in this copy. Higher quality 6" x 9" black and white photographic prints are available for any photographs or illustrations appearing in this copy for an additional charge. Contact UMI directly to order.

ProQuest Information and Learning
300 North Zeeb Road, Ann Arbor, MI 48106-1346 USA
800-521-0600

Université d'Ottawa · University of Ottawa

OPTION PRICING FROM A BAYESIAN PERSPECTIVE USING THE DIRICHLET PROCESS

By
Thierry Bédard, B.Sc.
August 2001

A M.Sc. Thesis
submitted to the School of Graduate Studies and Research
in partial fulfillment of the requirements
for the degree of
Master of Science in Mathematics[1]

University of Ottawa
Ottawa, Ontario
Canada

[1]The M.Sc. Program is a joint program with Carleton University, administered by the Ottawa-Carleton Institute of Mathematics and Statistics

Abstract

There exist a wide variety of models for the pricing of derivative securities such as call and put options. This thesis introduces an alternative option pricing methodology based on a Monte Carlo simulation of the Dirichlet process. The model is constructed in a Bayesian framework, using the properties initially described by Ferguson [10, 11].

Given historical stock prices up to the present, we simulate various sample paths for future stock prices. This procedure is conducted under the hypothesis that the prior distribution of the stock returns has a Dirichlet process structure. The predicted option prices are then computed by averaging the option prices obtained for each simulated sample path.

A considerable advantage of this model is that random draws are sampled from a mixed distribution which consists of a prior guess and the empirical process based on the initial random sample of stock returns.

The methodology is applied to various examples throughout this thesis. The results are compared with some existing models, including exponential Brownian motion and the Black-Scholes option pricing formula.

Acknowledgements

I would like to thank my supervisors, Prof. André Dabrowski and Prof. Mahmoud Zarepour, for their useful advice throughout my research. The financial contributions provided by the University of Ottawa, the Natural Science and Engineering Research Council of Canada, and the Gordon E. Swartzen Memorial Fund were also greatly appreciated. Special thanks to my colleagues Gilles Lamothe and Sarah Sumner for their technical support, and to Cynthia Martel for the proof-reading and the moral support.

Dedication

Je dédie cet ouvrage à mes parents qui m'ont toujours encouragé malgré tout.

Contents

List of Tables

List of Figures

Chapter 1

Introduction to Options

Modern capital markets offer investors a wide array of financial instruments that can be classified into two major categories. On one hand, *fundamental securities* include *stocks*, *bonds*, *Treasury bills*, and any other security issued directly by a corporation or a government. On the other hand, *derivative securities* or *derivative products* are financial instruments whose value is determined upon the value of another security, called the underlying security.

An example of derivative security is the *option contract* which gives its holder the right (but not the obligation) to buy or sell the underlying security at a certain price by a certain date. The option to buy is referred to as a *call*, while the option to sell is referred to as a *put*. If the holder of an option contract decides to exercise his right, then the seller of the option contract has the obligation to either sell the underlying security to the holder in the case of a call, or buy the underlying security from the holder in the case of a put. Of course, the holder's privileges are acquired in return for a compensation, called *option premium* or *option price*. This premium is paid by the buyer when the option is traded and is kept by the seller whether the option is exercised or not.

Options are traded on various assets, but most frequently on stocks, *stock indices*, *futures contracts*, and foreign currencies. In this paper, we will focus our discussion on options where the underlying asset is a stock, commonly referred to as equity options or options on stock.

Equity options are exchange-traded since 1973. Among the exchanges that offer equity options trading, the oldest and most important is the Chicago Board Options Exchange. Other markets in United States are the American Stock Exchange, the Philadelphia Stock Exchange, the Pacific Stock Exchange, and the New York Stock Exchange. In Canada, options are exclusively traded on the Montreal Exchange. In each of these exchanges, option contracts are standardized in terms of the underlying stock, the *exercise prices*, the number of shares, and the *expiration dates* available. By convention, options always expire on the Saturday following the third Friday of the month of expiration. The underlying asset of a typical equity option contract is 100 shares of stock.

1.1 Example

We illustrate the mechanics of the options market with an example. Consider a call option on one share of TBX Inc. stock. Suppose that this option has the following characteristics: the exercise price (or strike price) is \$125, the option premium is \$15, and the expiration date (or maturity) is September 22. In other words, this call option allows its holder to buy one share of TBX stock at \$125 on September 22, and the holder must pay \$15 to acquire this right.

If the holder of the call decides to exercise his option, the seller has the obligation to sell him one share of TBX at \$125, no matter what the current price of TBX may be. Obviously, if TBX trades above the exercise price of \$125 at expiration date, the holder will exercise his call option and buy an asset for less than its market value. However, for the whole operation to be worthwhile, the profit generated by the exercise must be greater than the option premium of \$15. If TBX's price is \$137, the holder will exercise the option, but still make a negative profit equal to $\$137 - \$125 - \$15 = -\$3$. Conversely, if TBX trades at \$144, his profit will be positive: $\$144 - \$125 - \$15 = \$4$. Note that in the event of TBX trading below \$125, the holder will let his call option expire since an exercise of his right would not be profitable. In this case, the only loss incurred by the holder is the option premium of \$15.

Put options work in a similar way. Consider a put option on one share of TBX stock with the following characteristics: the option premium is \$5, the exercise price is \$125, and the expiration date is September 22. Thus, to receive the right to sell one share of TBX stock at \$125 on September 22, an investor must pay a \$5 premium. The seller of the option receives \$5 and promises to buy one share for \$125 if the holder decides to exercise his put option. If TBX trades above \$125, the holder will not exercise his put option since he would be selling an asset for less than its market value. If TBX trades below \$125, the holder will exercise his put option and sell one share to the option seller for \$125.

Note that in any option contract, the holder's gains (losses) are exactly equal to the seller's losses (gains). In a competitive market, investors must rely on the misjudgement of less fortunate investors in order to generate profits. In this regard, an option contract is considered a zero-sum game since the combined profits of the holder and the seller are always zero.

Options trading can be highly speculative. As in the previous example, the buyer of an option contract pays a predetermined small amount of money (option premium) in exchange for an uncertain profit, while the seller receives a small fixed amount but has unlimited loss potential. Nevertheless, investors generally trade options to protect their portfolio from market fluctuations.

1.2 American, European, and Exotic Options

The two basic types of options traded on the exchanges are the *European option* and the *American option*. The fundamental difference between these two kinds of options lies in the time allowed to exercise them. While European options can only be exercised at the expiration date, American options can be exercised at any time during the life of the option.

Other types of options with non-standard contingencies are referred to as *exotic options*. For example, an *Asian option* has a payoff structure based on the average price of the underlying stock over the life of the option; a chooser option allows its holder to decide whether the option is a put or a call after the contract is purchased,

etc. There exist a great variety of exotic options, but we will not discuss them further. Unless otherwise specified, this thesis will only be concerned with European options.

For more on options and derivative securities in general, we refer the reader to Cox and Rubinstein [7], Hull [16], Kolb [22], or Reilly and Brown [31].

1.3 The Fundamental Problem

The obvious question arising when trading options is: how do we determine the premium? The financial literature includes an impressive number of articles presenting various solutions to the problem of option pricing. The best-known works are perhaps those of Black and Scholes [3] and Merton [27] which rely on the lognormality assumption for stock prices. The validity of this assumption, however, has been widely questioned by various experts who believe that stock markets have heavier tails.

The objective of this thesis is to introduce an alternative option pricing methodology based on Monte Carlo simulation and the Dirichlet process. The model is constructed in a Bayesian context using the properties initially described by Ferguson [10, 11].

1.3.1 Organization of the Thesis

Before we develop our model, we present some background theory about the Dirichlet process and option pricing in general. In Chapter 2, we describe some general conditions relative to European option pricing and capital markets modelling. In particular, we discuss the properties of the Brownian motion process and describe three existing option pricing models: the binomial model, the Black-Scholes option pricing formula, and Monte Carlo simulation.

Chapter 3 is divided into five major sections. The first four consist of a mathematical review of the Dirichlet process and its properties. We describe the Dirichlet distribution and present the formal definition of the Dirichlet process in the context defined by Ferguson [10, 11]. Alternative representations of the process are also discussed, including the Dirichlet process sum-construction by Ferguson [10, 11], the

Pólya urn representation by Blackwell and MacQueen [4], the stick-breaking approach by Sethuraman [35], and the truncated Dirichlet process by Ishwaran and Zarepour [17].

In the last section of Chapter 3, we present an original application of the Dirichlet process to the pricing of European options. Assuming that the stock returns have a Dirichlet process structure, we derive a pricing formula for European options that can be viewed as an alternative model to those described in Chapter 2.

Chapter 4 describes a numerical procedure of the model introduced in the latter part of Chapter 3. We begin by developing an algorithm to compute the price of European options whose stock returns have a Dirichlet process prior distribution. This is achieved by performing a Monte Carlo simulation where the underlying stochastic process is the Dirichlet process. Predicted stock prices and corresponding option prices are then computed for fictive random samples that were constructed using an exponential random walk model with either normal, heavy-tailed, or skewed residuals. The results obtained using the Dirichlet process approach are compared with some of the existing pricing techniques described in Chapter 2.

The same analysis is performed in Chapter 5, with the exception that the underlying random sample is a series of monthly closing prices from the Standard & Poor's 500 Total Return Index.

Readers with limited knowledge in modern finance are encouraged to consult the glossary of financial terminology provided in Appendix A. Appendix B presents a review of some useful notions in probability, including a brief summary of the principal probability distributions. The S-PLUS simulation programs used in this work are provided in Appendix C, while the data sets can be found in Appendix D.

1.3.2 Notation

Throughout the remainder of this thesis, the *rate of return* of a security will be defined as the logarithmic increase of its price S_t over the time interval $(t-1, t]$, that is

$$Y_t = \log S_t - \log S_{t-1},$$

which implies

$$\begin{aligned} S_t &= S_{t-1}e^{Y_t} \\ &= \dots \\ &= S_0 e^{Y_1+\cdots+Y_t}. \end{aligned}$$

The following notation will also be used to denote the various variables included in our analyses:

- c_t is the price of a European call at time t,
- p_t is the price of a European put at time t,
- C_t is the random variable of the payoff of a European call at time t,
- P_t is the random variable of the payoff of a European put at time t,
- S_t is the price of the underlying stock at time t,
- T is the expiration date of the option,
- K is the exercise price of an option,
- r is the *risk-free interest rate*, defined as the rate of return that can be earned without assuming any risks.

Moreover, the estimates of c_t, p_t, S_t, and Y_t that are obtained via simulation will be denoted by $\hat{c}_t$, $\hat{p}_t$, $\hat{S}_t$, and $\hat{Y}_t$. Note also that investors are assumed to be rational and as a result, options are only exercised when they can provide positive payoffs. *Dividends* and *transactions costs* are assumed to be nil.

Chapter 2

European Option Pricing

The literature on option pricing includes a wide variety of models, each based on different sets of hypotheses. A few of these models are described in this chapter, along with some general considerations relative to capital markets modelling. We begin by discussing the concepts of arbitrage and risk-neutral valuation, which then lead to the development of a general pricing formula for European options. We then present the Brownian motion process and conclude this chapter with a description of three option pricing approaches: the binomial model, the Black-Scholes option pricing formula, and Monte Carlo simulation. The concepts covered in this chapter are based on Hull [16], with some material taken from Karlin and Taylor [21] and Kolb [22].

2.1 Risk-Neutral Valuation and the No-Arbitrage Pricing Principle

As mentioned in Chapter 1, options are exchange-traded, which means that their prices are determined by the interaction between supply and demand forces. Nevertheless, these forces do not behave randomly. If an option was to be wrongly priced, this would result in an *arbitrage* opportunity and investors could be guaranteed a risk-free profit without making any investment. Every financial instrument is priced under the assumption that arbitrage situations do not occur. This is known as the

no-arbitrage pricing principle.

We demonstrate the no-arbitrage pricing principle with the following example. Consider a call option on TBX stock with exercise price of \$125, and suppose that this stock trades at \$130 at expiration date. According to the no-arbitrage pricing principle, the price of this call at expiration date must be \$5 because any other price would create an arbitrage opportunity. If the call is priced at \$4, an investor could realize a \$1 risk-free profit using the following strategy: buy a call for \$4, exercise this call for \$125, and then sell TBX stock for \$130. Of course, as many investors would follow this strategy, the increased demand for the call would create upward pressure on the option price. Conversely, if the call was priced at \$6, increased supply would put downward pressure on the option price. The interaction between these supply and demand forces would quickly eliminate the arbitrage opportunity and stabilize the call at its equilibrium price of \$5.

From these considerations, it is clear that the price of a call option at expiration date is the value of its payoff, or simply

$$\max(S_T - K, 0).$$

Prior to the expiration date, the price at time $t < T$ is determined by discounting the expected value of this payoff using the expected rate of return.[1]

To simplify the analysis, options are always priced under the assumption that investors are neutral to risk. In a risk-neutral world, investors do not require a premium to take more risks and the expected return for every security is the risk-free interest rate r. The price of a European call can then be written as

$$c_t = e^{-r(T-t)} E\left[\max(S_T - K, 0) \mid S_0, \ldots, S_t\right], \tag{2.1}$$

while that of a European put is

$$p_t = e^{-r(T-t)} E\left[\max(K - S_T, 0) \mid S_0, \ldots, S_t\right]. \tag{2.2}$$

Note that these equations are still valid if we remove the risk-neutral assumption and move to a risk-averse world. Because risk-averse investors require a premium μ for

[1] Readers who are not familiar with the concept of time value of money should consult Appendix A for more details.

taking risks, the expected payoff of a call becomes

$$e^{\mu(T-t)}E\left[\max\left(S_T-K,0\right)\mid S_0,\ldots,S_t\right].$$

However, since the expected rate of return of a risk-averse investor is $r+\mu$, the payoff must be discounted by a factor of $e^{-(r+\mu)(T-t)}$ instead of $e^{-r(T-t)}$, yielding

$$c_t = e^{-(r+\mu)(T-t)}e^{\mu(T-t)}E\left[\max\left(S_T-K,0\right)\mid S_0,\ldots,S_t\right].$$

After simplification, this expression becomes

$$c_t = e^{-r(T-t)}E\left[\max\left(S_T-K,0\right)\mid S_0,\ldots,S_t\right],$$

which is obviously equation (2.1) in the risk-neutral case.

An important step in the computation of an option price is the characterization of an appropriate distribution for the underlying stock S_t. Of course, the distribution selected must be as representative as possible of financial markets, since the option price calculated using an inappropriate distribution is most likely to be unrealistic. In most financial applications, the distribution of a stock price is modelled using a stochastic process called Brownian motion.

2.2 The Brownian Motion

The Brownian motion process (or Wiener process) is a model that was originally used in physics to describe the motion of a particle subject to perpetual collision with surrounding molecules. The process was later adopted by financial mathematicians to model the behaviour of asset returns. The formal definition is as follows:

Definition 2.1 (Brownian motion) *The Brownian motion $W(\cdot)$ is a stochastic process with the following characteristics:*

1. *Let $W(0)=0$ and $t_0<\cdots<t_n$, then the increments $W(t_1)-W(t_0),\ldots,W(t_n)-W(t_{n-1})$ are mutually independent random variables. (A process with this property is called an independent increment process.)*

2. *For $s < t$, $W(t) - W(s) \sim N(0, t-s)$, where $N(\mu, \sigma^2)$ denotes the normal distribution with mean μ and variance σ^2.*

A popular model based on the Brownian motion process is the Brownian motion with drift, where

$$X_t = \mu t + \sigma W_t,$$

with $t \geq 0$, $\mu \in \Re$, and $\sigma > 0$.

Brownian motion is applied to the modelling of stock prices using the following argument. Suppose that a stock price S increases at some constant rate μ. Then, for a short interval of time dt, the expected increase in S is $\mu S dt$. If the volatility of the stock price is zero, this implies

$$dS = \mu S dt.$$

However, a more realistic approach is to model the volatility using Brownian motion, which yields the following stochastic differential equation

$$dS = \mu S dt + \sigma S dW_t,$$

where σ is a volatility measure of the stock price S_t. This model is known as exponential Brownian motion, geometric Brownian motion, geometric Wiener process, or lognormal process.

From Itô's [19] lemma, the process followed by some function f of S and t is

$$df = \left(\frac{\partial f}{\partial t} + \mu S \frac{\partial f}{\partial S} + \frac{1}{2}\sigma^2 S^2 \frac{\partial^2 f}{\partial S^2}\right) dt + \sigma S \frac{\partial f}{\partial S} dW, \tag{2.3}$$

Applying this lemma to the logarithm of a stock price, we get that

$$d(\log S_t) = \left(\mu - \frac{\sigma^2}{2}\right) dt + \sigma dW_t.$$

Therefore, the stock return Y_t between times $t-1$ and t is normally distributed with mean $\left(\mu - \frac{\sigma^2}{2}\right)$ and variance σ^2, which implies that

$$S_t = S_{t-1} e^{\left(\mu - \frac{\sigma^2}{2}\right) + \sigma W_1}.$$

A sampling procedure for exponential Brownian motion can easily be constructed by drawing observations from a normal distribution. In practice, μ and σ are often taken to be the sample mean and sample standard deviation of the stock price over a certain period.

For more on the mathematical aspects of Brownian motion, consult Karlin and Taylor [21]. Readers interested in financial applications of this process should refer to Hull [16].

2.3 Binomial Option Pricing Model

The binomial model is a popular option pricing technique that was originally discussed in the late seventies by Cox et al. [6] and Rendleman and Bartter [32]. The basic idea behind the binomial approach is the construction of binomial trees which are used to replicate the behaviour of the stock price over the life of the option.

2.3.1 One-Step Binomial Model

Consider a European call option c, with underlying security S_t, expiration date T, and exercise price K. Assume that during the life of the option, the stock price can either increase to $S_t u$, or decrease to $S_t d$. If the stock price increases, we use c_u to denote the payoff of the option; if the stock price decreases, the payoff is denoted by c_d. This situation is illustrated in Figure 2.1.

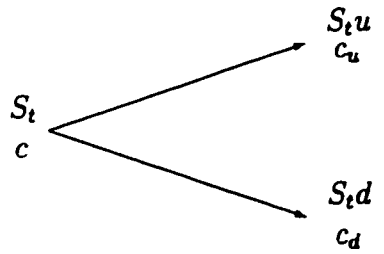

Figure 2.1: Stock and call option prices in a one-step binomial tree.

We describe the option pricing methodology with the following portfolio:

Portfolio Π_1 : -1 European call + Δ shares of the underlying stock.

As illustrated in Figure 2.2, the value of Π_1 at time t is $S_t\Delta - c$. At expiration of the option, the value of this portfolio becomes $S_t u\Delta - c_u$ if the stock price moves up, or $S_t d\Delta - c_d$ if the stock price moves down.

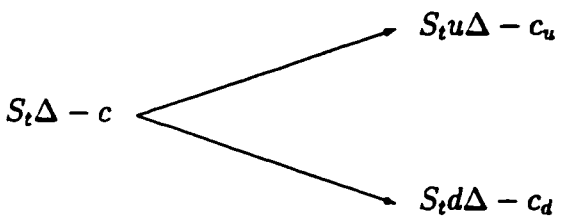

Figure 2.2: Value of portfolio Π_1.

Now suppose we wish to set up Π_1 so that it becomes a risk-free portfolio. This will be the case if the value of Π_1 at expiration date is the same regardless of whether the stock price moves up or down, i.e.

$$S_t u\Delta - c_u = S_t d\Delta - c_d,$$

which implies

$$\Delta = \frac{c_u - c_d}{S_t\,(u-d)}. \tag{2.4}$$

From the risk-neutral valuation principles, Π_1 is then a risk-free portfolio and must earn the risk-free rate r over the life of the option. Thus, the present value of Π_1 is

$$e^{-r(T-t)}\,(S_t u\Delta - c_u)\,,$$

and since the initial value of the portfolio is $S_t\Delta - c$, then it follows that

$$S_t\Delta - c = e^{-r(T-t)}\,(S_t u\Delta - c_u)\,.$$

Substituting from equation (2.4) and solving for c, we obtain

$$c = e^{-r(T-t)}\left[qc_u + (1-q)\,c_d\right],$$

where

$$q = \frac{e^{r(T-t)} - d}{u - d}$$

is the probability that the stock price will increase over the time interval considered.

2.3.2 Generalization

The single-step model previously described can be extended to a general model with multiple steps. Consider the same European call option c and divide the life of the option into n equal subintervals. Assume that over each subinterval, the stock price can either move up or down. The case with $n = 2$ is illustrated in Figure 2.3.

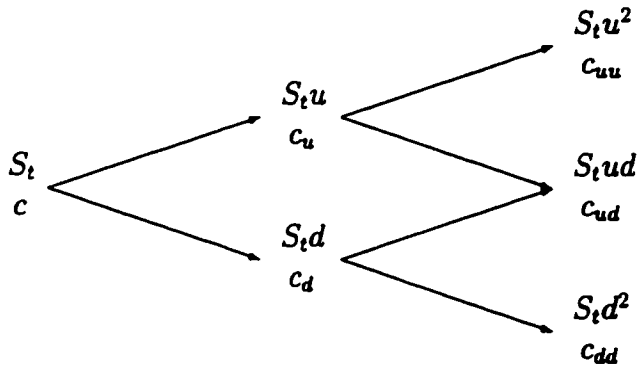

Figure 2.3: Stock and call option prices in a two-step binomial tree.

The methodology used to calculate c is relatively simple. In fact, the call option price is obtained by repeatedly applying the procedure described for the single-step case. For a model with n steps, the resulting option pricing formula is as follows

$$c = e^{-nr\Delta t}\sum_{j=0}^{n}\binom{n}{j}q^j\,(1-q)^{n-j}\,c_{ju+(n-j)d},$$

where $\Delta t = (T-t)/n$,

$$q = \frac{e^{r\Delta t} - d}{u - d},$$

and $c_{ju+(n-j)d}$ represents the value of a call option whose underlying security moved up j times and moved down $(n-j)$ times over the n subintervals.

The corresponding relationship for a European put option is

$$p = e^{-nr\Delta t} \sum_{j=0}^{n} \binom{n}{j} q^j (1-q)^{n-j} p_{ju+(n-j)d}.$$

In practice, the parameters u and d are generally chosen to match the stock price volatility. This is achieved by setting

$$u = e^{\sigma\sqrt{\Delta t}}, \quad \text{and} \quad d = e^{-\sigma\sqrt{\Delta t}},$$

where σ is the standard deviation of S_t over some time interval.

The binomial approach is characterized by its flexibility, which allows for pricing of various types of options, including options on dividend-bearing securities, American options, and options on currencies. Consult Hull [16] or Kolb [22] for complete details.

2.4 Black-Scholes Option Pricing Formula

Perhaps the best known and most commonly used option pricing model is the Black-Scholes formula. This model was developed by Black and Scholes [3] under the assumptions that stock prices change continuously, adjust to prevent arbitrage, and follow exponential Brownian motion

$$dS = \mu S dt + \sigma S dW_t, \tag{2.5}$$

where μ is the mean return and σ is the volatility of the stock price.

Suppose that c is the price of a European call option with underlying asset S and consider the following portfolio:

$$\text{Portfolio } \Pi_2 \ : \ \text{-1 European call} + \frac{\partial c}{\partial S} \text{ shares of the underlying stock.}$$

By definition, the value of this portfolio is given by

$$\Pi_2 = -c + \frac{\partial c}{\partial S} S.$$

Using Itô's lemma (2.3) and equation (2.5), the change in the value of Π_2 during time interval Δt can be written as

$$\begin{aligned} \Delta\Pi_2 &= -\Delta c + \frac{\partial c}{\partial S}\Delta S \\ &= \left(-\frac{\partial c}{\partial t} - \frac{1}{2}\frac{\partial^2 c}{\partial S^2}\sigma^2 S^2\right)\Delta t, \end{aligned}$$

which is a risk-free portfolio since it does not depend on ΔW. In a risk-neutral world, this portfolio must earn the risk-free interest rate r and hence

$$\Delta\Pi_2 = r\Pi_2\Delta t.$$

Substituting from the previous results, we obtain the following differential equation

$$\frac{\partial c}{\partial t} + rS\frac{\partial c}{\partial S} + \frac{1}{2}\sigma^2 S^2\frac{\partial^2 c}{\partial S^2} = rc,$$

which known as the Black-Scholes-Merton differential equation. The Black-Scholes option pricing formula is then obtained by solving this differential equation under certain initial conditions. We refer the reader to Hull [16] for the complete argument.

Definition 2.2 (Black-Scholes option pricing formula) *Let c_t be the price of a European call option with underlying security S_t, expiration date T, and exercise price K. If S_t does not pay dividends, r is the risk-free interest rate, and σ is a volatility measure of S_t, then the Black-Scholes option pricing formula is*

$$c_t = S_t\Phi(d_1) - Ke^{-r(T-t)}\Phi(d_2),$$

where $\Phi(\cdot)$ is the distribution function of a $N(0,1)$ random variable,

$$d_1 = \frac{\log\left(\frac{S_t}{K}\right) + \left(r + \frac{\sigma^2}{2}\right)(T-t)}{\sigma\sqrt{T-t}},$$

and

$$d_2 = d_1 - \sigma\sqrt{T-t}.$$

The Black-Scholes formula is recognized for its capability of valuing options under numerous circumstances. Another major contributor to its popularity is the relative simplicity of the final equation. Besides the option characteristics, only two other inputs are required: the risk-free interest rate r and the stock volatility σ. In practice, r is estimated by the yield of a government bond with the same maturity as the option and σ is often taken as the sample variance of historical stock returns over a certain period.

For the put option, we use the put-call parity relationship for European options. This result was developed by Stoll [36] and establishes the connection between a call and a put with the same characteristics.

Theorem 2.1 (Put-call parity for European options) *Let c_t and p_t be European call and put options, both with underlying security S_t, expiration date T, and exercise price K. If S_t does not pay dividends and r is the risk-free interest rate, then*

$$c_t + Ke^{-r(T-t)} = p_t + S_t.$$

The proof of this theorem is straightforward and consists of demonstrating that a portfolio containing a call option and a cash amount equal to $Ke^{-r(T-t)}$ has the same value as another portfolio containing a put option and one share of the underlying stock. Merging this result with the Black-Scholes call option formula, we obtain the following relationship

$$p_t = Ke^{-r(T-t)}\Phi(-d_2) - S_t\Phi(-d_1),$$

where d_1 and d_2 are as defined previously.

Note that both the Black-Scholes formula and the put-call parity relationship are only valid for European options whose underlying security does not pay dividends. Adjusted models for securities paying dividends are described in the literature, but we will not discuss them. See Merton [27] for more on that subject. For articles on American option pricing, please consult Geske [15], Roll [33], and Whaley [37] for the American call, or Barone-Adesi and Whaley [1], and Johnson [20] for the American put.

2.5 Monte Carlo Simulation

The third option pricing model described in this chapter is a sampling procedure called Monte Carlo simulation. This procedure is performed by drawing stock returns from the following process

$$d(\log S_t) = \left(\mu - \frac{\sigma^2}{2}\right) dt + \sigma dG_t,$$

where G_t is a stochastic process modelling the volatility in a stock return. In practice, G_t is often chosen to be the Brownian motion process W_t.

The option price estimate is then computed by averaging the option prices calculated for each simulated sample path. For European options, the algorithm is as follows:

A. Simulate future stock returns $\hat{Y}_{t+1}, \ldots, \hat{Y}_T$ by drawing observations from a normal distribution with mean $\left(\mu - \frac{\sigma^2}{2}\right)$ and variance σ^2.

B. Create the corresponding sample paths for the predicted stock prices:

$$\hat{S}_{t+i} = \hat{S}_{t+i-1} e^{\hat{Y}_{t+i}}, \quad \text{for } i = 1, \ldots, T-t.$$

C. Repeat steps 1–2 for $j = 1, \ldots, m$ to obtain $\hat{S}_T^{(1)}, \ldots, \hat{S}_T^{(m)}$.

D. Calculate the option price for each sample path:

1. Call: $\hat{C}_t^{(j)} = e^{-r(T-t)} \max\left(\hat{S}_T^{(j)} - K, 0\right)$.
2. Put: $\hat{P}_t^{(j)} = e^{-r(T-t)} \max\left(K - \hat{S}_T^{(j)}, 0\right)$.

E. Estimate the option price by computing the sample mean of the resulting prices:

1. Call: $\hat{c}_t = \frac{\hat{C}_t^{(1)} + \cdots + \hat{C}_t^{(m)}}{m}$.
2. Put: $\hat{p}_t = \frac{\hat{P}_t^{(1)} + \cdots + \hat{P}_t^{(m)}}{m}$.

Note that this algorithm is not restricted to the case with European options as Monte Carlo simulation can be extended to price certain types of exotic options. In fact, because plain-vanilla European options can be priced almost exactly by the Black-Scholes formula, most option prices computed using Monte Carlo simulation tend to have non-standard provisions.

Another major advantage of this procedure is that it can accommodate any stochastic process, not just Brownian motion. A drawback however is its poor efficiency in handling options with early exercise opportunities, like American options for example. We refer the reader to Hull [16] for more properties of Monte Carlo simulation.

Chapter 3

The Dirichlet Process

The Dirichlet process is a stochastic process named after the 19^{th} century mathematician Johann Peter Gustav Lejeune Dirichlet. Although this process was first discussed by Freedman [13] and Fabius [8] in the early sixties, most of its theory and properties were developed only ten years later in two seminal papers by Ferguson [10, 11].

This chapter presents a review of the Dirichlet process. We begin our discussion with a description of the Dirichlet distribution and its principal properties. Then, we define the Dirichlet process and present its various representations, including Ferguson's [10, 11] definition and sum-construction, Blackwell and MacQueen's [4] Pólya urn representation, Sethuraman's [35] stick-breaking approach, and Ishwaran and Zarepour's [17] truncated Dirichlet process. Important properties are also reviewed.

We close this chapter with an original application of the Dirichlet process to the pricing of European options. Using the Dirichlet process as the prior distribution of stock returns, we derive an option pricing formula that can be viewed as an alternative to the binomial, Black-Scholes, and Monte Carlo models described in Chapter 2.

3.1 The Dirichlet Distribution

Consider the gamma distribution with shape parameter $\alpha > 0$ and scale parameter $\beta > 0$, denoted by $Ga(\alpha, \beta)$. If $\alpha = 1$, the gamma distribution is called the exponential distribution with parameter β, denoted by $Exp(\beta)$. If $\alpha = \beta = 1$, we speak

of standard exponential. Perhaps one of the main characteristics of the gamma distribution is its closure under additivity. If X_1 and X_2 are two independent gamma random variables such that $X_j \sim Ga(\alpha_j, \beta)$, then the variable $X_1 + X_2$ follows a $Ga(\alpha_1 + \alpha_2, \beta)$.

This characteristic is useful in determining another property of the gamma distribution, namely its relationship with the beta distribution. If X_1 and X_2 are independent gamma variables such that $X_j \sim Ga(\alpha_j, 1)$, then the variable

$$Y = \frac{X_1}{X_1 + X_2}$$

has a beta distribution with parameters α_1 and α_2, denoted by $Be(\alpha_1, \alpha_2)$.

The Dirichlet distribution can be constructed as a generalization of the beta construction. Let $X_1, \ldots, X_{k+1}$ be a collection of independent random variables with $X_j \sim Ga(\alpha_j, 1)$, where $\alpha_j \geq 0$ for all $j = 1, \ldots, k+1$ and $\alpha_j > 0$ for some j. For $j = 1, \ldots, k+1$, let

$$Y_j = \frac{X_j}{\sum_{i=1}^{k+1} X_i}.$$

By the additive property of the gamma distribution, the denominator follows a $Ga\left(\sum_{i=1}^{k+1} \alpha_i, 1\right)$ and consequently the marginal distribution of each variable Y_j is $Be\left(\alpha_j, \sum_{i=1}^{k+1} \alpha_i - \alpha_j\right)$.

The Dirichlet distribution with parameter $\boldsymbol{\alpha} = (\alpha_1, \ldots, \alpha_{k+1})$, denoted $Dir(\boldsymbol{\alpha})$, is defined as the joint distribution of $Y_1, \ldots, Y_k$ (note the absence of Y_{k+1}). If $\alpha_j > 0$ for all j, then the k-dimensional distribution of $(Y_1, \ldots, Y_k)$ is absolutely continuous and has density function

$$f(y_1, \ldots, y_k \mid \boldsymbol{\alpha}) = \frac{\Gamma(\alpha_1 + \cdots + \alpha_{k+1})}{\Gamma(\alpha_1) \ldots \Gamma(\alpha_{k+1})} y_1^{\alpha_1 - 1} \ldots y_k^{\alpha_k - 1} (1 - y_1 - \cdots - y_k)^{\alpha_{k+1} - 1},$$

over the simplex

$$\mathbf{S} = \left\{ (y_1, \ldots, y_k) : y_j \geq 0, \quad \sum_{j=1}^{k} y_j \leq 1 \right\}.$$

It can easily be verified that the integral of f over $\mathbf{S}$ is unity. Note that if $k = 1$, this density reduces to a $Be(\alpha_1, \alpha_2)$. In this regard, the Dirichlet distribution can be

viewed as the k-variate analogue of the beta distribution. It is frequently used in a Bayesian context as a conjugate prior for the multinomial distribution.

We now state some general properties of the Dirichlet distribution.

1. If $(Y_1, \ldots, Y_k) \sim Dir(\alpha_1, \ldots, \alpha_{k+1})$ and $r_1, \ldots, r_n$ are integers such that $0 < r_1 < \cdots < r_n = k$, then

$$\left(\sum_{j=1}^{r_1} Y_j, \sum_{r_1+1}^{r_2} Y_j, \ldots, \sum_{r_{n-1}+1}^{r_n} Y_j\right) \sim Dir\left(\sum_{j=1}^{r_1} \alpha_j, \sum_{r_1+1}^{r_2} \alpha_j, \ldots, \sum_{r_{n-1}+1}^{r_n} \alpha_j, \alpha_{k+1}\right).$$

   In particular, if $r_1 = k$, the distribution of $\sum_{j=1}^{k} Y_j$ is $Be\left(\sum_{j=1}^{k} \alpha_j, \alpha_{k+1}\right)$.

2. If $(Y_1, \ldots, Y_k) \sim Dir(\alpha_1, \ldots, \alpha_{k+1})$, then the general moment of the Dirichlet distribution has the following representation

$$E[Y_1^{r_1} \ldots Y_k^{r_k}] = \frac{\Gamma(\alpha_1 + r_1) \ldots \Gamma(\alpha_k + r_k)\, \Gamma(\alpha_1 + \cdots + \alpha_{k+1})}{\Gamma(\alpha_1 + \cdots + \alpha_{k+1} + r_1 + \cdots + r_k)\, \Gamma(\alpha_1) \ldots \Gamma(\alpha_k)}.$$

   Consequently, the principal moments are as follows

$$\begin{aligned}
E[Y_j] &= \frac{\alpha_j}{\sum_{i=1}^{k+1} \alpha_i}, \\
E[Y_j^2] &= \frac{\alpha_j(\alpha_j + 1)}{\left(\sum_{i=1}^{k+1} \alpha_i\right)\left(\sum_{i=1}^{k+1} \alpha_i + 1\right)}, \\
E[Y_i Y_j] &= \frac{\alpha_i \alpha_j}{\left(\sum_{i=1}^{k+1} \alpha_i\right)\left(\sum_{i=1}^{k+1} \alpha_i + 1\right)}, \quad \text{for } i \neq j,
\end{aligned}$$

   and these can be used to derive the variance, covariance, and correlation coefficient

$$\begin{aligned}
Var[Y_j] &= \frac{\alpha_j\left(\sum_{i=1}^{k+1} \alpha_i - \alpha_j\right)}{\left(\sum_{i=1}^{k+1} \alpha_i\right)^2\left(\sum_{i=1}^{k+1} \alpha_i + 1\right)}, \\
Cov[Y_i, Y_j] &= \frac{-\alpha_i \alpha_j}{\left(\sum_{i=1}^{k+1} \alpha_i\right)^2\left(\sum_{i=1}^{k+1} \alpha_i + 1\right)}, \quad \text{for } i \neq j, \\
Corr[Y_i, Y_j] &= -\left[\frac{\alpha_i \alpha_j}{\left(\sum_{i=1}^{k+1} \alpha_i - \alpha_i\right)\left(\sum_{i=1}^{k+1} \alpha_i - \alpha_j\right)}\right]^{1/2}, \quad \text{for } i \neq j.
\end{aligned}$$

3. If $(Y_1, \ldots, Y_k) \sim Dir(\alpha_1, \ldots, \alpha_{k+1})$ and if

$$\Pr[X = j \mid Y_1, \ldots, Y_k] = Y_j, \quad \text{for } j = 1, \ldots, k,$$

then the posterior distribution of $(Y_1, \ldots, Y_k)$ given $X = j$ follows a $Dir\left(\alpha_1^{(j)}, \ldots, \alpha_{k+1}^{(j)}\right)$, where

$$\alpha_i^{(j)} = \begin{cases} \alpha_i & \text{if } i \neq j, \\ \alpha_i + 1 & \text{if } i = j. \end{cases}$$

An excellent summary of the principal applications and properties of the Dirichlet distribution may be found in Wilks [38].

3.2 Definition of the Dirichlet Process

As mentioned earlier, Ferguson [10, 11] is responsible for the formal definition of the Dirichlet process, which is characterized by a stochastic process defined on an arbitrary measurable space $\mathcal{X}$ and indexed by elements of a Borel σ-algebra $\mathcal{B}$. In fact, this stochastic process is equivalent to a random probability measure whose existence is secured by Kolmogorov's existence theorem.[1] It follows from this theorem that such a measure is equivalent to a stochastic process. The formal definition is as follows:

Definition 3.1 (Dirichlet process) *Suppose $\alpha H(\cdot)$ is a finite non-null measure on space $(\mathcal{X}, \mathcal{B})$ and let $\mathcal{P}(\cdot)$ be a stochastic process indexed by elements of $\mathcal{B}$. We say $\mathcal{P}$ is a Dirichlet process with parameter αH and write $\mathcal{P} \in DP(\alpha H)$ if, for every finite measurable partition $\{B_1, \ldots, B_{k+1}\}$ of $\mathcal{X}$, the random vector $(\mathcal{P}(B_1), \ldots, \mathcal{P}(B_k))$ follows a Dirichlet distribution with parameter $(\alpha H(B_1), \ldots, \alpha H(B_{k+1}))$.*

For each sample point $\omega \in \Omega$, $\mathcal{P}$ is a random probability measure on $\mathcal{X}$. If $\{B_1, \ldots, B_{k+1}\}$ is a partition of $\mathcal{X}$, $(\mathcal{P}_\omega(B_1), \ldots, \mathcal{P}_\omega(B_k))$ defines the probability that a point chosen from $\mathcal{X}$ falls in $B_1, \ldots, B_k$ respectively. Of course, this changes

[1] The statement of Kolmogorov's theorem is provided in Appendix B.

with ω and $(\mathcal{P}(B_1), \ldots, \mathcal{P}(B_k))$ must have a $Dir(\alpha H(B_1), \ldots, \alpha H(B_{k+1}))$ distribution. Note that since the marginal distribution of each $\mathcal{P}(B_j)$, $j = 1, \ldots, k+1$, is a $Be(\alpha H(B_j), \alpha H(\mathcal{X}) - \alpha H(B_j))$, then

$$E[\mathcal{P}(B_j)] = \frac{\alpha H(B_j)}{\alpha H(\mathcal{X})} = H(B_j), \quad \text{for } j = 1, \ldots, k+1.$$

An interesting characteristic of the Dirichlet process is described in the following theorem: (see Ferguson [10])

Theorem 3.1 *Let $\mathcal{P} \in DP(\alpha H)$ on $(\mathcal{X}, \mathcal{B})$ and let $\mathcal{Q}$ be a fixed probability measure on $(\mathcal{X}, \mathcal{B})$, with $\mathcal{Q} \ll \alpha H$. Then, for any positive integer k and measurable sets $B_1, \ldots, B_{k+1}$, and for $\varepsilon > 0$,*

$$\Pr[|\mathcal{P}(B_i) - \mathcal{Q}(B_i)| < \varepsilon] > 0, \quad \text{for } i = 1, \ldots, k+1.$$

Consequently, the Dirichlet process is dense in the space of probability measures and can be used to approximate any fixed probability measure.

3.2.1 Dirichlet Process Sum-Construction

The Dirichlet process sum-construction is an alternative representation describing the Dirichlet process as a random probability measure with an infinite sum-construction. Exploiting the fact that the Dirichlet distribution can be expressed through the joint distribution of a set of independent gamma variables divided by their sum, Ferguson [10] proposed that the Dirichlet process can be defined using a gamma process with independent increments. The Dirichlet process is obtained using a representation which divides the height of a jump at a time given by the gamma process by the total height of all the jumps over all times to specify the probabilities of randomly specified points. This results in a random discrete probability measure satisfying Definition 3.1. The result is as follows:

Theorem 3.2 (Dirichlet process sum-construction) *Let $E_1, \ldots, E_k$ be independent and identically distributed (i.i.d.) standard exponential random variables, and define $\Gamma_k = E_1 + \cdots + E_k$. Let $Z_1, \ldots, Z_k$ be i.i.d. elements, independent of $\Gamma_1, \ldots, \Gamma_k$,*

with a distribution H over $(\mathcal{X}, \mathcal{B})$. The Dirichlet process with parameter αH, with $\alpha \in \Re^+$, is realized by the random probability measure

$$\mathcal{P}(\cdot) = \sum_{k=1}^{\infty} \frac{N^{-1}(\Gamma_k)}{\sum_{k=1}^{\infty} N^{-1}(\Gamma_k)} \delta_{Z_k}(\cdot),$$

where $\delta_{Z_k}(\cdot)$ denotes the measure concentrated at Z_k

$$\delta_{Z_k}(A) = \begin{cases} 1 & \text{if } Z_k \in A, \\ 0 & \text{if } Z_k \notin A, \end{cases}$$

and N is the Lévy measure[2] for a $Ga(\alpha, 1)$ random variable

$$N(x) = \alpha \int_x^{\infty} u^{-1} e^{-u} du, \quad \text{for } x > 0.$$

As shown in Ishwaran and Zarepour [17], this infinite sum-construction can be approached using point process methods. Let J be an infinitely divisible non-normal random variable whose support is positive with characteristic function

$$\phi(\theta) = \exp\left[\int_0^{\infty} \left(e^{i\theta u} - 1\right) dN(u)\right], \quad \text{for } -\infty < \theta < \infty.$$

Assume that for all $\varepsilon > 0$, the Lévy measure N has a finite inverse function

$$\int_{\varepsilon}^{\infty} N^{-1}(u)\, du < \infty.$$

Let $J_1, J_2, \ldots$ be an infinite collection of random variables such that

$$\Pr[J_1 \leq x_1] = e^{-N(x_1)}, \quad \text{for } x_1 > 0,$$

and for $k = 2, 3, \ldots$

$$\Pr[J_k \leq x_k \mid J_{k-1} = x_{k-1}] = e^{-(N(x_k) - N(x_{k-1}))}, \quad \text{for } 0 < x_k < x_{k-1}.$$

It then follows from Ferguson and Klass [12] that $\sum_{k=1}^{\infty} J_k$ converges to a random variable J almost surely and therefore

$$\mathcal{P}(\cdot) = \sum_{k=1}^{\infty} \frac{J_k}{\sum_{k=1}^{\infty} J_k} \delta_{Z_k}(\cdot)$$

[2]See Appendix B for a description of Lévy measures and characteristic functions for infinitely divisible random variables.

is a random probability measure with random weights based on an infinitely divisible distribution such as the gamma distribution.

As demonstrated by Ferguson [10], the Dirichlet process can be expressed using this representation. Let $\Gamma_1, \Gamma_2, \ldots$ be an infinite collection of gamma random variables and let N be the Lévy measure of a $Ga(\alpha, 1)$

$$N(x) = \alpha \int_x^\infty u^{-1} e^{-u} du, \quad \text{for } x > 0.$$

Then, for $x_1 > 0$,

$$\begin{aligned} \Pr\left[N^{-1}(\Gamma_1) \leq x_1\right] &= \Pr\left[\Gamma_1 \leq N(x_1)\right] \\ &= e^{-N(x_1)} \\ &= \Pr\left[J_1 \leq x_1\right], \end{aligned}$$

and for $0 < x_k < x_{k-1}$ and $k = 2, 3, \ldots,$

$$\begin{aligned} \Pr\left[N^{-1}(\Gamma_k) \leq x_k \mid N^{-1}(\Gamma_{k-1}) = x_{k-1}\right] &= \Pr\left[\Gamma_k \leq N(x_k) \mid \Gamma_{k-1} = N(x_{k-1})\right] \\ &= e^{-(N(x_k) - N(x_{k-1}))} \\ &= \Pr\left[J_k \leq x_k \mid J_{k-1} = x_{k-1}\right]. \end{aligned}$$

Obviously, $J_k = N^{-1}(\Gamma_k)$ and therefore

$$\mathcal{P}(\cdot) = \sum_{k=1}^\infty \frac{N^{-1}(\Gamma_k)}{\sum_{k=1}^\infty N^{-1}(\Gamma_k)} \delta_{Z_k}(\cdot).$$

If $\{B_1, \ldots, B_{k+1}\}$ is a partition of $\mathcal{X}$, then it follows from Ferguson and Klass [12] that

$$\sum_{k=1}^\infty N^{-1}(\Gamma_k)\, \delta_{Z_k}(B_j) \sim Ga(\alpha H(B_j), 1).$$

Since $\sum_{k=1}^\infty N^{-1}(\Gamma_k)$ is the sum of these gamma variables, then

$$\sum_{k=1}^\infty N^{-1}(\Gamma_k) \sim Ga(\alpha, 1),$$

and from the definition of the Dirichlet distribution

$$(\mathcal{P}(B_1), \ldots, \mathcal{P}(B_k)) \sim Dir(\alpha H(B_1), \ldots, \alpha H(B_{k+1})).$$

3.2.2 Pólya Urn Representation

An easier proof of Ferguson's [10, 11] sum-construction was provided by Blackwell and MacQueen [4] via Pólya urn schemes. Consider the sequence $\{X_k\}$ representing the results of successive draws from an urn containing $\mu(x)$ balls of colour x. After each draw, the ball drawn is returned to the urn along with another ball of the same colour. Then for every $B \in \mathcal{B}$, the probability that the first ball drawn has colour B is

$$\Pr[X_1 \in B] = \frac{\mu(B)}{\mu(\mathcal{X})},$$

and the probability that the $(k+1)^{th}$ ball drawn has colour B, given the first k observations is

$$\Pr[X_{k+1} \in B \mid X_1, \ldots, X_k] = \frac{\mu_k(B)}{\mu_k(\mathcal{X})} = \frac{\mu(B) + \sum_1^k \delta_{X_i}(B)}{\mu(\mathcal{X}) + \sum_1^k \delta_{X_i}(\mathcal{X})} = \frac{\mu(B) + \sum_1^k \delta_{X_i}(B)}{\mu(\mathcal{X}) + k}.$$

As $k \to \infty$, Blackwell and MacQueen [4] showed that this expression converges almost surely to a discrete probability measure $\mu^* \in DP(\mu)$.

3.3 Stick-Breaking Representation

Although Ferguson's [10, 11] sum-construction is equivalent to the definition of the Dirichlet process, the complex structure of the random weights

$$v_k = \frac{N^{-1}(\Gamma_k)}{\sum_{k=1}^{\infty} N^{-1}(\Gamma_k)}$$

made this representation difficult to manipulate. The lack of interest toward the sum-construction disappeared when Sethuraman [35] introduced an alternative approach which models the random weights using beta random variables in a stick-breaking procedure. According to the stick-breaking representation, the random weights are defined by

$$v_k = \begin{cases} V_1 & \text{if } k = 1, \\ (1 - V_1)(1 - V_2)\ldots(1 - V_{k-1})V_k & \text{if } k = 2, 3, \ldots, \end{cases}$$

where $V_1, V_2, \ldots$ are i.i.d. $Be(1, \alpha)$ random variables. Under independence among the V_k's and Z_k's, the Dirichlet process $DP(\alpha H)$ can be written

$$\mathcal{P}(\cdot) = \sum_{k=1}^{\infty} v_k \delta_{Z_k}(\cdot) = V_1 \delta_{Z_1}(\cdot) + \sum_{k=2}^{\infty} (1 - V_1)(1 - V_2) \ldots (1 - V_{k-1}) V_k \delta_{Z_k}(\cdot).$$

3.3.1 Relationship to Poisson Process

Consider a sequence of events, where X_1 is the waiting time for the first event, X_2 is the waiting time between the first and second events, etc. Suppose that $X_1, X_2, \ldots$ are i.i.d. exponential variables with parameter α. Under these conditions, the number N_t of events that occur during a time interval has a Poisson distribution with parameter αt and

$$\Pr[N_t = n] = \frac{e^{-\alpha t}(\alpha t)^n}{n!}, \quad \text{for } n = 0, 1, \ldots.$$

N_t is called a Poisson process with rate α.

There exists a useful connection between the Dirichlet process and the Poisson process. This connection was observed by Ishwaran and Zarepour [17] who noted that Sethuraman's [35] construction can be written as

$$\mathcal{P}(\cdot) = \sum_{k=1}^{\infty} v_k \delta_{Z_k}(\cdot) \stackrel{d}{=} \sum_{k=1}^{\infty} \left(e^{-\Gamma_{k-1}/\alpha} - e^{-\Gamma_k/\alpha}\right) \delta_{Z_k}(\cdot),$$

where $\Gamma_0 = 0$ and $\stackrel{d}{=}$ denotes the equality of the distributions. This relationship was derived from the fact that

$$1 - Be(1, \alpha) \stackrel{d}{=} Be(\alpha, 1) \stackrel{d}{=} e^{-E_1/\alpha},$$

where E_1 denotes a standard exponential random variable. Thus,

$$\begin{aligned} v_k &= (1 - V_1)(1 - V_2) \ldots (1 - V_{k-1}) V_k \\ &\stackrel{d}{=} e^{-E_1/\alpha} \ldots e^{-E_{k-1}/\alpha} \left(1 - e^{-E_k/\alpha}\right) \\ &= e^{-\Gamma_{k-1}/\alpha} - e^{-\Gamma_k/\alpha}. \end{aligned}$$

3.3.2 Almost Sure Truncations

An approximation to the Dirichlet process can be obtained by truncating the higher-order terms in Sethuraman's [35] stick-breaking representation. This results in an approximating random probability measure of the form

$$\mathcal{P}_N(\cdot) = \sum_{k=1}^{N} v_k \delta_{Z_k}(\cdot) = V_1 \delta_{Z_1}(\cdot) + \sum_{k=2}^{N} (1-V_1)(1-V_2)\dots(1-V_{k-1}) V_k \delta_{Z_k}(\cdot),$$

where

$$v_k = \begin{cases} V_1 & \text{if } k = 1, \\ (1-V_1)(1-V_2)\dots(1-V_{k-1}) V_k & \text{if } k = 2, 3, \dots, N, \end{cases}$$

$V_1, \dots, V_{N-1}$ are i.i.d. $Be(1, \alpha)$ random variables, and V_N is set to one to ensure that the random weights sum to unity. Note that if we exploit the Poisson process connection described earlier, the almost sure truncation can also be written as

$$\mathcal{P}_N(\cdot) = \sum_{k=1}^{N} v_k \delta_{Z_k}(\cdot) \stackrel{d}{=} \sum_{k=1}^{N} \left(e^{-\Gamma_{k-1}/\alpha} - e^{-\Gamma_k/\alpha}\right) \delta_{Z_k}(\cdot),$$

with $\Gamma_0 = 0$. Note that Γ_k converges to k almost surely.

In both representations, the value of N is chosen to control the size of the tail probability

$$\sum_{k=N+1}^{\infty} v_k.$$

This can be achieved using various methods. According to Ishwaran and Zarepour [17], a fixed stopping rule is to pick N such that

$$\begin{aligned} \Pr\left[\sum_{k=N+1}^{\infty} v_k > \varepsilon\right] &\leq \frac{E\left[\sum_{k=N+1}^{\infty} v_k\right]}{\varepsilon} \\ &= \frac{\left(\frac{\alpha}{1+\alpha}\right)^{N-1}}{\varepsilon} \\ &< 1. \end{aligned}$$

An alternative approach is to use Muliere and Tardella's [29] random stopping rule where

$$N_\varepsilon = \inf\{k : (1 - V_1)(1 - V_2)\dots(1 - V_{k-1})V_k < \varepsilon\}.$$

The next result was shown by Ishwaran and Zarepour [17]:

Theorem 3.3 *Let $\mathcal{P} \in DP(\alpha H)$ and let $\mathcal{P}_N$ denote the Dirichlet process truncated at N. Then, for each real-valued measurable function g, integrable with respect to H, $\mathcal{P}_N(g) \to \mathcal{P}(g)$.*

As N becomes large, the distribution of the truncation converges to the true distribution of the Dirichlet process. Thus, integrable functionals of the Dirichlet process can be approximated by $\mathcal{P}_N$. This result is powerful in the sense that it allows for simulation of the Dirichlet process. First, the distribution of $\mathcal{P}_N$ is obtained by simulating the random variables $V_1, \dots, V_N \sim Be(1, \alpha)$ and $Z_1, \dots, Z_N \sim H$. The resulting distribution is then used to approximate that of the Dirichlet process $\mathcal{P}$. Further applications of the truncated Dirichlet process are presented in Ishwaran and Zarepour [18].

3.4 Dirichlet Process Posteriors

A major property of the Dirichlet process is this theorem of Ferguson [10, 11]:

Theorem 3.4 *If F is a random probability from $DP(\alpha H)$ and $X_1, \dots, X_n$ is a random sample from F_ω, then the posterior distribution of F given $X_1, \dots, X_n$ is $DP(\alpha H + \sum_1^n \delta_{X_i})$, where δ_x is a point mass at x.*

Note that the parameter of the new process can be written as

$$\begin{aligned} \alpha H + \sum_{i=1}^{n} \delta_{X_i} &= (\alpha + n)\left(\frac{\alpha}{\alpha + n} H + \frac{1}{\alpha + n} \sum_{i=1}^{n} \delta_{X_i}\right) \\ &= (\alpha + n)\left(w_n H + (1 - w_n)\frac{1}{n} \sum_{i=1}^{n} \delta_{X_i}\right), \end{aligned}$$

where

$$w_n = \frac{\alpha}{\alpha + n}.$$

Therefore, the concentration measure in a $DP\left(\alpha H + \sum_1^n \delta_{X_i}\right)$ is $\alpha + n$, while the distribution of each Z_k is $\left(w_n H + (1 - w_n)\frac{1}{n}\sum_1^n \delta_{X_i}\right)$.

In other words, the posterior distribution is a Dirichlet process whose parameter was updated by the information contained in the random sample. This property is very useful in Bayesian decision theoretic problems. If we can find a Bayes rule for the no-sample problem, then a Bayes rule for the general problem may be found by replacing αH with $\left(\alpha H + \sum_1^n \delta_{X_i}\right)$ in the Dirichlet process. We demonstrate the importance of this property with some examples.

3.4.1 Estimation of a Distribution Function

The easiest application of Dirichlet process priors is the estimation of an unknown distribution function F by a suitable $\hat{F}$. This application was first discussed by Ferguson [10, 11]. The objective is to find the Bayes estimate $\hat{F}$ that will minimize the loss incurred by the estimation. The procedure is performed using the squared error loss function

$$L\left(F, \hat{F}\right) = \int \left[F(t) - \hat{F}(t)\right]^2 dG(t),$$

where $G(\cdot)$ is a given non-random weight function (finite measure) on $(\Re, \mathcal{B})$. The Bayes estimate is found by minimizing the Bayes risk

$$E\left[L\left(F, \hat{F}\right)\right] = \int E\left[F(t) - \hat{F}(t)\right]^2 dG(t),$$

which is achieved by choosing $\hat{F}(t) = E[F(t)]$.

Now suppose that the prior distribution of F is $DP(\alpha H)$. Then, for the no-sample problem,

$$F(t) \sim Be\left(\alpha H(-\infty, t], \alpha H(t, \infty)\right),$$

and hence

$$\hat{F}(t) = E[F(t)] = \frac{\alpha H(-\infty, t]}{\alpha H(\Re)} = H(-\infty, t] = H(t).$$

The function $H(t)$ represents our prior guess at $F(t)$.

Next, consider a random sample $X_1, \ldots, X_n$ from F_ω. Since the posterior distribution of F given the sample is $DP(\alpha H + \sum_1^n \delta_{X_i})$, then the Bayes estimate is

$$\hat{F}_n(t) = E[F(t) \mid X_1, \ldots, X_n] = \frac{\alpha H(-\infty, t] + \sum_{i=1}^n \delta_{X_i}(-\infty, t]}{\alpha + n}.$$

This can be rewritten as

$$\hat{F}_n(t) = w_n H(t) + (1 - w_n) F_n(t \mid x_1, \ldots, x_n), \tag{3.1}$$

where

$$F_n(t \mid x_1, \ldots, x_n) = \frac{1}{n} \sum_{i=1}^n \delta_{X_i}(-\infty, t]$$

is the usual empirical distribution function, and of course

$$w_n = \frac{\alpha}{\alpha + n}.$$

Consequently, the Bayes estimate is a weighted average of our prior guess H and the sample distribution function F_n. When α is large compared to n, the Bayes estimate gives more weight to the prior guess H. However, as the number of observations n increases, this weight is gradually shifted towards F_n. For this reason, Ferguson [10, 11] suggested that the concentration measure α can be interpreted as the strength of belief in the prior guess. Note also that as α tends to zero, the Bayes estimate $\hat{F}_n$ is asymptotically equivalent to the sample distribution function F_n, and since F_n converges almost surely to F as $n \to \infty$, then $\hat{F}_n$ is a consistent estimator.

3.4.2 Estimation of the Median

The next application was also discussed by Ferguson [10] and is concerned with the estimation of the median. Using absolute error loss

$$L(\mathcal{P}, m) = |m - \hat{m}|,$$

we wish to estimate the median m of an unknown probability measure $\mathcal{P}$ on $(\Re, \mathcal{B})$. In this case, any median of the distribution of m is a Bayes estimate of m.

If $\mathcal{P} \in DP(\alpha H)$, the median of the distribution of m is a number t such that

$$\Pr[m < t] \leq \frac{1}{2} \leq \Pr[m \leq t],$$

or equivalently

$$\Pr\left[F(t) \geq \frac{1}{2}\right] \leq \frac{1}{2} \leq \Pr\left[F(t) > \frac{1}{2}\right].$$

Since $F(t) \sim Be(\alpha H(-\infty, t], \alpha H(t, \infty))$, this relationship is satisfied if and only if t is the median of $E[\mathcal{P}]$, i.e.

$$\frac{\alpha H(-\infty, t)}{\alpha H(\Re)} \leq \frac{1}{2} \leq \frac{\alpha H(-\infty, t]}{\alpha H(\Re)},$$

or

$$H(-\infty, t) \leq \frac{1}{2} \leq H(-\infty, t].$$

For the no-sample problem, the Bayes estimate $\hat{m}$ satisfying the previous inequality is the median of H; for a random sample $X_1, \ldots, X_n$, the Bayes estimate $\hat{m}_n$ is the median of $\hat{F}_n$.

The analysis of the previous examples can be extended to many situations, including the estimation of the mean, variance, covariance, or any other statistic. See Ferguson [10] for further details.

3.5 Application: European Option Pricing

We now present an application of Dirichlet process priors to the derivation of a pricing formula for European options. The model is developed under the hypothesis that the prior distribution of the underlying stock returns is the $DP(\alpha H)$. We begin our demonstration by deriving general expressions for the expected value and variance of an option price conditional on the historical prices of the underlying stock. These results are then combined with the Dirichlet process theory to obtain an estimated option price.

Expected Value

Consider a European call option with underlying security S_t, expiration date T, and exercise price K. The expected price of a European option is defined as the present value of its expected payoff at maturity (for example, see Hull [16]). In Section 2.1, we saw that the payoff at maturity of a European call option is equal to $\max(S_T - K, 0)$. If we condition on the historical stock prices $S_0, \ldots, S_t$ (and of course the historical stock returns $\mathbf{Y} = (Y_1, \ldots, Y_t)$), then the conditional expected call option price at time t is given by

$$\begin{aligned} c_{t|\mathbf{y}} &= e^{-r(T-t)} E\left[\max(S_T - K, 0) \mid S_0, \ldots, S_t\right] \\ &= e^{-r(T-t)} E\left[\max\left(S_t e^{Y_{t+1}+\cdots+Y_T} - K, 0\right) \mid S_0, \ldots, S_t\right] \\ &= e^{-r(T-t)} E\left[\max\left(S_t e^{Y_{t+1}+\cdots+Y_T} - K, 0\right) \mid Y_1, \ldots, Y_t\right], \end{aligned}$$

where r is the risk-free interest rate. Define $X = Y_{t+1} + \cdots + Y_T$, a random variable measuring the cumulative stock return between times t and T, then

$$\begin{aligned} c_{t|\mathbf{y}} &= e^{-r(T-t)} E\left[\max\left(S_t e^{X} - K, 0\right) \mid Y_1, \ldots, Y_t\right] \\ &= e^{-r(T-t)} \int_{-\infty}^{\infty} \max\left(S_t e^{x} - K, 0\right) dF(x \mid \mathbf{y}), \end{aligned}$$

where $dF(x \mid \mathbf{y})$ is the density function of the variable X conditional on the historical returns $\mathbf{Y} = (Y_1, \ldots, Y_t)$. Using the identity

$$\max(a, b) = \frac{a + b + |a - b|}{2},$$

we can write

$$\max\left(S_t e^{X} - K, 0\right) = \frac{S_t e^{X} - K + \left|S_t e^{X} - K\right|}{2},$$

and consequently

$$\begin{aligned} c_{t|\mathbf{y}} &= e^{-r(T-t)} E\left[\left(\frac{S_t e^{X} - K + \left|S_t e^{X} - K\right|}{2}\right) \middle| \mathbf{Y}\right] \\ &= \frac{e^{-r(T-t)}}{2} \left\{E\left[\left(S_t e^{X} - K\right) \mid \mathbf{Y}\right] + E\left[\left|S_t e^{X} - K\right| \mid \mathbf{Y}\right]\right\}. \end{aligned} \tag{3.2}$$

Developing the second expectation, we obtain

$$\begin{aligned} & E\left[\left|S_t e^X - K\right| \mid \mathbf{Y}\right] \\ &= \int_{-\infty}^{\infty} \left|S_t e^x - K\right| dF\left(x \mid \mathbf{y}\right) \\ &= \int_{\log(K/S_t)}^{\infty} \left(S_t e^x - K\right) dF\left(x \mid \mathbf{y}\right) - \int_{-\infty}^{\log(K/S_t)} \left(S_t e^x - K\right) dF\left(x \mid \mathbf{y}\right), \end{aligned}$$

where $\log\left(K/S_t\right)$ represents the value of x for which the investor will be indifferent between exercising the call option or not. It is the point at which the function $\left(S_t e^x - K\right)$ intersects with the x-axis. By rearranging the integrals, we obtain

$$\begin{aligned} & E\left[\left|S_t e^X - K\right| \mid \mathbf{Y}\right] \\ &= \int_{\log(K/S_t)}^{\infty} \left(S_t e^x - K\right) dF\left(x \mid \mathbf{y}\right) \\ &\quad - \left\{\int_{-\infty}^{\infty} \left(S_t e^x - K\right) dF\left(x \mid \mathbf{y}\right) - \int_{\log(K/S_t)}^{\infty} \left(S_t e^x - K\right) dF\left(x \mid \mathbf{y}\right)\right\} \\ &= 2\int_{\log(K/S_t)}^{\infty} \left(S_t e^x - K\right) dF\left(x \mid \mathbf{y}\right) - \int_{-\infty}^{\infty} \left(S_t e^x - K\right) dF\left(x \mid \mathbf{y}\right) \\ &= 2\int_{\log(K/S_t)}^{\infty} \left(S_t e^x - K\right) dF\left(x \mid \mathbf{y}\right) - E\left[\left(S_t e^X - K\right) \mid \mathbf{Y}\right], \end{aligned}$$

and merging this result with (3.2), we get

$$c_{t|\mathbf{y}} = e^{-r(T-t)} \int_{\log(K/S_t)}^{\infty} \left(S_t e^x - K\right) dF\left(x \mid \mathbf{y}\right). \tag{3.3}$$

This is the exact conditional price at time t of a European call option that matures at time T, where r is the known risk-free interest rate, K is the exercise price, S_t is the price of the underlying security at time t, and $F\left(x \mid \mathbf{y}\right)$ is the distribution of the cumulative return $X = Y_{t+1} + \cdots + Y_T$ conditional on $\mathbf{Y} = (Y_1, \ldots, Y_t)$. Similarly, the conditional price of a European put with the same characteristics is

$$p_{t|\mathbf{y}} = e^{-r(T-t)} \int_{\log(K/S_t)}^{\infty} \left(K - S_t e^x\right) dF\left(x \mid \mathbf{y}\right).$$

Variance

The conditional variance of the call option price can be determined from the fact that

$$Var\left[C_{t|\mathbf{y}}\right] = E\left[C_{t|\mathbf{y}}^2\right] - c_{t|\mathbf{y}}^2,$$

where

$$E\left[C_{t|\mathbf{y}}^2\right] = e^{-2r(T-t)} E\left[\left(\max\left(S_t e^X - K, 0\right)\right)^2 \mid \mathbf{Y}\right].$$

Using an argument similar to that for $c_{t|\mathbf{y}}$, the squared expectation becomes

$$E\left[C_{t|\mathbf{y}}^2\right] = e^{-2r(T-t)} \int_{\log(K/S_t)}^{\infty} \left(S_t e^x - K\right)^2 dF\left(x \mid \mathbf{y}\right),$$

and the variance is then equal to

$$Var\left[C_{t|\mathbf{y}}\right] = e^{-2r(T-t)} \int_{\log(K/S_t)}^{\infty} \left(S_t e^x - K\right)^2 dF\left(x \mid \mathbf{y}\right) - c_{t|\mathbf{y}}^2.$$

For a European put option, the expression for the variance is written

$$Var\left[P_{t|\mathbf{y}}\right] = e^{-2r(T-t)} \int_{\log(K/S_t)}^{\infty} \left(K - S_t e^x\right)^2 dF\left(x \mid \mathbf{y}\right) - p_{t|\mathbf{y}}^2.$$

Option Pricing Under Dirichlet Process Prior

To numerically approximate the conditional expected price and variance of European options, we need to adopt a distribution for the random variable X conditional on $\mathbf{Y}$. Whereas the Black-Scholes formula assumes normal distributions using historical means and variances, the Dirichlet process approach employs a prior distribution updated by the historical returns $Y_1, \ldots, Y_t$.

The Dirichlet process theory is adapted for the option pricing formula by assuming that the stock returns Y_i's are observations from F_ω, a realization of $DP\left(\alpha H\right)$. By Theorem 3.4, the posterior distribution of $\mathcal{P}$ given $Y_1, \ldots, Y_t$ is $DP\left(\alpha H + \sum_{i=1}^{t} \delta_{Y_i}\right)$. If F_ω is the common conditional distribution of the Y_i's, then using squared error loss, the Bayes estimate of F_ω is found in equation (3.1), yielding

$$\hat{F}\left(x\right) = E\left[F_\omega\left(x\right) \mid \mathbf{y}\right] = w_t H\left(x\right) + \left(1 - w_t\right) F_t\left(x \mid \mathbf{y}\right),$$

where $H(x)$ is our prior guess at $F_\omega(x \mid \mathbf{y})$,

$$F_t(x \mid \mathbf{y}) = \frac{1}{t}\sum_{i=1}^{t} \delta_{Y_i}(-\infty, x]$$

is the empirical distribution function, and

$$w_t = \frac{\alpha}{\alpha + t}.$$

Special Case $T = t + 1$

Let us first consider the special case where $T = t + 1$ and

$$c_{t|\mathbf{y}} = e^{-r}\int_{\log(K/S_t)}^{\infty} (S_t e^{y_{t+1}} - K)\, dF(y_{t+1} \mid \mathbf{y}).$$

Although this case has little practical value, it represents a good starting point for the discussion of longer periods. Assuming a Dirichlet process prior, the conditional call option price estimated by using $\hat{F}$ in (3.3) is as follows

$$\begin{aligned}
c_{t|\mathbf{y}} &= e^{-r}\int_{\log(K/S_t)}^{\infty} (S_t e^{y_{t+1}} - K)\, dE\left[F_\omega(y_{t+1} \mid \mathbf{y})\right] \\
&= e^{-r}\int_{\log(K/S_t)}^{\infty} (S_t e^{y_{t+1}} - K)\left[w_t dH(y_{t+1}) + (1 - w_t)\, dF_t(y_{t+1} \mid \mathbf{y})\right] \\
&= e^{-r}\left[w_t \int_{\log(K/S_t)}^{\infty} (S_t e^{y_{t+1}} - K)\, dH(y_{t+1})\right. \\
&\quad \left. + (1 - w_t)\int_{\log(K/S_t)}^{\infty} (S_t e^{y_{t+1}} - K)\, dF_t(y_{t+1} \mid \mathbf{y})\right] \\
&= e^{-r}\left[w_t \int_{\log(K/S_t)}^{\infty} (S_t e^{y_{t+1}} - K)\, dH(y_{t+1})\right. \\
&\quad \left. + (1 - w_t)\left(\frac{1}{t}\right)\sum_{i=1}^{t} \max(S_t e^{y_i} - K, 0)\right].
\end{aligned}$$

The conditional expected call option price $c_{t|\mathbf{y}}$ is a weighted average of two expressions. The first term represents the expected value of the payoff using the distribution guessed initially, H, while the second term is the expected value of the payoff using the empirical distribution of $Y_1, \ldots, Y_t$. This second term is the major advantage of

this pricing formula since it is based on the historical behaviour of the stock price. A wrong guess for the distribution H would be corrected by the empirical distribution if t is large enough compared to α. Remember that α is the strength of belief in the prior guess, so it should be small when little is known and larger when the trader has a more strongly held opinion on the distribution.

For the squared expectation, we get

$$E\left[C_{t|\mathbf{y}}^2\right] = e^{-2r}\int_{\log(K/S_t)}^{\infty}\left(S_t e^{y_{t+1}} - K\right)^2 dE\left[F_\omega\left(y_{t+1} \mid \mathbf{y}\right)\right],$$

and hence,

$$\begin{aligned}
E\left[C_{t|\mathbf{y}}^2\right] &= e^{-2r}\int_{\log(K/S_t)}^{\infty}\left(S_t e^{y_{t+1}} - K\right)^2\left[w_t dH\left(y_{t+1}\right) + \left(1-w_t\right) dF_t\left(y_{t+1} \mid \mathbf{y}\right)\right] \\
&= e^{-2r}\left[w_t\int_{\log(K/S_t)}^{\infty}\left(S_t e^{y_{t+1}} - K\right)^2 dH\left(y_{t+1}\right)\right. \\
&\quad \left. + \left(1-w_t\right)\int_{\log(K/S_t)}^{\infty}\left(S_t e^{y_{t+1}} - K\right)^2 dF_t\left(y_{t+1} \mid \mathbf{y}\right)\right] \\
&= e^{-2r}\left[w_t\int_{\log(K/S_t)}^{\infty}\left(S_t e^{y_{t+1}} - K\right)^2 dH\left(y_{t+1}\right)\right. \\
&\quad \left. + \left(1-w_t\right)\left(\frac{1}{t}\right)\sum_{i=1}^{t}\left(\max\left(S_t e^{y_i} - K, 0\right)\right)^2\right].
\end{aligned}$$

The corresponding expressions for a European put option are

$$\begin{aligned}
p_{t|\mathbf{y}} &= e^{-r}\left[w_t\int_{\log(K/S_t)}^{\infty}\left(K - S_t e^{y_{t+1}}\right) dH\left(y_{t+1}\right)\right. \\
&\quad \left. + \left(1-w_t\right)\left(\frac{1}{t}\right)\sum_{i=1}^{t}\max\left(K - S_t e^{y_i}, 0\right)\right],
\end{aligned}$$

and

$$\begin{aligned}
E\left[P_{t|\mathbf{y}}^2\right] &= e^{-2r}\left[w_t\int_{\log(K/S_t)}^{\infty}\left(K - S_t e^{y_{t+1}}\right)^2 dH\left(y_{t+1}\right)\right. \\
&\quad \left. + \left(1-w_t\right)\left(\frac{1}{t}\right)\sum_{i=1}^{t}\left(\max\left(K - S_t e^{y_i}, 0\right)\right)^2\right].
\end{aligned}$$

General Case for all T

For the case where the expiration date is more than one period away ($T \geq t+1$), we assume that $Y_{t+1}, \ldots, Y_T$ are conditionally independent and identically distributed, i.e. the conditional distribution of the stock returns does not change over the remaining life of the option. Thus, for $j = 1, \ldots, T-t$, each Y_{t+j} is drawn from $\hat{F}_{t+j}(x)$, an independent realization of $DP\left(\alpha H + \sum_{i=1}^{t} \delta_{Y_i}\right)$.

This is a simple generalization of the single-period case that we will refer to as the predicted Dirichlet process method. According to this approach, future stock prices $S_{t+1}, \ldots, S_T$ are all predicted using the distribution of $Y_{t+1} \mid Y_1, \ldots, Y_t$. This method exactly parallels that used in the exponential Brownian motion estimation scheme described in Chapter 2.

The option price formulae are derived from the expressions

$$c_{t|\mathbf{y}} = e^{-r(T-t)} \int_{\log(K/S_t)}^{\infty} (S_t e^x - K)\, dE\left[F_\omega\left(X = x \mid \mathbf{y}\right)\right],$$

and

$$p_{t|\mathbf{y}} = e^{-r(T-t)} \int_{\log(K/S_t)}^{\infty} (K - S_t e^x)\, dE\left[F_\omega\left(X = x \mid \mathbf{y}\right)\right],$$

where the conditional distribution of $X = Y_{t+1} + \cdots + Y_T$ is determined from our assumption. For $j = 1, \ldots, T-t$, we can write

$$E\left[F\left(y_{t+j}\right) \mid \mathbf{y}\right] \;=\; w_t H\left(y_{t+j}\right) + \left(1 - w_t\right) F_t\left(y_{t+j} \mid \mathbf{y}\right).$$

The expected conditional distribution of the cumulative stock return X is given by the expected value of the $(T-t)$-fold convolution of $\hat{F}_{t+1}$ to $\hat{F}_T$ so that from (3.3),

$$c_{t|\mathbf{y}} = e^{-r(T-t)} \int_{\log(K/S_t)}^{\infty} (S_t e^x - K)\, dF_X^*\left(x \mid \mathbf{y}\right),$$

where $F_X^*\left(x \mid \mathbf{y}\right)$ denotes the convolution distribution. This integral is not easily computable. As $T \to \infty$, a conditional central limit theorem could perhaps be employed to obtain asymptotic distributions, but the interest in option pricing lies in short time horizons. Simulation of these short-term distributions represent the most practical approach, and is described in the next chapter.

Chapter 4

Predicted Dirichlet Process Simulation

This chapter discusses a sampling procedure based on the predicted Dirichlet process method that will allow us to bypass the analytical expressions developed in Section 3.5. We consider scenarios where the stock price evolves according to an exponential random walk model with either Gaussian, heavy-tailed, or skewed distributions. Given observed stock prices up to the present, we wish to compute the predicted stock prices and corresponding European option prices by performing a Monte Carlo simulation of the future using three different methods:

1. The actual exponential random walk model.
2. The exponential Brownian motion.
3. The truncated Dirichlet process.

The objective is to match as closely as possible the distribution of the option price under an exponential random walk model by that generated by the exponential Brownian motion and the predicted Dirichlet process sampling procedures. The performance of the Dirichlet process estimation method is assessed by a comparison with exponential Brownian motion, using criteria such as histograms and quantile-quantile plots (qq-plots) of the predicted stock prices and their corresponding option prices, histograms

of the residuals, and sum of squared errors (SSE). The mean option prices and their estimated standard deviations are also compared for each method.

We begin by discussing the methodology used to construct a random sample of stock prices based on an exponential random walk model, and then describe each of the three simulation procedures. For the predicted Dirichlet process simulation, we first consider the special case where the expiration date is one period ahead and then generalize our results to farther horizons. The general case is conducted under the assumption that the prior distribution of a stock return follows a $DP(\alpha H)$, and thus its posterior distribution given the observed sample is a $DP\left(\alpha H + \sum_1^t \delta_{Y_i}\right)$.

Throughout Chapters 4 and 5, we will use the following notation:

X_t	is the cumulative stock return between times 0 and t,
$Y_1, \ldots, Y_t$	are the observed stock returns up to time t,
$\hat{Y}_{t+1}, \ldots, \hat{Y}_T$	are a sequence of stock returns predicted using one of the simulation methods for times $t+1 \ldots, T$,
$S_0, \ldots, S_t$	are the observed stock prices up to time t,
$\hat{S}_{t+1}, \ldots, \hat{S}_T$	are a sequence of predicted stock prices corresponding to $\hat{Y}_{t+1}, \ldots, \hat{Y}_T$ and S_t,
$\hat{C}_t^{(j)}, \hat{P}_t^{(j)}$	are the call and put option prices computed for the j^{th} sample path using one of the simulation methods,
$\hat{c}_t, \hat{p}_t$	are the European call and put option price estimates computed by averaging the option prices obtained for each simulated sample path,
$\hat{c}_t^A, \hat{p}_t^A$	are the Asian call and put option price estimates computed by averaging the option prices obtained for each simulated sample path.

Moreover, the call and put option prices are always computed at time t, with underlying stock S_t, expiration date T, and exercise price K. Note that the dependence of c_t, C_t, p_t, and P_t on the initial history $Y_1, \ldots, Y_t$ is suppressed in the notation. The risk-free interest rate is denoted by r.

4.1 Description of the Methodologies

4.1.1 Exponential Random Walk Model

Construction of the Initial Random Sample

We first describe the construction of a random sample based on an exponential random walk model. Suppose that the cumulative return of a security between times 0 and t is distributed according to a random walk model with drift

$$X_t = \mu + X_{t-1} + \varepsilon_t \quad \text{for } t = 1, 2, \ldots, \tag{4.1}$$

where μ is the drift term and the random errors ε_t are assumed to follow either a normal, heavy-tailed, or chi-square distribution. Then, the rate of return for period t is given by

$$Y_t = X_t - X_{t-1} = \mu + \varepsilon_t. \tag{4.2}$$

A series of stock returns $Y_1, \ldots, Y_t$ is built from this model by simulating the random errors ε_t. The corresponding stock prices $S_0, \ldots, S_t$ are then calculated using the relationship $S_t = S_{t-1}e^{Y_t}$.

Simulation of the Future Stock Prices

Given the observed stock prices $S_0, \ldots, S_t$ (and stock returns $Y_1, \ldots, Y_t$), we wish to compute the price at time t of a European call option with underlying security S_t, expiration date T, and exercise price K.

This is achieved by performing a Monte Carlo simulation of the future option prices based on the exponential random walk model. First, we generate m different random paths for the stock price over the life of the option by projecting (4.1) between times t and T. The option price for each sample path is then calculated using

$$\hat{C}_t^{(j)} = e^{-r(T-t)} \max\left(\hat{S}_T^{(j)} - K, 0\right),$$

where $\hat{S}_T^{(j)}$ is the predicted stock price at time T for the j^{th} path produced by the simulation. The mean option price is found by averaging the predicted option prices

over the number of sample paths considered using

$$\hat{c}_t = \frac{\hat{C}_t^{(1)} + \cdots + \hat{C}_t^{(m)}}{m}.$$

The complete algorithm for the Monte Carlo simulation of the exponential random walk model is as follows:[1]

A. Simulate a future stock return $\hat{Y}_{t+i}$:

   1. Simulate the residuals using one of the following models:
      (a) $\varepsilon_{t+i} \sim N(0, \sigma^2)$.
      (b) $\varepsilon_{t+i} \sim S_\alpha(\sigma, 0, 0)$, where $S_\alpha(\sigma, \beta, 0)$ denotes the symmetric stable distribution with index α, scale parameter σ, skewness parameter β, and shift parameter μ.
      (c) $\varepsilon_{t+i} \sim \chi^2(p) - p$, where $\chi^2(p) - p$ denotes the centred chi-square distribution with p degrees of freedom.
   2. Compute the simulated stock return $\hat{Y}_{t+i} = \mu + \varepsilon_{t+i}$.

B. Simulate the future stock returns $\hat{Y}_{t+1}, \ldots, \hat{Y}_T$:

   1. Repeat step A for $i = 1, \ldots, T-t$.
   2. Compute the future stock price $\hat{S}_T = S_t e^{\hat{Y}_{t+1} + \cdots + \hat{Y}_T}$.

C. Repeat steps A–B for $j = 1, \ldots, m$ to obtain $\hat{S}_T^{(1)}, \ldots, \hat{S}_T^{(m)}$.

D. Compute the corresponding option prices $\hat{C}_t^{(1)}, \ldots, \hat{C}_t^{(m)}$ and $\hat{P}_t^{(1)}, \ldots, \hat{P}_t^{(m)}$:

   1. Call: $\hat{C}_t^{(j)} = e^{-r(T-t)} \max\left(\hat{S}_T^{(j)} - K, 0\right)$.
   2. Put: $\hat{P}_t^{(j)} = e^{-r(T-t)} \max\left(K - \hat{S}_T^{(j)}, 0\right)$.

E. Compute the mean option prices $\hat{c}_t$ and $\hat{p}_t$:

   1. Call: $\hat{c}_t = \frac{\hat{C}_t^{(1)} + \cdots + \hat{C}_t^{(m)}}{m}$.
   2. Put: $\hat{p}_t = \frac{\hat{P}_t^{(1)} + \cdots + \hat{P}_t^{(m)}}{m}$.

[1] A S-PLUS program of this simulation algorithm is provided in Appendix C.

4.1.2 Exponential Brownian Motion Sampling

Like the exponential random walk model, the exponential Brownian motion sampling procedure is built using a Monte Carlo simulation of the future given the observed stock prices $S_0, \ldots, S_t$. However, instead of computing the future stock prices using (4.1) or (4.2), we use the following process

$$\hat{S}_{t+1} = S_t e^{\left(\hat{\mu} - \frac{\hat{\sigma}^2}{2}\right) + \hat{\sigma} W_1}, \tag{4.3}$$

where $\hat{\mu}$ and $\hat{\sigma}$ are the estimated return and volatility of the stock returns $Y_1, \ldots, Y_t$, and W_t is the Brownian motion process.

To prevent arbitrage, the analysis is performed assuming risk-neutral valuation. In a risk-neutral environment, the expected return on any security is the risk-free rate r and thus (4.3) becomes

$$\hat{S}_{t+1} = S_t e^{\left(r - \frac{\hat{\sigma}^2}{2}\right) + \hat{\sigma} W_1}.$$

In practice, the risk-free interest rate r is estimated by the yield of a government bond with the same maturity as the option.

The following algorithm describes the detailed methodology used to simulate option prices from exponential Brownian motion:[2]

A. Simulate a future stock return $\hat{Y}_{t+i}$:

   1. Simulate $\hat{z}_{t+i} \sim N(0, \hat{\sigma}^2)$.
   2. Compute the simulated stock return $\hat{Y}_{t+i} = \left(r - \frac{\hat{\sigma}^2}{2}\right) + \hat{z}_{t+i}$.

B. Simulate the future stock returns $\hat{Y}_{t+1}, \ldots, \hat{Y}_T$:

   1. Repeat step A for $i = 1, \ldots, T - t$.
   2. Compute the future stock price $\hat{S}_T = S_t e^{\hat{Y}_{t+1} + \cdots + \hat{Y}_T}$.

C. Repeat steps A–B for $j = 1, \ldots, m$ to obtain $\hat{S}_T^{(1)}, \ldots, \hat{S}_T^{(m)}$.

[2]Consult Appendix C for a S-PLUS program of this algorithm.

D. Compute the corresponding option prices $\hat{C}_t^{(1)}, \ldots, \hat{C}_t^{(m)}$ and $\hat{P}_t^{(1)}, \ldots, \hat{P}_t^{(m)}$:

1. Call: $\hat{C}_t^{(j)} = e^{-r(T-t)} \max\left(\hat{S}_T^{(j)} - K, 0\right)$.
2. Put: $\hat{P}_t^{(j)} = e^{-r(T-t)} \max\left(K - \hat{S}_T^{(j)}, 0\right)$.

E. Compute the mean option prices $\hat{c}_t$ and $\hat{p}_t$:

1. Call: $\hat{c}_t = \frac{\hat{C}_t^{(1)} + \cdots + \hat{C}_t^{(m)}}{m}$.
2. Put: $\hat{p}_t = \frac{\hat{P}_t^{(1)} + \cdots + \hat{P}_t^{(m)}}{m}$.

4.1.3 Predicted Dirichlet Process Sampling for $T = t + 1$

We now discuss a similar methodology based on the Dirichlet process. Let us first consider the special case of a European call option whose expiration date is only one period ahead ($T = t+1$). In Section 3.5, we found that if the prior distribution of the underlying stock returns is a $DP(\alpha H)$, then the analytical expression for this option price is

$$\begin{aligned} c_t &= e^{-r}\left[w_t \int_{\log(K/S_t)}^{\infty} \left(S_t e^{y_{t+1}} - K\right) dH\left(y_{t+1}\right)\right. \\ &\quad \left. + (1 - w_t)\left(\frac{1}{t}\right) \sum_{i=1}^{t} \max\left(S_t e^{y_i} - K, 0\right)\right], \end{aligned}$$

where

$$w_t = \frac{\alpha}{\alpha + t}.$$

A Dirichlet process sampling procedure for estimating this mean option price can be constructed using a Monte Carlo simulation of the future given the observed stock returns $Y_1, \ldots, Y_t$. Because the prior distribution of the stock returns is assumed to be $DP(\alpha H)$, then we know that the posterior distribution of Y_T given $Y_1, \ldots, Y_t$ can be drawn from a $DP\left(\alpha H + \sum_1^t \delta_{Y_i}\right)$.

Assuming risk-neutral valuation, the simulation is performed using the following process

$$\hat{S}_{t+1} = S_t e^{\left(r - \frac{\hat{\sigma}^2}{2}\right) + \hat{\sigma} G_t}, \tag{4.4}$$

where r is the risk-free rate modelled by the yield of a government bond, $\hat{\sigma}$ is the sample standard deviation of $Y_1, \ldots, Y_t$, and G_t is a stochastic variable drawn from $\mathcal{P} \in DP\left(\alpha H + \sum_1^t \delta_{Y_i}\right)$, with $\mathcal{P}$ approximated by the truncated Dirichlet process described in Section 3.3.2. We use the stick-breaking approach to obtain

$$\mathcal{P}_N(\cdot) = \sum_{k=1}^{N} v_k \delta_{Z_k}(\cdot),$$

where

$$v_k = \begin{cases} V_1 & \text{if } k = 1, \\ (1 - V_1)(1 - V_2)\ldots(1 - V_{k-1})\, V_k & \text{if } k = 2, 3, \ldots, N. \end{cases}$$

The reason behind using the truncated process is motivated by the fact that the real Dirichlet process has an infinite sum and seems impossible to simulate exactly. As mentioned in Section 3.3.2, this truncation provides an excellent approximation to the Dirichlet process.

The first step of the procedure is to sample a random path for the future stock price $\hat{Y}_{t+1}$ by drawing an observation from the truncated Dirichlet process $\mathcal{P}_N$. Using the stick-breaking approach, we simulate the random variables $V_1, \ldots, V_N$ and $Z_1, \ldots, Z_N$, where $V_k \sim Be(1, \alpha + t)$ and $Z_k \sim \left(w_t H + (1 - w_t)\frac{1}{t}\sum_1^t \delta_{Y_i}\right)$. Thus, Z_k is drawn from the distribution H with probability w_t, or from F_t with probability $1 - w_t$. The value of N is chosen using Muliere and Tardella's [29] random stopping rule

$$N_\epsilon = \inf\left\{k : (1 - V_1)(1 - V_2)\ldots(1 - V_{k-1})\, V_k < \epsilon\right\}. \tag{4.5}$$

The next step is to calculate the option price estimate, which is achieved by repeating this methodology m times and then computing the sample mean of the option prices obtained for each sample path. The detailed algorithm is as follows:

A. Simulate a future stock return $\hat{Y}_{t+1}$:

1. Simulate the truncated Dirichlet process $\mathcal{P}_N$:

   (a) Simulate $V_k \sim Be(1, \alpha + t)$.

(b) Compute the random weights:

$$v_k = \begin{cases} V_1 & \text{if } k = 1, \\ (1 - V_1)(1 - V_2)\dots(1 - V_{k-1})V_k & \text{if } k = 2, 3, \dots . \end{cases}$$

(c) Simulate Z_k by drawing an observation from H with probability w_t, or from F_t with probability $1 - w_t$.

(d) Repeat steps (a)–(c) for $k = 1, 2, \dots$, as long as $v_k > \epsilon$.

2. Simulate the future stock return $\hat{Y}_{t+1}$ using the $\mathcal{P}_N$ fixed in 1:

(a) Simulate $u \sim U(0, 1)$.

(b) Compute the simulated stock return $\hat{Y}_{t+1}$:

$$\hat{Y}_{t+1} = \left(r - \frac{\hat{\sigma}^2}{2}\right) + \sum_{k=1}^{N} Z_k I\left(\sum_{j=1}^{k-1} v_j < u \leq \sum_{j=1}^{k} v_j\right).$$

B. Compute the future stock price $\hat{S}_{t+1} = S_t e^{\hat{Y}_{t+1}}$.

C. Repeat steps A–B for $j = 1, \dots, m$ to obtain $\hat{S}_{t+1}^{(1)}, \dots, \hat{S}_{t+1}^{(m)}$.

D. Compute the corresponding option prices $\hat{C}_t^{(1)}, \dots, \hat{C}_t^{(m)}$ and $\hat{P}_t^{(1)}, \dots, \hat{P}_t^{(m)}$:

1. Call: $\hat{C}_t^{(j)} = e^{-r} \max\left(\hat{S}_{t+1}^{(j)} - K, 0\right)$.

2. Put: $\hat{P}_t^{(j)} = e^{-r} \max\left(K - \hat{S}_{t+1}^{(j)}, 0\right)$.

E. Compute the mean option prices $\hat{c}_t$ and $\hat{p}_t$:

1. Call: $\hat{c}_t = \frac{\hat{C}_t^{(1)} + \dots + \hat{C}_t^{(m)}}{m}$.

2. Put: $\hat{p}_t = \frac{\hat{P}_t^{(1)} + \dots + \hat{P}_t^{(m)}}{m}$.

4.1.4 Predicted Dirichlet Process Sampling for all T

Let us now consider the general case where $T \geq t + 1$. In Section 3.5, we developed the analytical expressions associated with the predicted Dirichlet process method under the assumptions that the future conditional distribution of a stock return does

not change over time, and that it follows a $DP\left(\alpha H + \sum_1^t \delta_{Y_i}\right)$. We now discuss the implementation of this method using the same hypothesis.

The algorithm for the general case is a simple generalization of the single-period algorithm described in Section 4.1.3. In fact, because every stock return is predicted using the same distribution, the only additional step is to rerun the single-period algorithm $T-t-1$ times to obtain the predictions for the stock returns $\hat{Y}_{t+2}, \ldots, \hat{Y}_T$ and their corresponding stock prices $\hat{S}_{t+2}, \ldots, \hat{S}_T$. European option prices are then computed by plugging the results into the appropriate equations. The complete algorithm is as follows:[3]

A. Simulate a future stock return $\hat{Y}_{t+i}$:

1. Simulate the truncated Dirichlet process $\mathcal{P}_N$:
   (a) Simulate $V_k \sim Be(1, \alpha + t)$.
   (b) Compute the random weights:
   $$v_k = \begin{cases} V_1 & \text{if } k = 1, \\ (1 - V_1)(1 - V_2)\ldots(1 - V_{k-1})\, V_k & \text{if } k = 2, 3, \ldots. \end{cases}$$
   (c) Simulate Z_k by drawing an observation from H with probability w_t, or from F_t with probability $1 - w_t$.
   (d) Repeat steps (a)–(c) for $k = 1, 2, \ldots$, as long as $v_k > \varepsilon$.
2. Simulate the future stock return $\hat{Y}_{t+i}$ using the $\mathcal{P}_N$ fixed in 1:
   (a) Simulate $u \sim U(0, 1)$.
   (b) Compute the simulated stock return $\hat{Y}_{t+i}$:
   $$\hat{Y}_{t+i} = \left(r - \frac{\hat{\sigma}^2}{2}\right) + \sum_{k=1}^{N} Z_k I\left(\sum_{j=1}^{k-1} v_j < u \leq \sum_{j=1}^{k} v_j\right).$$

B. Simulate the future stock returns $\hat{Y}_{t+1}, \ldots, \hat{Y}_T$:

1. Repeat step A for $i = 1, \ldots, T - t$.

[3] A S-PLUS program of this simulation algorithm is provided in Appendix C.

2. Compute the future stock price $\hat{S}_T = S_t e^{\hat{Y}_{t+1}+\cdots+\hat{Y}_T}$.

C. Repeat steps A–B for $j = 1, \ldots, m$ to obtain $\hat{S}_T^{(1)}, \ldots, \hat{S}_T^{(m)}$.

D. Compute the corresponding option prices $\hat{C}_t^{(1)}, \ldots, \hat{C}_t^{(m)}$ and $\hat{P}_t^{(1)}, \ldots, \hat{P}_t^{(m)}$:

1. Call: $\hat{C}_t^{(j)} = e^{-r(T-t)} \max\left(\hat{S}_T^{(j)} - K, 0\right)$.
2. Put: $\hat{P}_t^{(j)} = e^{-r(T-t)} \max\left(K - \hat{S}_T^{(j)}, 0\right)$.

E. Compute the mean option prices $\hat{c}_t$ and $\hat{p}_t$:

1. Call: $\hat{c}_t = \frac{\hat{C}_t^{(1)}+\cdots+\hat{C}_t^{(m)}}{m}$.
2. Put: $\hat{p}_t = \frac{\hat{P}_t^{(1)}+\cdots+\hat{P}_t^{(m)}}{m}$.

The asymptotic consistency of this simulation algorithm follows from Theorem 3.3 and the convergence of the empirical cumulative distribution function to F.

4.2 Application to Option Pricing

4.2.1 European Option Pricing with $t = 60$ and $T = 72$

This section presents some results obtained with the sampling procedures described in Section 4.1. The first analysis was conducted using a random sample of 61 monthly stock prices that were simulated from an exponential random walk model with drift term $\mu = 0.01$. Errors in the random walk model were assumed to be i.i.d. $N\left(0, (0.04)^2\right)$ random variables. The price behaviour of this model over the time period considered is illustrated in Figures 4.1 and 4.2.[4]

[4]The complete data set is provided in Appendix D.

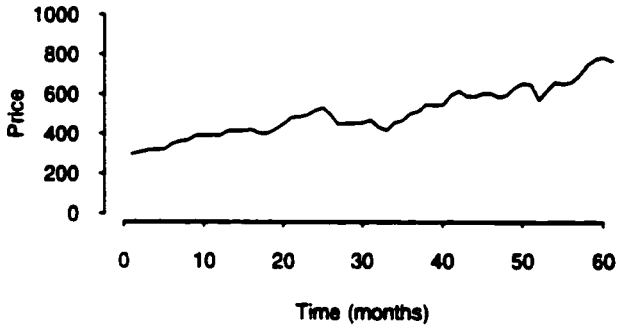

Figure 4.1: Prices from an exponential random walk model $S_t = S_{t-1}e^{Y_t}$, where $Y_t = 0.01 + \varepsilon_t$ and $\varepsilon_t \sim N\left(0, (0.04)^2\right)$. The initial value was set to $S_0 = 300$.

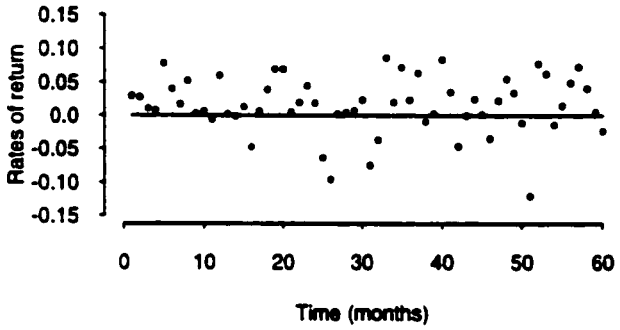

Figure 4.2: Rates of return $Y_1, \ldots, Y_{60}$ from an exponential random walk model $S_t = S_{t-1}e^{Y_t}$, where $Y_t = 0.01 + \varepsilon_t$ and $\varepsilon_t \sim N\left(0, (0.04)^2\right)$.

Given these observed stock prices $S_0, \ldots, S_{60}$ (and stock returns $Y_1, \ldots, Y_{60}$), the Monte Carlo simulations of the future were performed using the exponential random walk, the exponential Brownian motion, and the predicted Dirichlet process procedures described in Section 4.1. All three approaches were conducted under the risk-neutral valuation assumption, with $r = 0.005$ per month.

For the exponential Brownian motion simulation, the predicted stock prices were

computed using process (4.3) with $r = 0.005$ and $\hat{\sigma}$ equal to the sample standard deviation of $Y_1, \ldots, Y_{60}$, which was found to be $\hat{\sigma} = 0.04273449$.

The predicted Dirichlet process simulation was implemented using process (4.4), also with $r = 0.005$ and $\hat{\sigma} = 0.04273449$. For the parameter α, we picked a value of $\alpha = 6$ so that the predicted stock returns are drawn from the distribution $H \sim N(0, \hat{\sigma}^2)$ with probability $w_{60} = 6/(6 + 60) = 1/11$, or from the random sample $Y_1, \ldots, Y_{60}$ with probability $1 - w_{60} = 10/11$. When sampling from the random sample $Y_1, \ldots, Y_{60}$, each observation was assigned an equal probability $1/60$.

As for the exponential random walk simulation, it was performed using drift term $\mu = r = 0.005$ and normal residuals with mean 0 and standard deviation $\sigma = 0.04$. This revised drift for the future observations of the exponential random walk model was chosen to be consistent with the exponential Brownian motion and the predicted Dirichlet process simulations, which were performed under the risk-neutral assumption. In fact, because the residuals are normally distributed, the only difference between the exponential random walk and the exponential Brownian motion simulations lies in the value chosen for the volatility parameter σ. For the random walk model, we use $\sigma = 0.04$, while for the Brownian motion, we use the sample estimate $\hat{\sigma} = 0.04273449$. Nevertheless, these methods will be treated separately since their resemblance is particular to this example. Later analyses will demonstrate the difference between these two approaches when the residuals are assumed to follow a non-normal distribution.

The algorithms were implemented using S-PLUS 5.0.[5] Each model was programmed to compute 1,000 stock price predictions for each time subinterval.

Figure 4.3 shows the conditional empirical distribution of $\hat{S}_{72}$ given $S_0, \ldots, S_{60}$ for each of the three sampling methods. On each graph, it appears that the empirical distribution obtained from the simulation is very close to the actual conditional distribution of $S_{72} \mid S_0, \ldots, S_{60}$, which is represented by the solid curve.

This fact should not be surprising since $S_{72} \mid S_0, \ldots, S_{60}$ is normally distributed and all three simulation procedures were performed using normal draws. The exponential random walk sampling used a $N(0, \sigma^2)$, the exponential Brownian motion used

[5]The simulation programs are provided in Appendix C.

a $N(0, \hat{\sigma}^2)$, and the mean of the posterior distribution used to generate the predicted Dirichlet process observations was a mixture of a normal distribution $N(0, \hat{\sigma}^2)$ and the empirical process based on $Y_1, \ldots, Y_{60}$, a random sample drawn from a normal distribution.

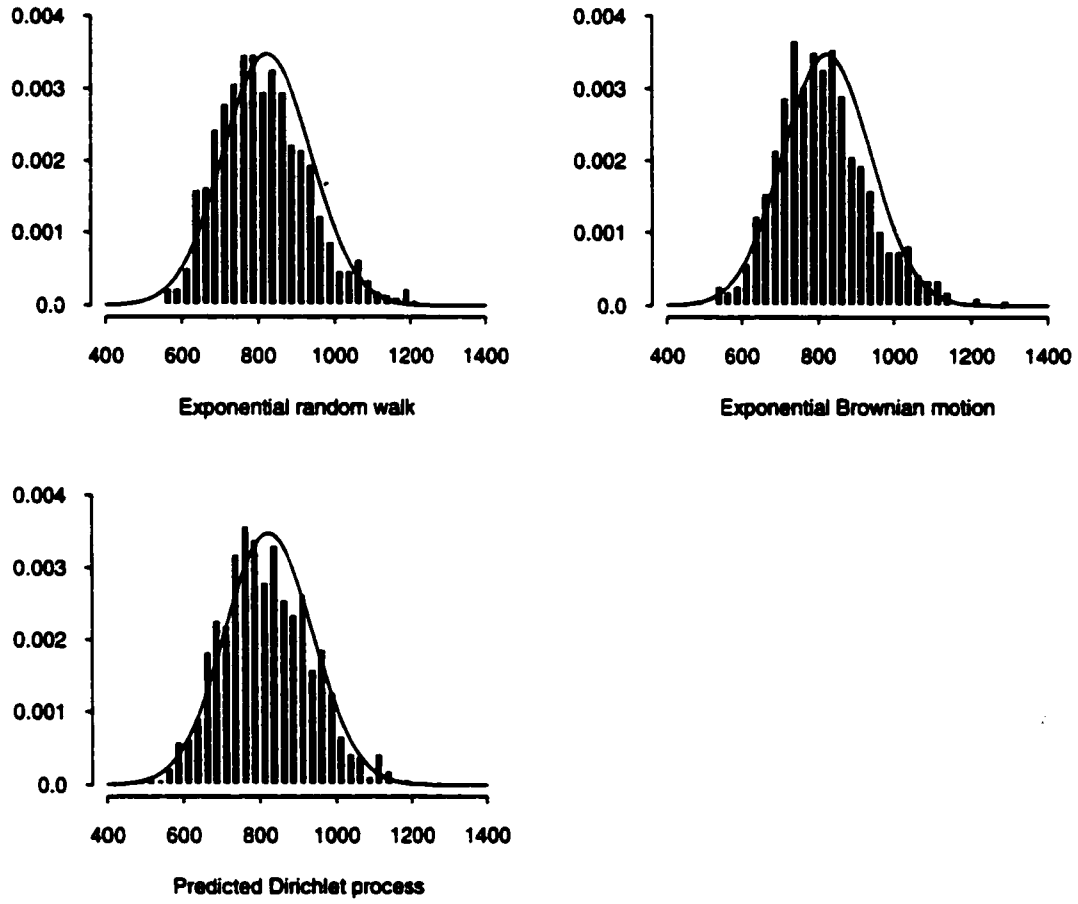

Figure 4.3: Empirical distributions of $\hat{S}_{72} \mid S_0, \ldots, S_{60}$ for 1,000 simulations of the exponential random walk, the exponential Brownian motion, and the predicted Dirichlet process procedures. The solid curve on each graph represents the actual conditional distribution of $S_{72} \mid S_0, \ldots, S_{60}$.

The plot of the quantiles of the exponential Brownian motion versus those obtained using the predicted Dirichlet process method is illustrated in Figure 4.4. Because this qqplot shows a relatively straight line, we can conclude normality of the predicted Dirichlet process observations.

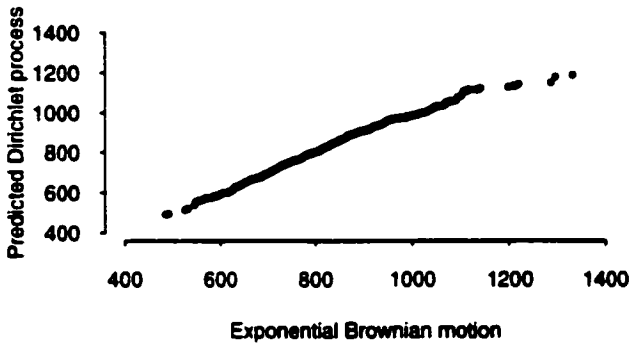

Figure 4.4: Qqplot of $\hat{S}_{72} \mid S_0, \ldots, S_{60}$ for 1,000 simulations of the exponential Brownian motion and the predicted Dirichlet process procedures.

Figure 4.5 displays the empirical distributions of the residuals obtained for the exponential Brownian motion and the predicted Dirichlet process procedures. These distributions were computed with respect to a particular sample path of the exponential random walk model. Note that both distributions are normal and centred around a positive mean: 43.02 for the exponential Brownian motion and 44.35 for the predicted Dirichlet process. These positive means were observed because both the Brownian motion and the Dirichlet process simulations outgrew the random walk model for this sample path. This fact however is negligible since our objective is not to fit the best model to the exponential random walk data, but to calculate option prices. Under risk-neutral valuation, the actual growth incurred by the stock price does not matter, only the expected growth rate must be considered. The SSE's computed for this sample path were 16,765,471 for exponential Brownian motion against 15,926,503 for the predicted Dirichlet process.

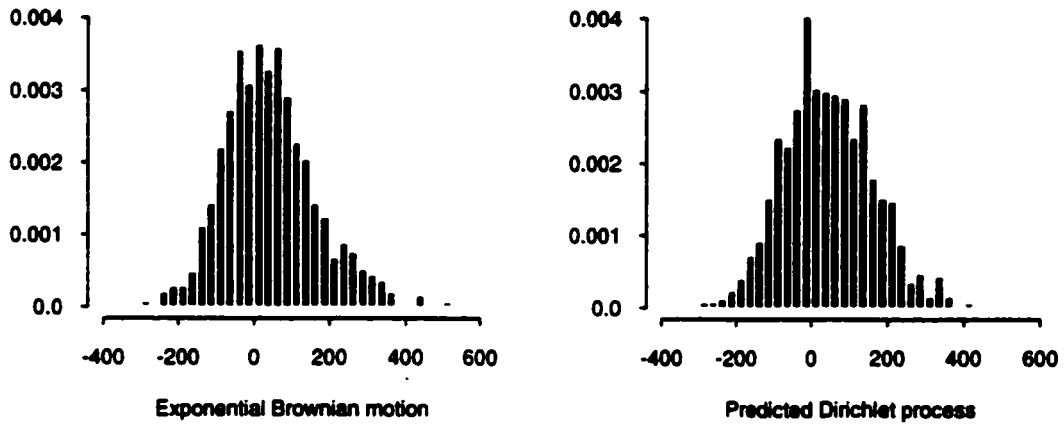

Figure 4.5: Empirical distributions of $\left(\hat{S}_{72} - S_{72}\right) \mid S_0, \ldots, S_{60}$ for one sample path of the exponential random walk model, based on 1,000 simulations.

We now use this information to compute the price at time $t = 60$ of European call and put options with expiration date $T = 72$ and exercise price $K = 800$. The empirical distributions of these option prices are shown for each simulation procedure in Figures 4.6 and 4.7. Note that these histograms represent the distributions of the non-zero values of the option prices. Figures 4.8 and 4.9 display the qqplots of the option prices for exponential Brownian motion and the predicted Dirichlet process methods. The mean option prices and their estimated standard deviations are displayed in Table 4.1, along with the option prices calculated using the Black-Scholes formula described in Section 2.4.

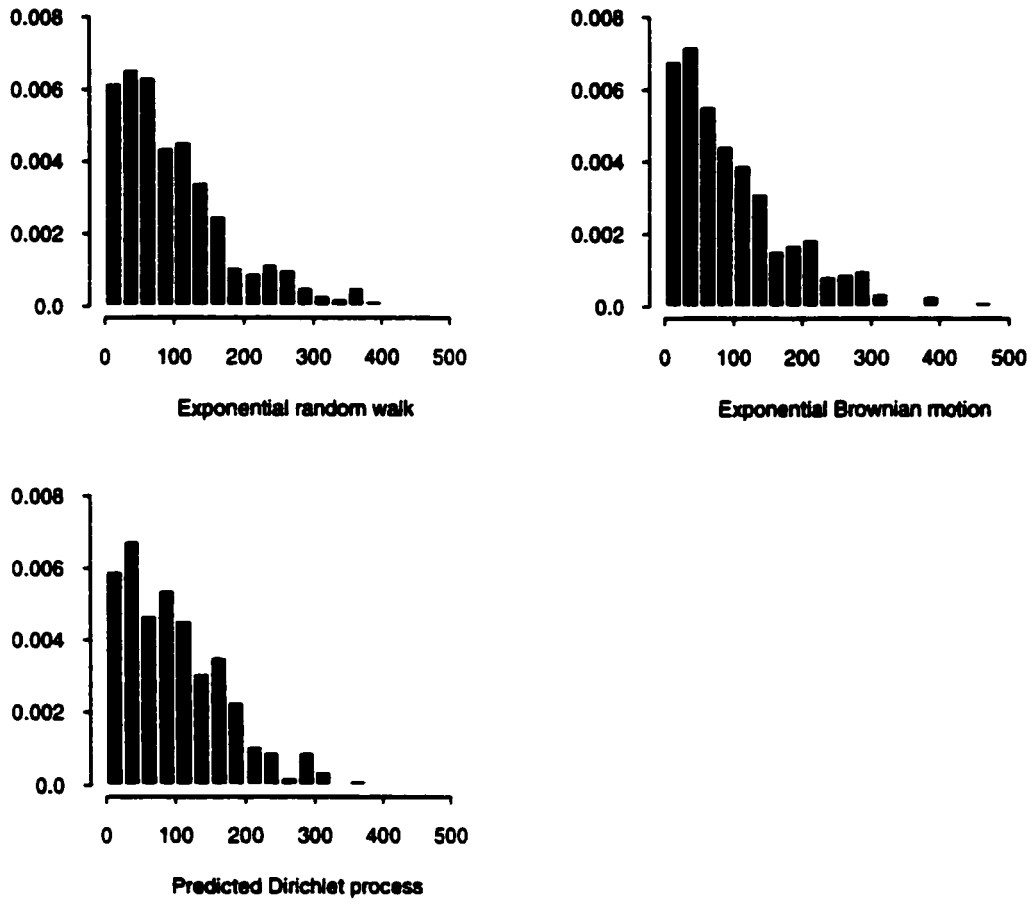

Figure 4.6: Empirical distributions for 1,000 simulations of a European call $\hat{c}_{60}$, with expiration date $T = 72$, exercise price $K = 800$, and underlying stock based on an exponential random walk model with normal residuals. Zero values were suppressed in the figures: 489 for the exponential random walk and the exponential Brownian motion, and 480 for the predicted Dirichlet process.

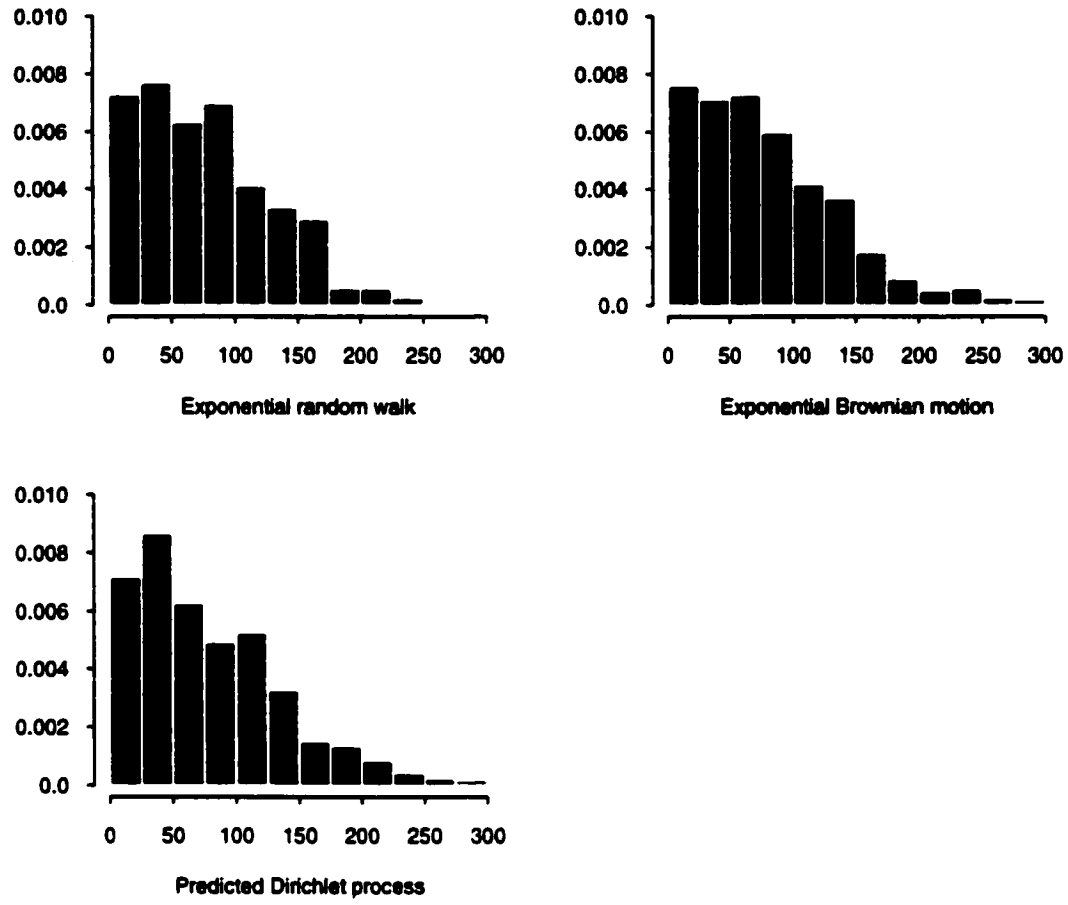

Figure 4.7: Empirical distributions for 1,000 simulations of a European put $\hat{p}_{60}$, with expiration date $T = 72$, exercise price $K = 800$, and underlying stock based on an exponential random walk model with normal residuals. Zero values were suppressed in the figures: 511 for the exponential random walk and the exponential Brownian motion, and 520 for the predicted Dirichlet process.

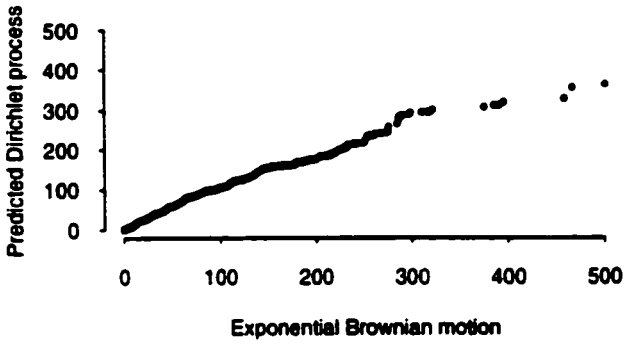

Figure 4.8: Qqplot of $\hat{c}_{60}$ for 1,000 simulations of the exponential Brownian motion and the predicted Dirichlet process procedures, with $T = 72$, $K = 800$, and underlying stock based on an exponential random walk model with normal residuals.

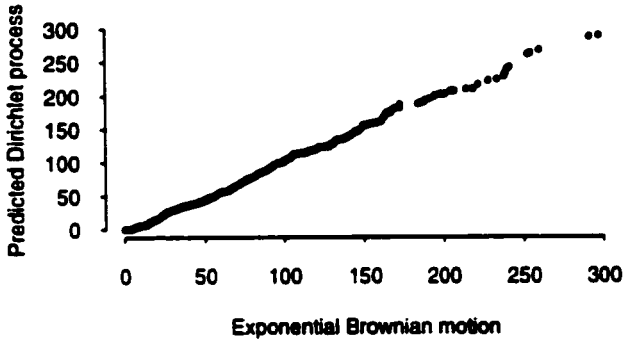

Figure 4.9: Qqplot of $\hat{p}_{60}$ for 1,000 simulations of the exponential Brownian motion and the predicted Dirichlet process procedures, with $T = 72$, $K = 800$, and underlying stock based on an exponential random walk model with normal residuals.

	$\hat{c}_{60}$		$\hat{p}_{60}$	
Prediction method	Mean	Std.dev.	Mean	Std.dev.
Exponential random walk	51.48	77.18	37.31	52.69
Exponential Brownian motion	51.25	78.96	38.19	55.57
Predicted Dirichlet process	51.94	72.89	37.62	56.29
Black-Scholes formula	52.55	–	37.97	–

Table 4.1: Mean prices and estimated standard deviations for 1,000 simulations of a European call $\hat{c}_{60}$ and a European put $\hat{p}_{60}$, both with expiration date $T = 72$, exercise price $K = 800$, and underlying stock based on an exponential random walk model with normal residuals.

According to Table 4.1, all three sampling methods produced option price estimates relatively close to those obtained with the Black-Scholes formula. The predicted Dirichlet process method provided the most accurate estimate of the Black-Scholes call option price and also a very good estimate of the Black-Scholes put option price.

Except for the Brownian motion put, all the option prices obtained via simulations are inferior to the Black-Scholes option prices. However, the differences are not significant and there is no other obvious explanation for this underestimation than the randomness of the simulations.

Moreover, because the estimated standard deviations lie in the same range, we can assume that the three sampling procedures contain the same risk. Consequently, there is no increased risk of overstating or understating the true price of an option when using any of the simulation methods discussed in this example.

The results obtained from this analysis lead to the conclusion that the predicted Dirichlet process simulation is an effective option pricing procedure. In fact, the methodology is not only valuable for this particular case, but also in general. Additional simulations using the same hypotheses and different random samples of the same length demonstrated the repeated effectiveness of the predicted Dirichlet process method.

4.2.2 European Option Pricing with $t = 120$ and $T = 132$

Let us now consider the pricing at time $t = 120$ of a European option expiring twelve months later at time $T = 132$. This example is analogous to the one described in Section 4.2.1, with the exception that initial random sample has now doubled in size. We assume once again that the exponential random walk model has a drift term $\mu = 0.01$ and normally distributed errors with mean 0 and standard deviation $\sigma = 0.04$.

The price pattern of the data set is displayed in Figures 4.10 and 4.11.[6] In this example, the exponential Brownian motion observations were drawn from a $N(0, \hat{\sigma}^2)$, with $\hat{\sigma}$ now equal to the sample standard deviation of $Y_1, \ldots, Y_{120}$, i.e. $\hat{\sigma} = 0.04033019$. As for the predicted Dirichlet process simulation, it was performed using $\alpha = 6$. The observations were sampled from the distribution $H \sim N(0, \hat{\sigma}^2)$ with probability $w_{120} = 6/(120 + 6) = 1/21$, or from $Y_1, \ldots, Y_{120}$ with probability $1 - w_{120} = 20/21$, where each observation in the random sample was assigned an equal probability $1/120$. Both these simulations were performed under risk-neutral valuation with $r = 0.005$ per month. The exponential random walk observations were sampled using a drift term $\mu = r = 0.005$ and i.i.d. $N\left(0, (0.04)^2\right)$ residuals.

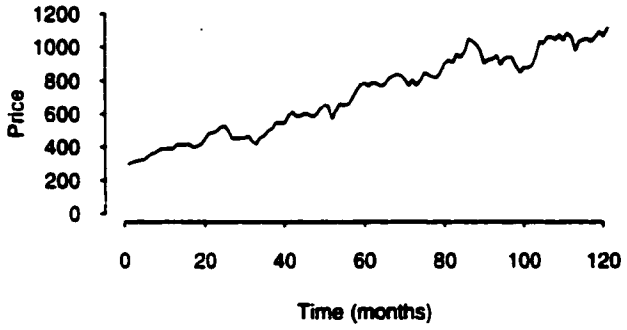

Figure 4.10: Prices from an exponential random walk model $S_t = S_{t-1}e^{Y_t}$, where $Y_t = 0.01 + \varepsilon_t$ and $\varepsilon_t \sim N\left(0, (0.04)^2\right)$. The initial value was set to $S_0 = 300$.

[6]The complete data set is provided in Appendix D.

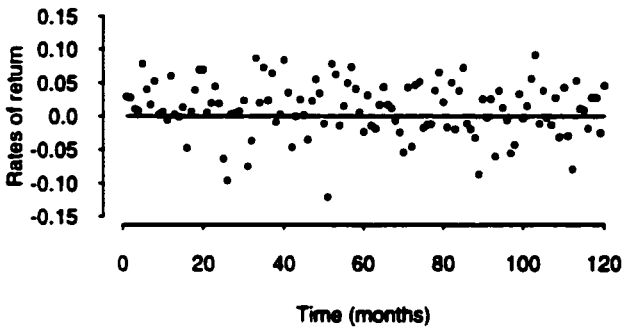

Figure 4.11: Rates of return $Y_1, \ldots, Y_{120}$ from an exponential random walk model $S_t = S_{t-1}e^{Y_t}$, where $Y_t = 0.01 + \varepsilon_t$ and $\varepsilon_t \sim N\left(0, (0.04)^2\right)$.

The conditional empirical distribution of $\hat{S}_{132}$ given the initial sample $S_0, \ldots, S_{120}$ is illustrated for each method in Figure 4.12. Despite a higher peak in the middle of the predicted Dirichlet process histogram, all three empirical distributions present a normal density that is quite representative of the actual conditional distribution of $S_{132} \mid S_0, \ldots, S_{120}$.

As in Section 4.2.1, this normality is due to the fact that the exponential random walk and the exponential Brownian motion simulations were performed using normal draws, and the mean of the posterior distribution used to generate the predicted Dirichlet process observations was a mixture of a normal distribution and the empirical process based on a normal random sample.

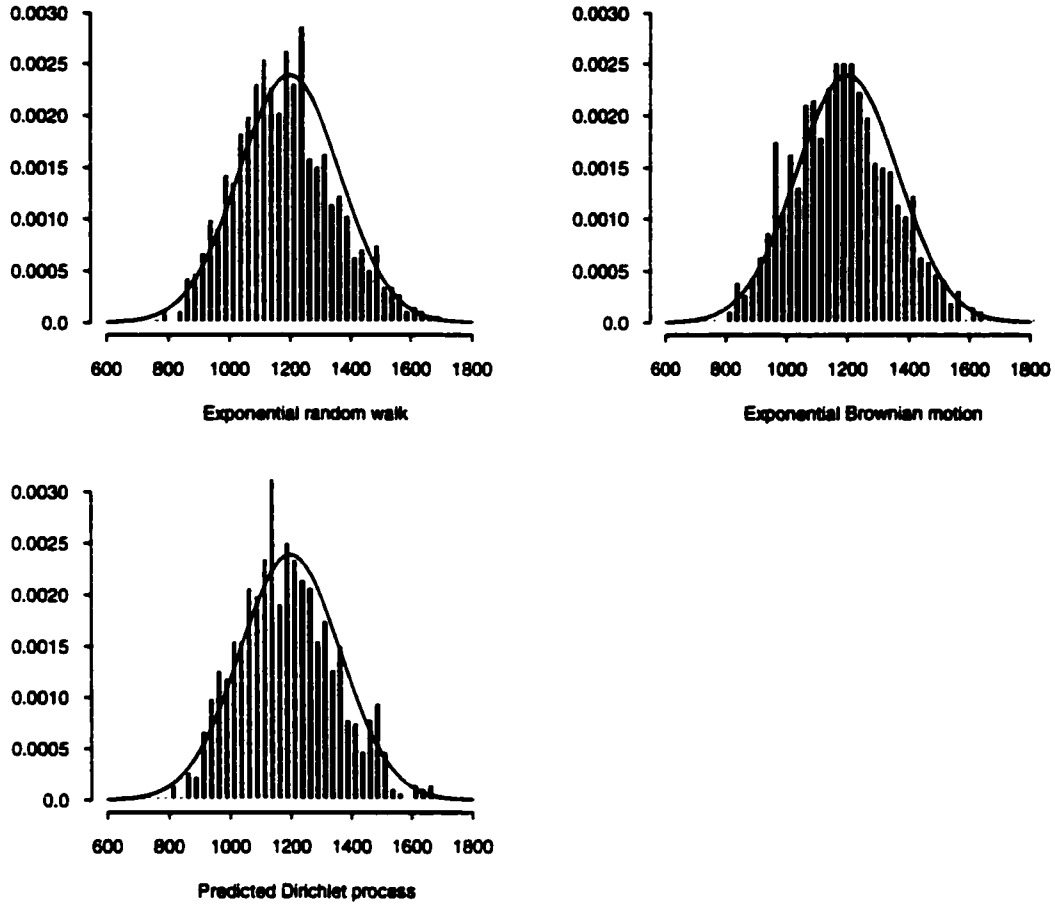

Figure 4.12: Empirical distributions of $\hat{S}_{132} \mid S_0, \ldots, S_{120}$ for 1,000 simulations of the exponential random walk, the exponential Brownian motion, and the predicted Dirichlet process procedures. The solid curve on each graph represents the actual conditional distribution of $S_{132} \mid S_0, \ldots, S_{120}$.

The qqplot of the predicted prices for the exponential Brownian motion and the predicted Dirichlet process methods is shown in Figure 4.13. Again, the straight line formed by the quantiles of these distributions confirms the normality of these methods.

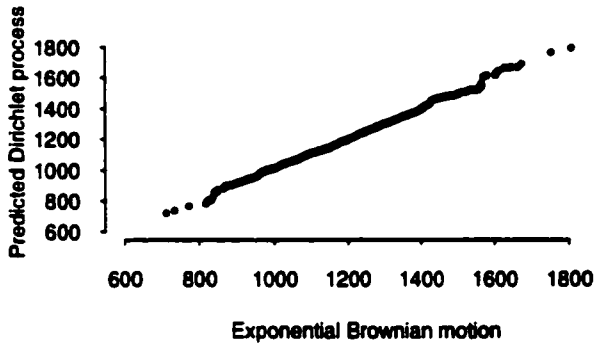

Figure 4.13: Qqplot of $\hat{S}_{132} \mid S_0, \ldots, S_{120}$ for $1,000$ simulations of the exponential Brownian motion and the predicted Dirichlet process procedures.

Figure 4.14 shows the empirical distributions of the residuals with respect to a specific sample path of the exponential random walk model. Note that both histograms have a comparable normal shape. The SSE's computed for this example were higher than for the previous example: $37,855,159$ for exponential Brownian motion versus $37,494,880$ for the predicted Dirichlet process. This slight increase is explained by the greater variability of the initial random sample during the later periods.

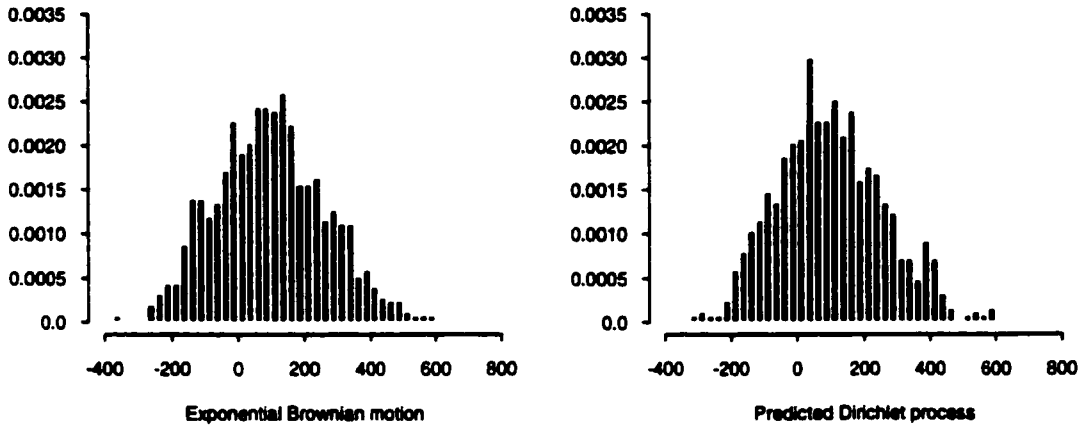

Figure 4.14: Empirical distributions of $\left(\hat{S}_{132} - S_{132}\right) \mid S_0, \ldots, S_{120}$ for one sample path of the exponential random walk model, based on 1,000 simulations.

If we apply these distributions to the pricing of European call and put options, we get the results displayed in Figures 4.15 to 4.18 and Table 4.2. In these figures, the prices are obtained at time $t = 120$ for options with expiration date $T = 132$ and exercise price $K = 1,200$. Figures 4.15 and 4.16 illustrate the empirical distributions obtained for each simulation procedure. The qqplots of these distributions are shown in Figures 4.17 and 4.18, while the mean option prices and their estimated standard deviations are displayed in Table 4.2.

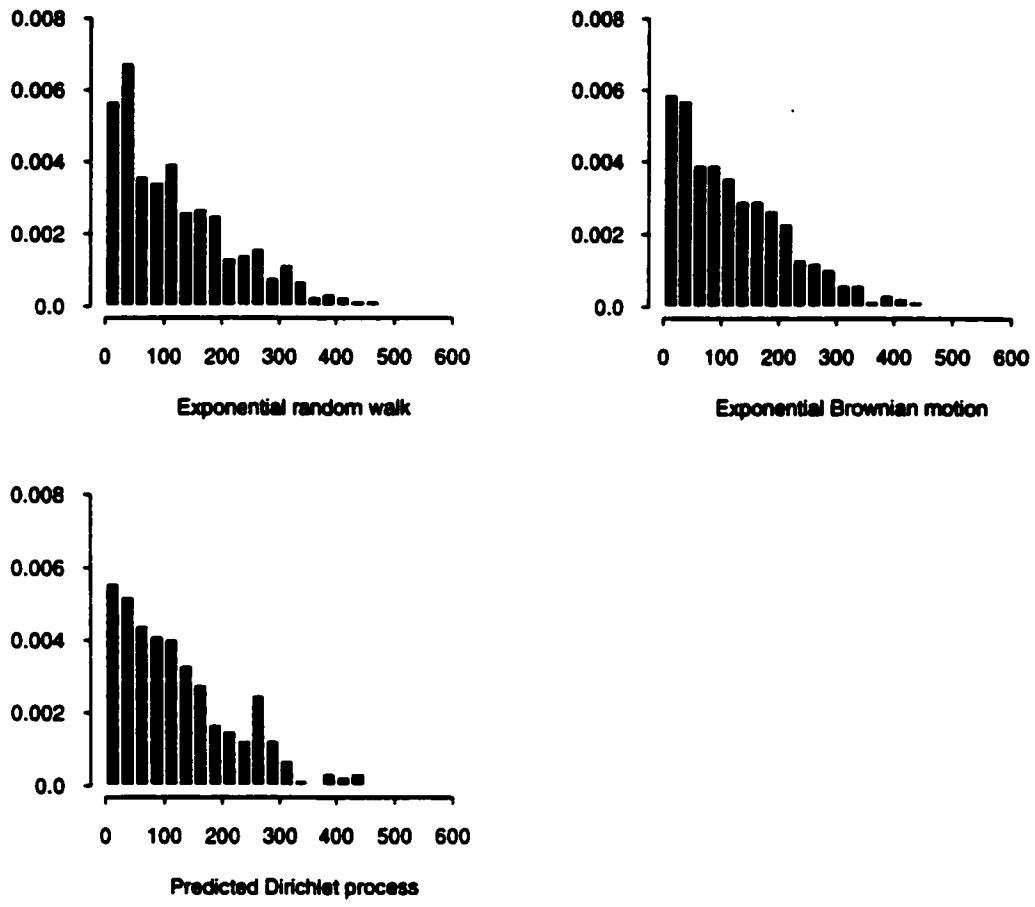

Figure 4.15: Empirical distributions for 1,000 simulations of a European call $\hat{c}_{120}$, with expiration date $T = 132$, exercise price $K = 1,200$, and underlying stock based on an exponential random walk model with normal residuals. Zero values were suppressed in the figures: 557 for the exponential random walk, 552 for the exponential Brownian motion, and 556 for the predicted Dirichlet process.

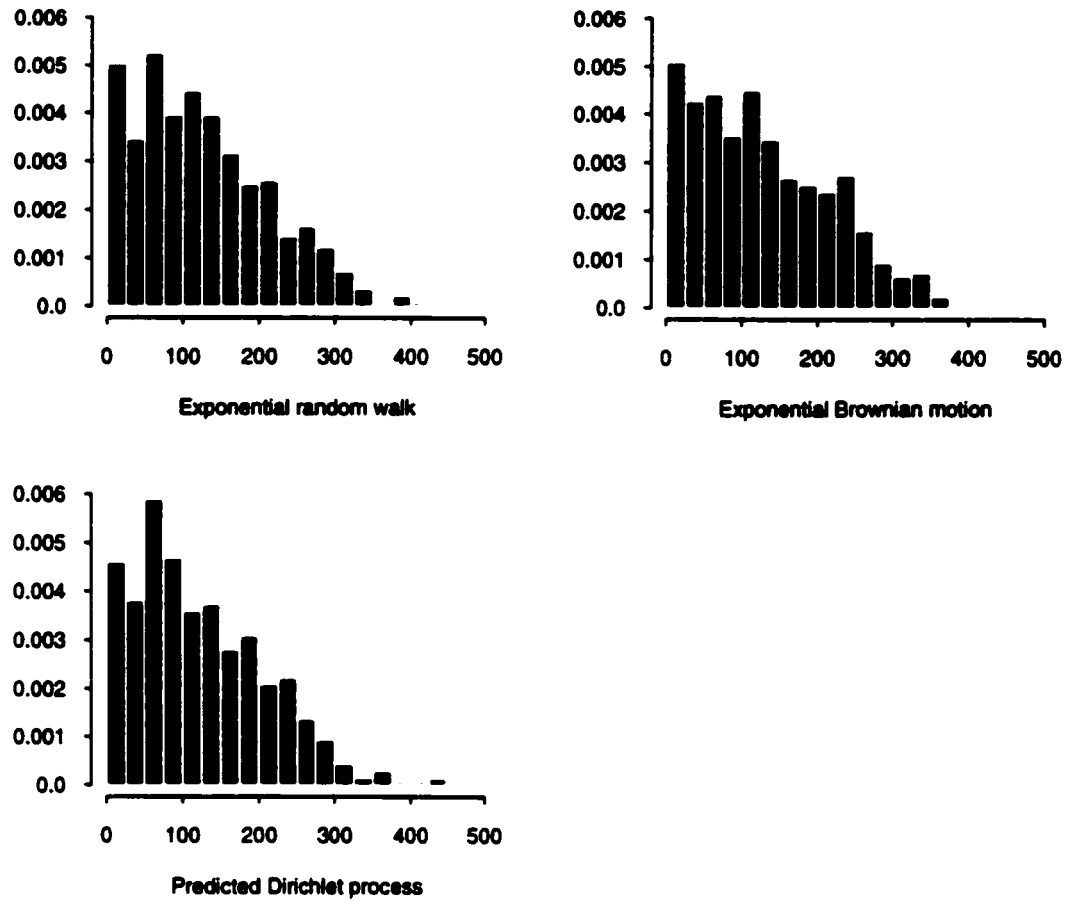

Figure 4.16: Empirical distributions for 1,000 simulations of a European put $\hat{p}_{120}$, with expiration date $T = 132$, exercise price $K = 1,200$, and underlying stock based on an exponential random walk model with normal residuals. Zero values were suppressed in the figures: 443 for the exponential random walk, 448 for the exponential Brownian motion, and 444 for the predicted Dirichlet process.

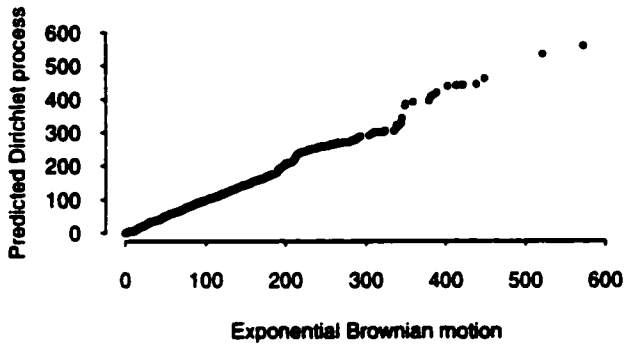

Figure 4.17: Qqplot of $\hat{c}_{120}$ for 1,000 simulations of the exponential Brownian motion and the predicted Dirichlet process procedures, with $T = 132$, $K = 1,200$, and underlying stock based on an exponential random walk model with normal residuals.

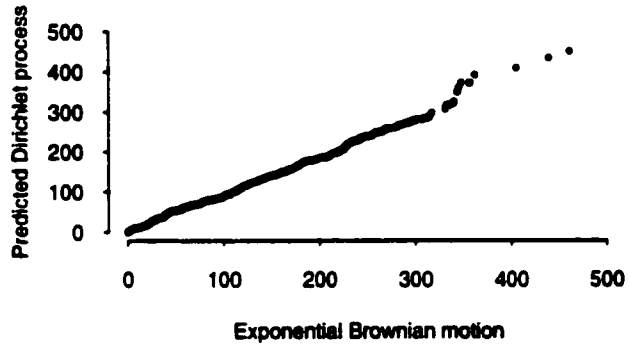

Figure 4.18: Qqplot of $\hat{p}_{120}$ for 1,000 simulations of the exponential Brownian motion and the predicted Dirichlet process procedures, with $T = 132$, $K = 1,200$, and underlying stock based on an exponential random walk model with normal residuals.

	$\hat{c}_{120}$		$\hat{p}_{120}$	
Prediction method	Mean	Std.dev.	Mean	Std.dev.
Exponential random walk	56.64	95.83	69.75	89.54
Exponential Brownian motion	55.98	91.33	71.23	93.13
Predicted Dirichlet process	56.23	92.49	68.37	88.55
Black-Scholes formula	56.31	-	69.26	-

Table 4.2: Mean prices and estimated standard deviations for 1,000 simulations of a European call $\hat{c}_{120}$ and a European put $\hat{p}_{120}$, both with expiration date $T = 132$, exercise price $K = 1,200$, and underlying stock based on an exponential random walk model with normal residuals.

It appears from Figures 4.15 to 4.18 that the empirical distributions obtained for each procedure are not significantly different from one another. Of course, this is reflected in the mean option prices and estimated standard deviations, which are also very close for all three methods.

According to Table 4.2, the best estimates for the Black-Scholes call and put option prices were produced by the predicted Dirichlet process and the exponential random walk models respectively. The predicted Dirichlet process put option estimate also performed well compared to the corresponding exponential Brownian motion price. As for the estimated standard deviations, their apparent closeness confirms that each simulation method presents the same risk.

Again, the conclusions obtained from this analysis are not specific to this particular example. Further simulations performed using a different initial random sample of the same length showed that these results are quite representative of the performance of the predicted Dirichlet process methodology.

4.2.3 Asian Option Pricing with $t = 120$ and $T = 132$

A considerable advantage of Monte Carlo simulation over the Black-Scholes formula is that it allows for the pricing of some types of exotic options, including options where the exercise price depends on certain values of the stock price during the life of the option.

For example, let us consider Asian call and put options, denoted c_t^A and p_t^A. In an Asian option, the exercise price is the average price of the underlying stock over the life of the option. Theoretically, this average price may be either arithmetic or geometric, but in practice most Asian options are based on an arithmetic average. For the current example, we use the arithmetic average of the stock price

$$K = \frac{\hat{S}_{121} + \cdots + \hat{S}_{132}}{12}.$$

Of course, this exercise price varies according to each sample path produced by the simulations.

The results obtained for each simulation procedure are displayed in Figures 4.19 to 4.22 and Table 4.3. These simulations were performed using the same exponential random walk model that was used in Section 4.2.2. In fact, we simply used the conditional distributions that were displayed in Figure 4.12, but we calculated Asian option prices instead of European option prices.

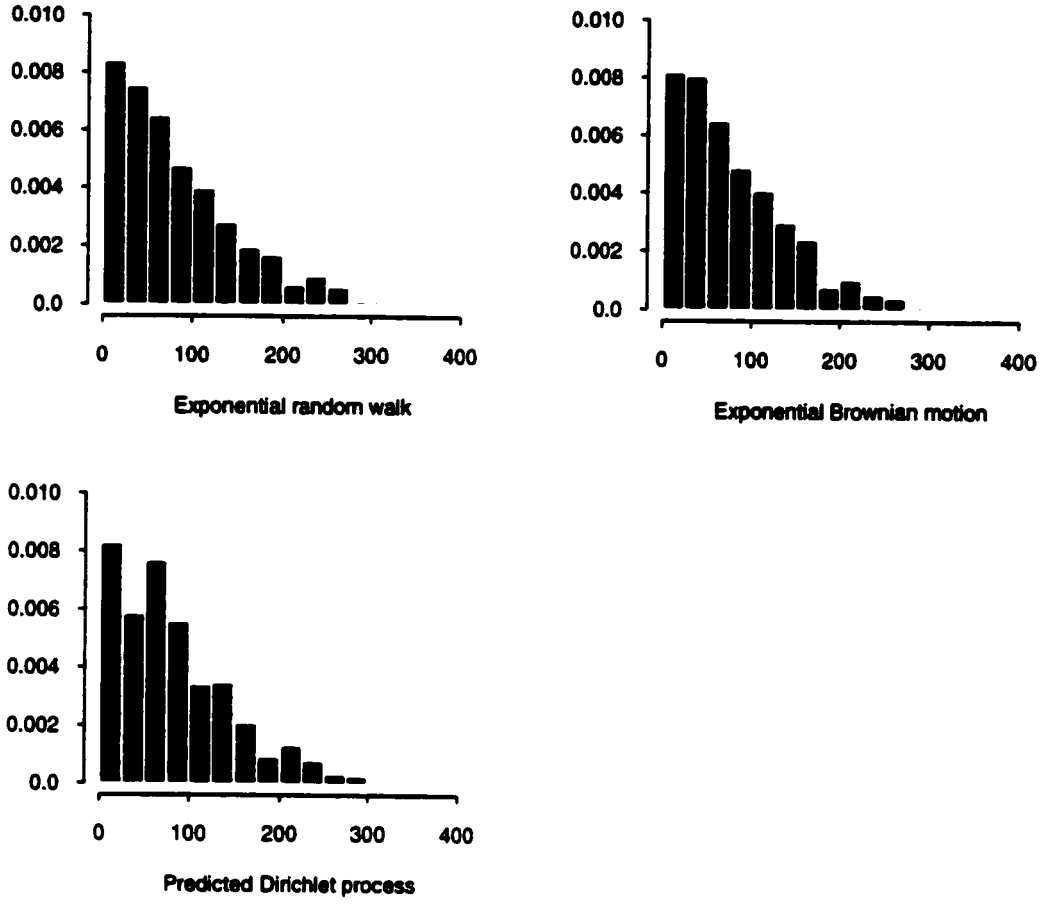

Figure 4.19: Empirical distributions for 1,000 simulations of an Asian call $\hat{c}^A_{120}$, with expiration date $T = 132$, exercise price K equal to the arithmetic average of the stock prices over the life of the option, and underlying stock based on an exponential random walk model with normal residuals. Zero values were suppressed in the figures: 383 for the exponential random walk, 382 for the exponential Brownian motion, and 390 for the predicted Dirichlet process.

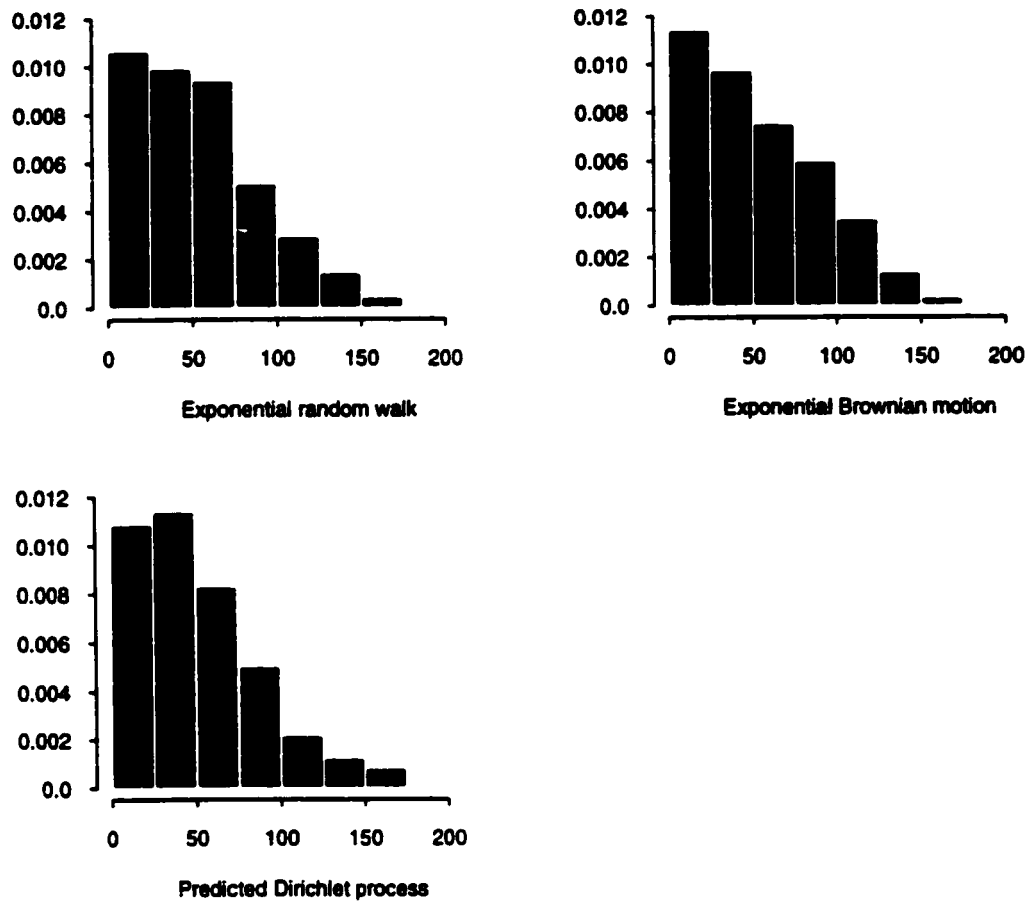

Figure 4.20: Empirical distributions for 1,000 simulations of an Asian put $\hat{p}^A_{120}$, with expiration date $T = 132$, exercise price K equal to the arithmetic average of the stock prices over the life of the option, and underlying stock based on an exponential random walk model with normal residuals. Zero values were suppressed in the figures: 617 for the exponential random walk, 618 for the exponential Brownian motion, and 610 for the predicted Dirichlet process.

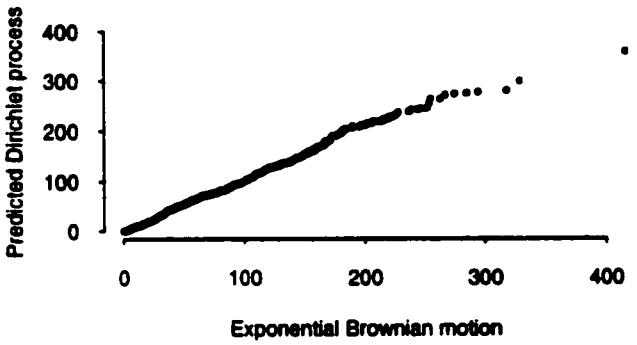

Figure 4.21: Qqplot of $\hat{c}^A_{120}$ for 1,000 simulations of the exponential Brownian motion and the predicted Dirichlet process procedures, with $T = 132$, K equal to the arithmetic average of the stock prices, and underlying stock based on an exponential random walk model with normal residuals.

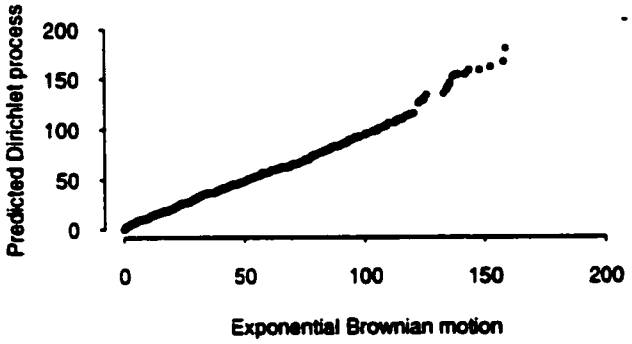

Figure 4.22: Qqplot of $\hat{p}^A_{120}$ for 1,000 simulations of the exponential Brownian motion and the predicted Dirichlet process procedures, with $T = 132$, K equal to the arithmetic average of the stock prices, and underlying stock based on an exponential random walk model with normal residuals.

	$\hat{c}^A_{120}$		$\hat{p}^A_{120}$	
Prediction method	Mean	Std.dev.	Mean	Std.dev.
Exponential random walk	50.51	65.09	20.14	34.39
Exponential Brownian motion	48.96	62.96	20.37	35.01
Predicted Dirichlet process	50.35	64.19	20.22	34.57

Table 4.3: Mean prices and estimated standard deviations for 1,000 simulations of an Asian call $\hat{c}^A_{120}$ and an Asian put $\hat{p}^A_{120}$, both with expiration date $T = 132$, exercise price equal to the arithmetic average of the underlying stock prices over the life of the option, and stock price based on an exponential random walk model with normal residuals.

As illustrated in Table 4.3, the differences between the mean option prices are not significant. Also, the estimated standard deviations are close enough to assume that there is no increased risk in using the predicted Dirichlet process method instead of the exponential random walk or exponential Brownian motion. Consequently, we can conclude that the type of option considered has no impact on the performance of the predicted Dirichlet process model.

4.2.4 European Option Pricing with Heavy-Tailed Residuals

In some financial applications, stock prices are assumed to follow an exponential random walk model where the residuals have a symmetric stable distribution, also known as a stable Paretian distribution. This type of assumption is generally made to allow for the modelling of rare events (like stock market crashes) through the higher probability of extreme observations possible in a stable non-Gaussian distribution.

The idea behind using the stable distribution as a statistical model for asset returns was initiated in the sixties by Mandelbrot [23, 24, 25, 26] and Fama [9]. Another excellent source of information about the financial applications of the stable distribution is the review paper by Mittnik and Rachev [28].

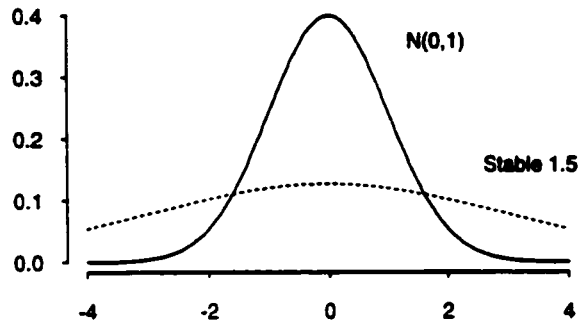

Figure 4.23: Probability density functions of normal and stable random variables.

The results presented in this section were obtained from an exponential random walk model where the residuals were assumed to follow a symmetric stable distribution with index $\alpha = 1.5$ and scale parameter $\sigma = 0.01$. The skewness and shift parameters were taken to be zero. We denote this distribution by $S_{1.5}(0.01, 0, 0)$. This change in the distribution assumed for the residuals represents the only difference between this analysis and that conducted in Section 4.2.2

The behaviour of this exponential random walk model is illustrated in Figures 4.24 and 4.25.[7] Notice the presence of a considerable drop at time $t = 62$ where the price decreased from 450.66 to 390.88. This 13.3% decline in the stock price is an example of a rare event resulting from the heavy-tailed distribution assumed for the residuals. The probability of such an event occurring in an exponential random walk model with $N(0, \sigma^2)$ residuals is practically nil.

The conditional empirical distribution of S_{132} given the historical stock prices $S_0, \ldots, S_{120}$ was predicted assuming risk-neutral valuation using the exponential random walk, the exponential Brownian motion, and the predicted Dirichlet process simulation procedures. Each simulation procedure was conducted assuming a risk-free rate equal to $r = 0.005$ per month.

[7]The complete data set is provided in Appendix D.

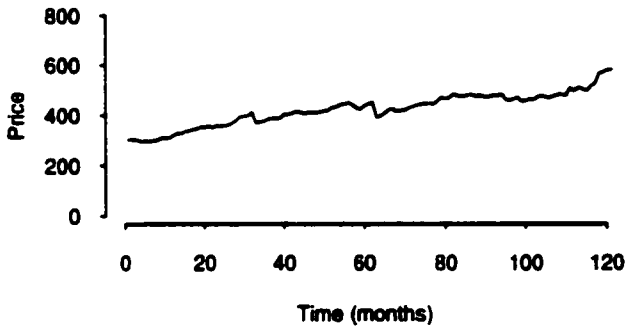

Figure 4.24: Prices from an exponential random walk model $S_t = S_{t-1}e^{Y_t}$, where $Y_t = 0.01 + \varepsilon_t$ and $\varepsilon_t \sim S_{1.5}(0.01, 0, 0)$. The initial value was set to $S_0 = 300$.

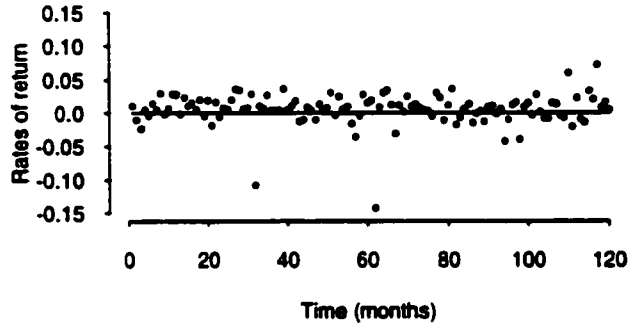

Figure 4.25: Rates of return $Y_1, \ldots, Y_{120}$ from an exponential random walk model $S_t = S_{t-1}e^{Y_t}$, where $Y_t = 0.01 + \varepsilon_t$ and $\varepsilon_t \sim S_{1.5}(0.01, 0, 0)$.

For the exponential Brownian motion simulation, the observations were drawn from a $N(0, \hat{\sigma}^2)$, with $\hat{\sigma}$ equal to the sample standard deviation of $Y_1, \ldots, Y_{120}$, i.e. $\hat{\sigma} = 0.02451886$. The predicted Dirichlet process simulation was performed using $\alpha = 6$, by drawing from the distribution $H \sim N(0, \hat{\sigma}^2)$ with probability $w_{120} = 1/21$, or from the heavy-tailed random sample $Y_1, \ldots, Y_{120}$ with probability $1 - w_{120} = 20/21$. Each observation in $Y_1, \ldots, Y_{120}$ was assigned an equal probability $1/120$.

Because the residuals in the random walk model have a heavy-tail distribution, we expect the predicted Dirichlet process simulation to provide a better match of the exponential random walk distribution than the exponential Brownian motion, which is performed using normal draws. Even if we assumed the prior guess H to be normal, it is expected that the heavy tail component provided by the random sample draws will take over and create a heavy tail histogram for the predicted Dirichlet process simulation.

The results displayed in Figure 4.26 are not very conclusive as both the exponential Brownian motion and the predicted Dirichlet process graphs seem to have a normal density. The normality of exponential Brownian motion was expected, but that of the predicted Dirichlet process is mostly due to the small number of observations (120) contained in the initial data set. Since only a few of these observations were drawn from the tails of the stable distribution, the initial sample $Y_1, \ldots, Y_{120}$ tends to have a normal shape which was then reproduced by the simulation of the Dirichlet process. The exponential random walk simulation generated 14 values far more extreme than found in $Y_1, \ldots, Y_{120}$. Consequently, the predicted Dirichlet process method could not replicate these values.

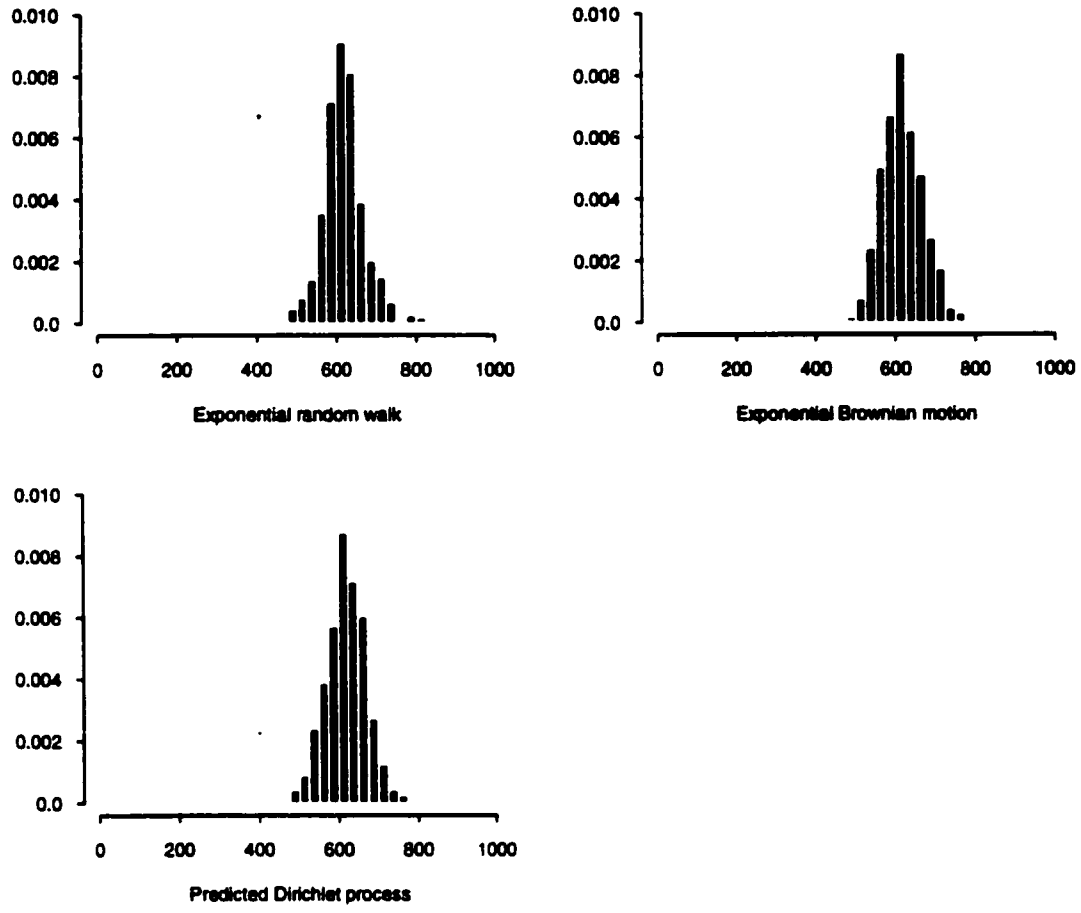

Figure 4.26: Empirical distributions of $\hat{S}_{132} \mid S_0, \ldots, S_{120}$ for 1,000 simulations of the exponential random walk, the exponential Brownian motion, and the predicted Dirichlet process procedures. The exponential random walk histogram includes 6 values above 1,000 and 8 values below 400 that are not shown on this figure.

Figure 4.27 presents the plot of the quantiles of exponential Brownian motion versus those of the predicted Dirichlet process method. The downward concavity of this qqplot means slightly heavier tails for exponential Brownian motion. This should not be frequently observed in this kind of analysis, but the low number of extreme observations contained in the initial sample and the randomness of the simulations decided otherwise.

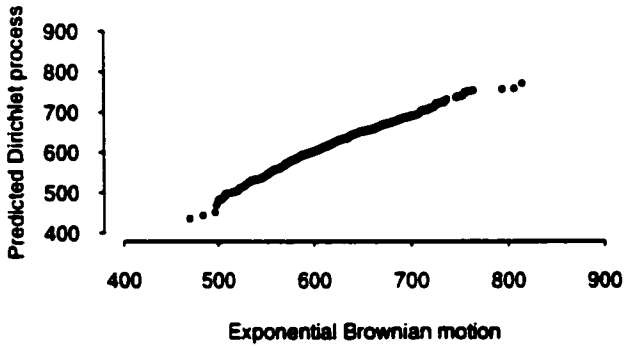

Figure 4.27: Qqplot of $\hat{S}_{132} \mid S_0, \ldots, S_{120}$ for 1,000 simulations of the exponential Brownian motion and the predicted Dirichlet process procedures.

The histograms of the residuals obtained for a specific sample path of the exponential random walk model are displayed in Figure 4.28. The SSE's computed for this path were 3,246,096 for exponential Brownian motion and 3,152,312 for the predicted Dirichlet process.

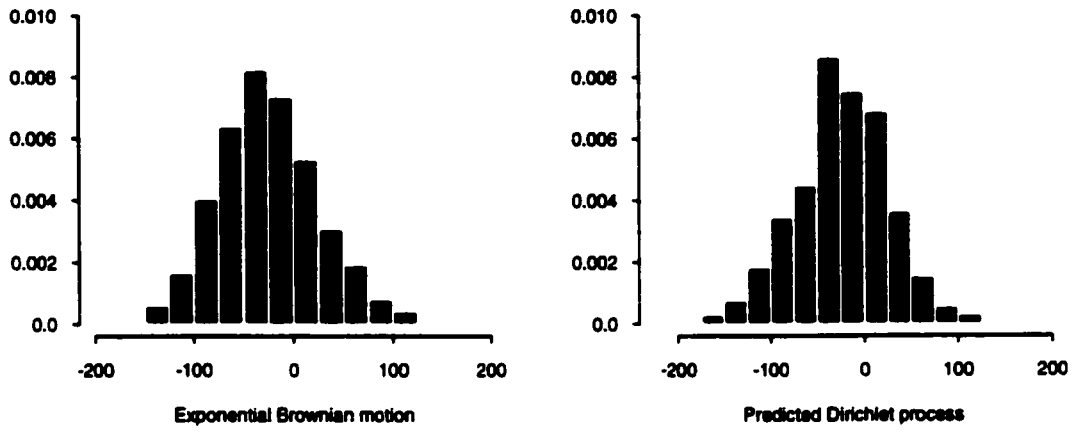

Figure 4.28: Empirical distributions of $\left(\hat{S}_{132} - S_{132}\right) \mid S_0, \ldots, S_{120}$ for one sample path of the exponential random walk model, based on 1,000 simulations.

Figures 4.29 to 4.32 illustrate the empirical distributions and the qqplots of European call and put option prices with expiration date $T = 132$ and exercise price $K = 600$. The mean prices and estimated standard deviations obtained for each simulation method are presented in Table 4.4.

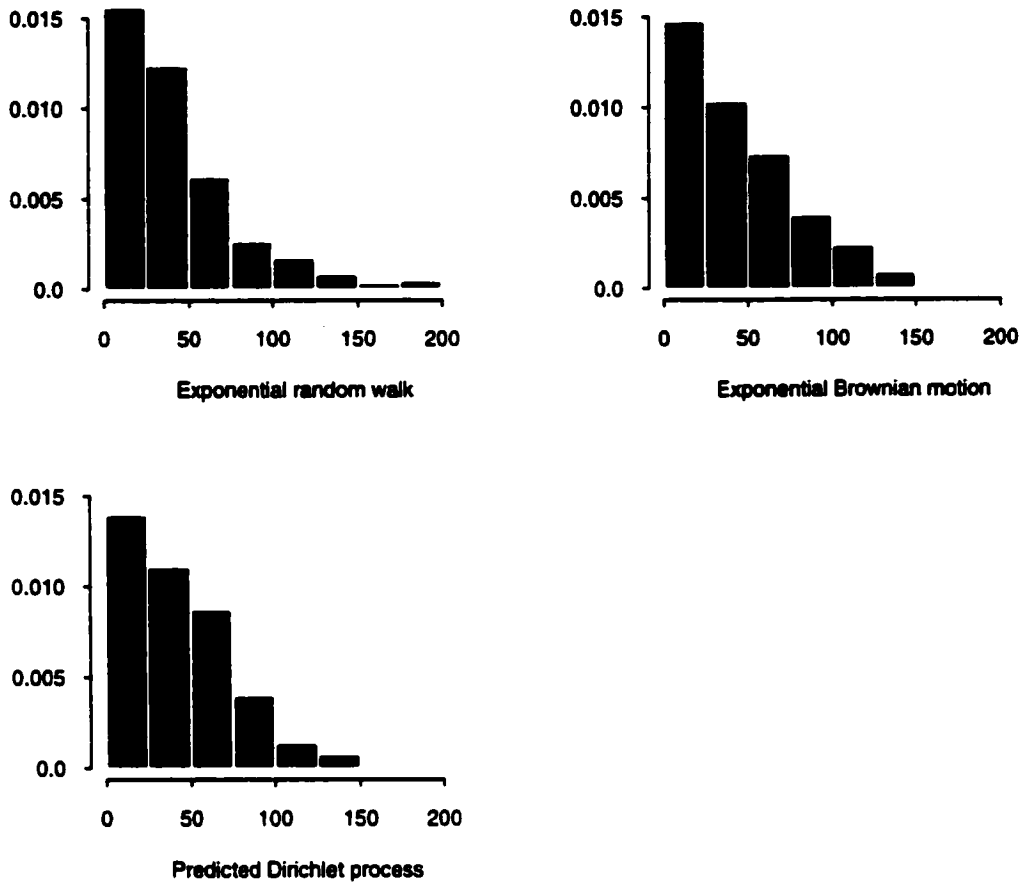

Figure 4.29: Empirical distributions for 1,000 simulations of a European call $\hat{c}_{120}$, with $T = 132$, $K = 600$, and underlying stock based on an exponential random walk model with stable residuals. Zero values were suppressed in the figures: 345 for the exponential random walk, 376 for the exponential Brownian motion, and 336 for the predicted Dirichlet process. The exponential random walk histogram also includes 16 values above 200 that are not shown on this figure.

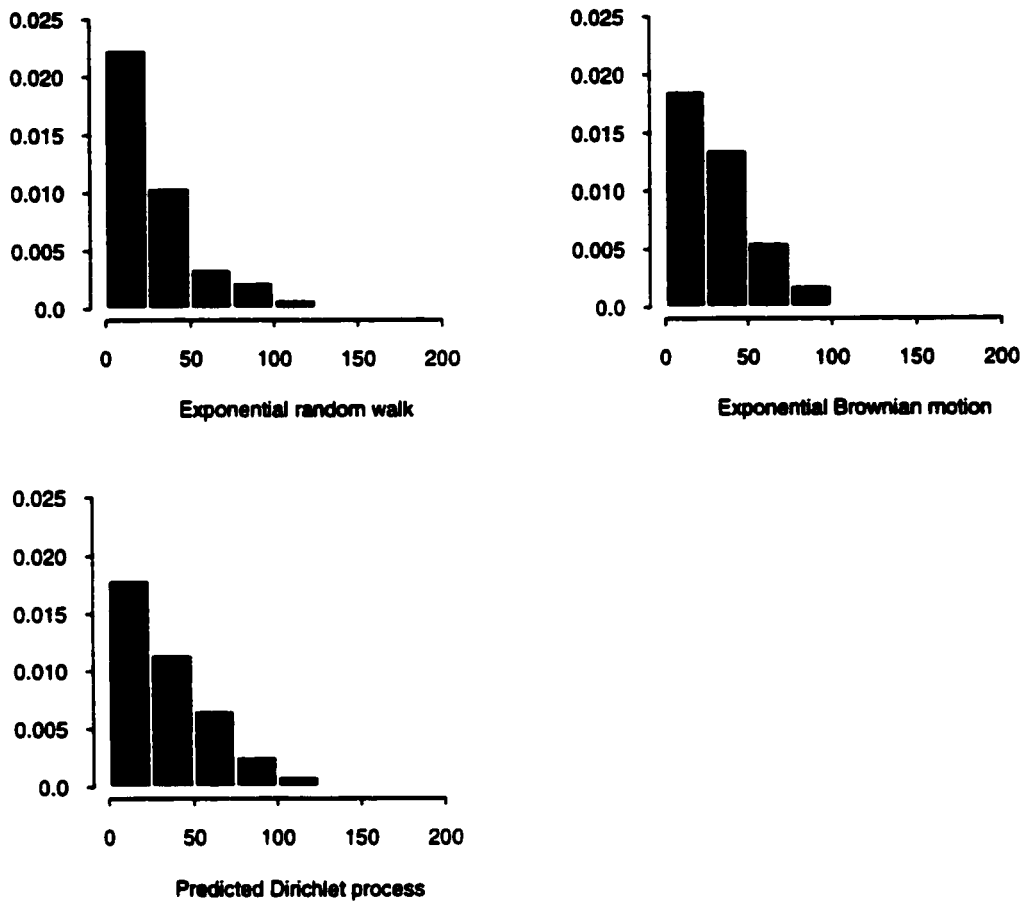

Figure 4.30: Empirical distributions for 1,000 simulations of a European put $\hat{p}_{120}$, with $T = 132$, $K = 600$, and underlying stock based on an exponential random walk model with stable residuals. Zero values were suppressed in the figures: 655 for the exponential random walk, 624 for the exponential Brownian motion, and 664 for the predicted Dirichlet process. The exponential random walk histogram also includes 7 values above 200 that are not shown on this figure.

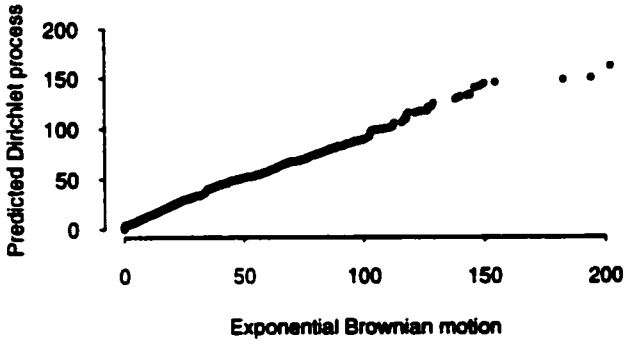

Figure 4.31: Qqplot of $\hat{c}_{120}$ for 1,000 simulations of the exponential Brownian motion and the predicted Dirichlet process procedures, with $T = 132$, $K = 600$, and underlying stock based on an exponential random walk model with stable residuals.

Figure 4.32: Qqplot of $\hat{p}_{120}$ for 1,000 simulations of the exponential Brownian motion and the predicted Dirichlet process procedures, with $T = 132$, $K = 600$, and underlying stock based on an exponential random walk model with stable residuals.

	$\hat{c}_{120}$		$\hat{p}_{120}$	
Prediction method	Mean	Std.dev.	Mean	Std.dev.
Exponential random walk	37.50	125.60	12.86	36.88
Exponential Brownian motion	27.96	35.22	11.76	20.82
Predicted Dirichlet process	28.33	32.57	11.70	23.32
Black-Scholes formula	28.79	-	12.26	-

Table 4.4: Mean prices and estimated standard deviations for 1,000 simulations of a European call $\hat{c}_{120}$ and a European put $\hat{p}_{120}$, both with expiration date $T = 132$, exercise price $K = 600$, and underlying stock based on an exponential random walk model with stable residuals.

As shown in Table 4.4, the option prices calculated using the exponential Brownian motion, the predicted Dirichlet process, and the Black-Scholes approaches are close to one another, but not in the same range as the exponential random walk prices. Moreover, because of the occurrence of extreme events, the standard deviations estimated using the exponential random walk are much higher than that of the other models. If we remove the lowest and two highest observations, the exponential random walk prices become more reasonable: 32.64 for the call and 12.31 for the put.

This whole example is not of practical use, however, since the pricing of options using an exponential random walk model with heavy-tailed residuals is not a common pricing technique. The increased variability caused by the higher frequency of extreme events observed in heavy-tailed distributions tends to reduce the degree of accuracy in the pricing of these options.

None of the exponential Brownian motion and the predicted Dirichlet process prices captured this variability since their estimated standard deviations are significantly inferior to those obtained from the exponential random walk model. From a practical standpoint, this underestimation creates an increased risk of wrongly estimating the true price of the option when using these two approaches.

As we mentioned earlier, the small number of extreme observations in the initial

data set is responsible for the poor performance of the predicted Dirichlet process method. For the Dirichlet model to replicate the exponential random walk prices more closely, the proportion of extreme observations in the initial random sample would have to be comparable to the probability of drawing an extreme observation in the stable distribution. This was not the case in this example as only two observations in the random sample were extreme. We expect that a similar analysis conducted with a larger initial random sample would show a slight improvement in the results obtained from the predicted Dirichlet process procedure.

Table 4.5 illustrates the mean prices and estimated standard deviations of European call and put options with expiration date $T = 252$ and exercise price $K = 2,700$. The option prices were evaluated at time $t = 240$, assuming that the historical prices $S_0, \ldots, S_{240}$ were known and came from an exponential random walk model with stable residuals. Note that because of the larger size of the initial random sample, the prices obtained are considerably more volatile than those displayed in Table 4.4. However, the exponential Brownian motion and the predicted Dirichlet process simulations were unable to replicate the volatility shown in the exponential random walk prices.

	$\hat{c}_{240}$		$\hat{p}_{240}$	
Prediction method	Mean	Std.dev.	Mean	Std.dev.
Exponential random walk	95.97	208.70	108.93	215.94
Exponential Brownian motion	102.29	151.63	100.31	139.96
Predicted Dirichlet process	78.59	110.84	101.62	185.33
Black-Scholes formula	104.36	-	104.48	-

Table 4.5: Mean prices and estimated standard deviations for 1,000 simulations of a European call $\hat{c}_{240}$ and a European put $\hat{p}_{240}$, both with expiration date $T = 252$, exercise price $K = 2,700$, and underlying stock based on an exponential random walk model with stable residuals.

4.2.5 European Option Pricing with Skewed Residuals

We now measure the performance of the predicted Dirichlet process approach for the case where the residuals in the exponential random walk model are asymmetric. This is achieved by simply reworking the example presented in Section 4.2.4 with a chi-square distribution instead of a stable distribution. As we know, the density of the chi-square distribution is skewed to the right.

The errors in the exponential random walk model were drawn from a chi-square distribution with $p = 4$ degrees of freedom, denoted $\chi^2(4)$. In order to obtain a distribution with mean 0, we subtracted the number of degrees of freedom from each observation. The residuals were also multiplied by a factor 0.015 so that the rates or return are on a scale comparable to that of the previous examples. The exponential random walk model is illustrated in Figures 4.33 and 4.34.[8]

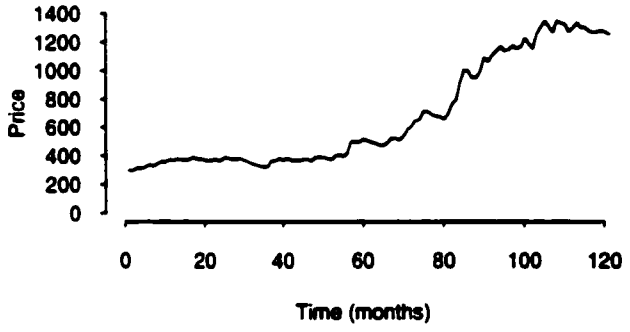

Figure 4.33: Prices from an exponential random walk model $S_t = S_{t-1}e^{Y_t}$, where $Y_t = 0.01 + \varepsilon_t$ and $\varepsilon_t \sim \chi^2(4) - 4$. The residuals were scaled down using a factor 0.015, while the initial value was set to $S_0 = 300$.

[8]The complete data set is provided in Appendix D.

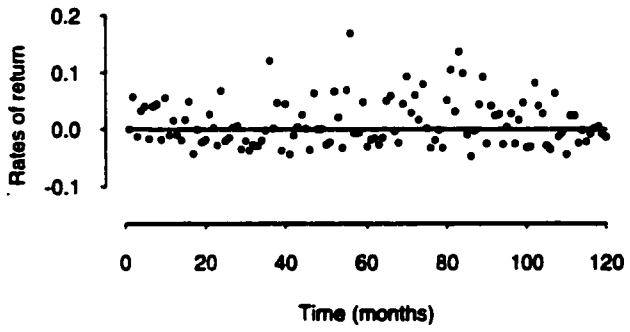

Figure 4.34: Rates of return $Y_1, \ldots, Y_{120}$ from an exponential random walk model $S_t = S_{t-1}e^{Y_t}$, where $Y_t = 0.01 + \varepsilon_t$ and $\varepsilon_t \sim \chi^2(4) - 4$. The residuals were scaled down using a factor 0.015.

Once again, the conditional distribution of $\hat{S}_{132}$ given $S_0, \ldots, S_{120}$ was predicted using the three sampling approaches previously described. The simulation of the exponential Brownian motion was performed using a $N(0, \hat{\sigma}^2)$, with $\hat{\sigma}$ equal to the standard deviation of $Y_1, \ldots, Y_{120}$, i.e. $\hat{\sigma} = 0.04129312$. The predicted Dirichlet process sampling was performed using $\alpha = 6$, by drawing observations from the distribution $H \sim N(0, \hat{\sigma}^2)$ with probability $w_{120} = 1/21$, or from the chi-square random sample $Y_1, \ldots, Y_{120}$ with probability $1 - w_{120} = 20/21$. When sampling from the random sample, each observation was assigned an equal probability $1/120$. All three simulation procedures were conducted assuming risk-neutral valuation and $r = 0.005$ per month.

Figure 4.35 shows the conditional empirical distribution of $\hat{S}_{132}$ obtained from each approach. According to these graphs, the predicted Dirichlet process produced a better match of the exponential random walk distribution than the exponential Brownian motion simulation. The exponential Brownian motion graph displays a normal density, while the exponential random walk and the predicted Dirichlet process histograms present skewness towards the right side of the distribution.

This assertion is confirmed by the graph of the kernel density estimates shown in the lower right corner of Figure 4.35. The kernel densities of the exponential

random walk and the predicted Dirichlet process (represented by the two dashed lines) clearly contain higher values than that of exponential Brownian motion. In the exponential random walk simulation, this tail was expected because the random draws were performed using a chi-square distribution. As for the Dirichlet process tail, it can be explained by the large proportion of observations that were drawn from the initial sample, which was constructed using chi-square random variables.

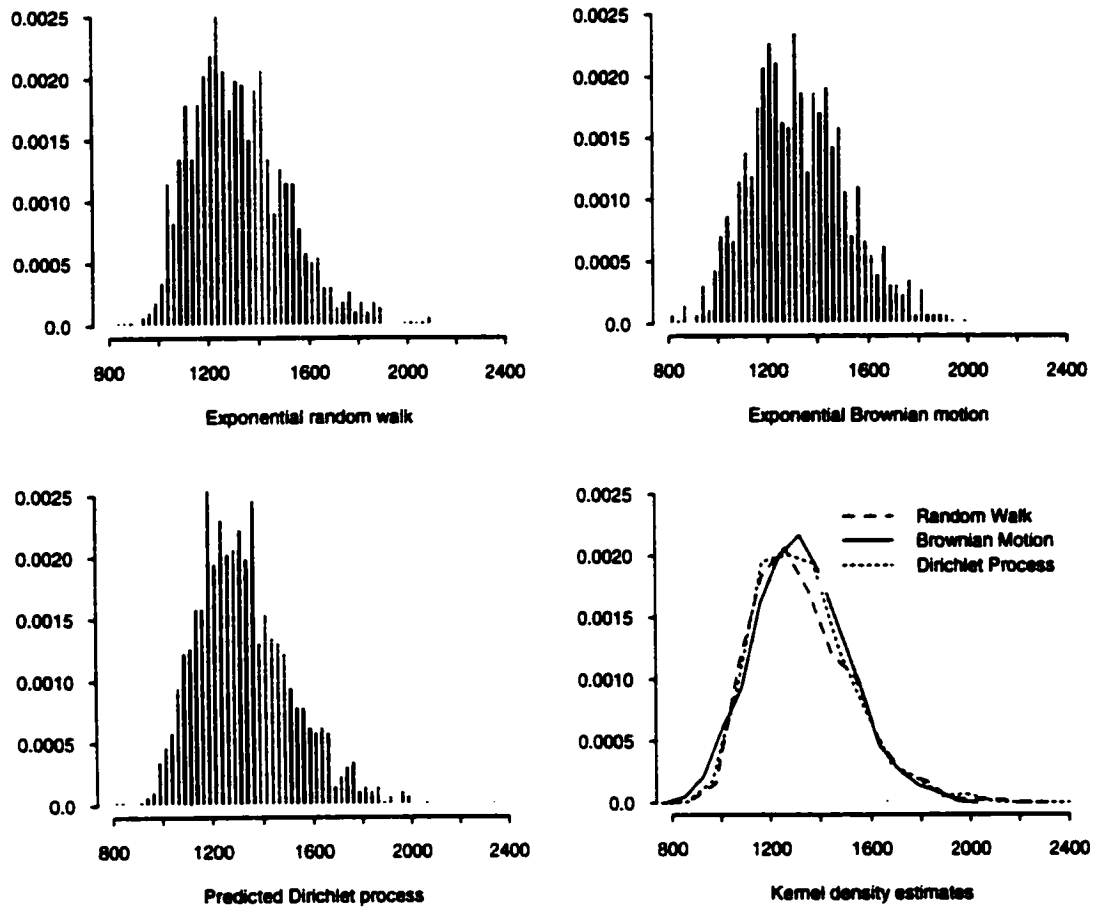

Figure 4.35: Empirical distributions of $\hat{S}_{132} \mid S_0, \ldots, S_{120}$ for 1,000 simulations of the exponential random walk, the exponential Brownian motion, and the predicted Dirichlet process procedures. The lower right figure represents the kernel density estimate of each distribution.

Figure 4.36 confirms the divergence between exponential Brownian motion and the predicted Dirichlet process. The slight upward concavity in the plot of their quantiles denotes a heavier right tail for the predicted Dirichlet process distribution.

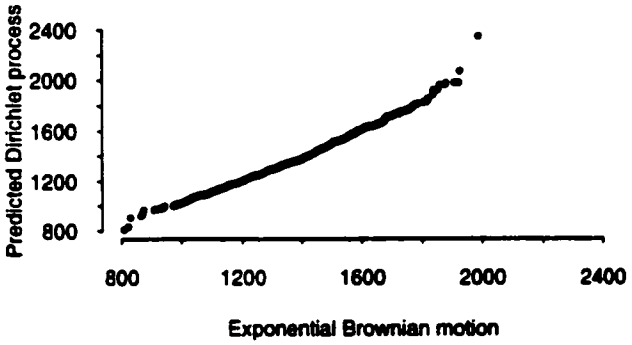

Figure 4.36: Qqplot of $\hat{S}_{132} \mid S_0, \ldots, S_{120}$ for 1,000 simulations of the exponential Brownian motion and the predicted Dirichlet process procedures.

This right tail is also noticeable in the histogram of the residuals displayed in Figure 4.37. The SSE's computed for this particular sample path were in a comparable range: 55,268,191 for exponential Brownian motion and 55,423,103 for the predicted Dirichlet process. Again, these graphs represent the residuals with respect to a specific sample path of the exponential random walk simulation.

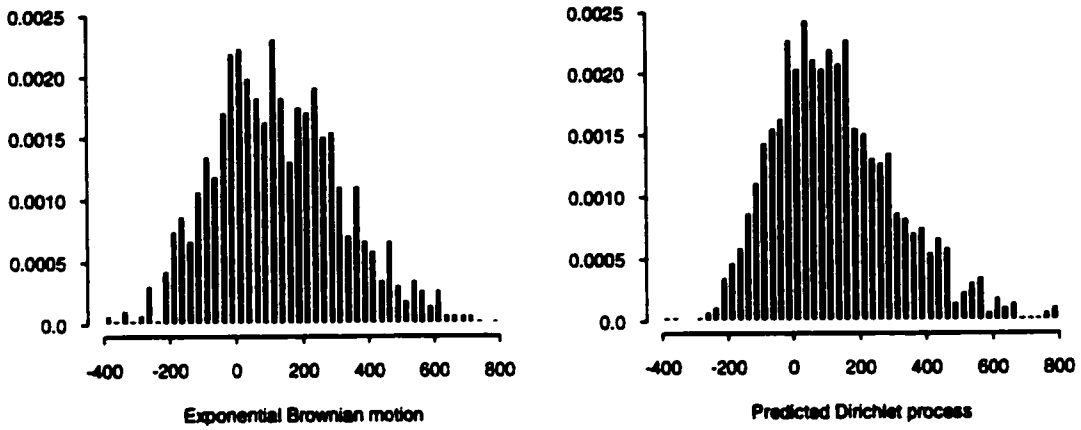

Figure 4.37: Empirical distributions of $\left(\hat{S}_{132} - S_{132}\right) \mid S_0, \ldots, S_{120}$ for one sample path of the exponential random walk model, based on 1,000 simulations. The predicted Dirichlet process histogram includes 2 values above 800 that are not shown on this figure.

Figures 4.38 to 4.39 illustrate the non-zero empirical distributions obtained for the pricing at time $t = 120$ of European call and put options with expiration date $T = 132$ and exercise price $K = 1,200$. The qqplots of the exponential Brownian motion and the predicted Dirichlet process prices are shown in Figures 4.40 and 4.41. The actual mean option prices and their estimated standard deviations are provided in Table 4.6.

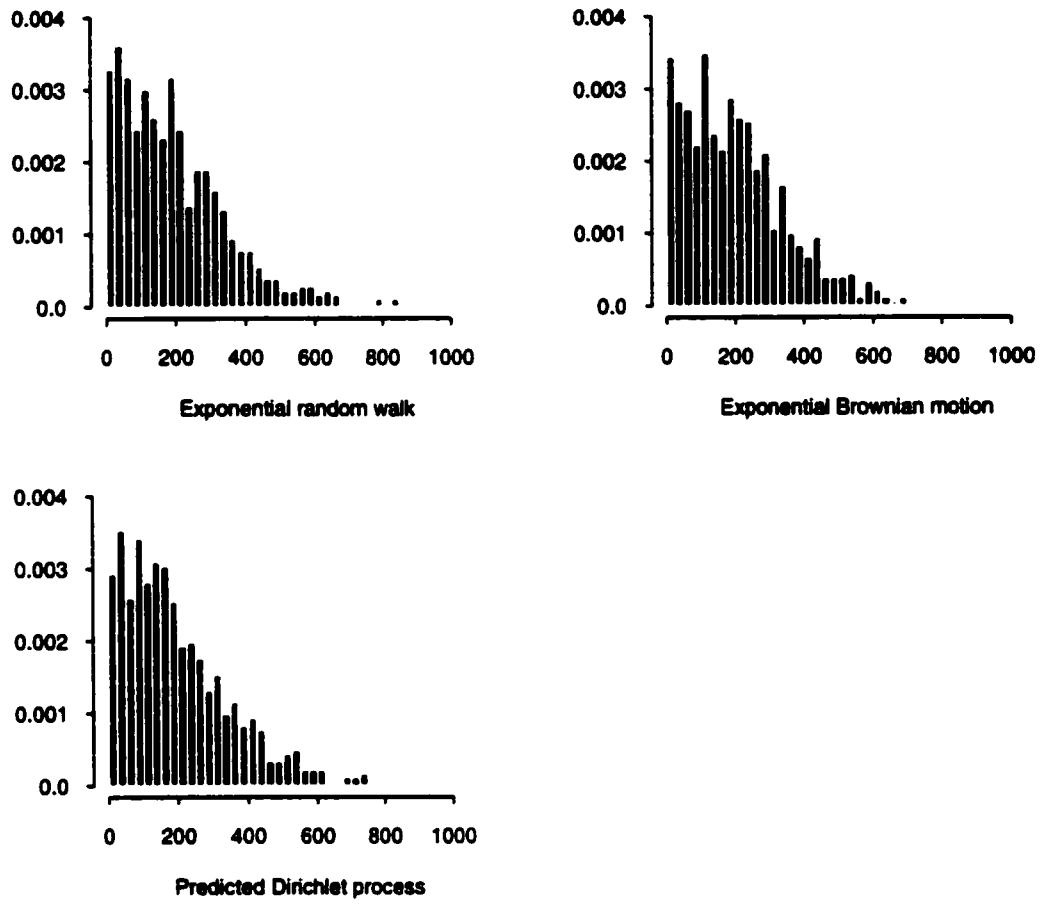

Figure 4.38: Empirical distributions for 1,000 simulations of a European call $\hat{c}_{120}$, with expiration date $T = 132$, exercise price $K = 1,200$, and underlying stock based on an exponential random walk model with chi-square residuals. Zero values were suppressed in the figures: 281 for the exponential random walk, 278 for the exponential Brownian motion, and 275 for the predicted Dirichlet process.

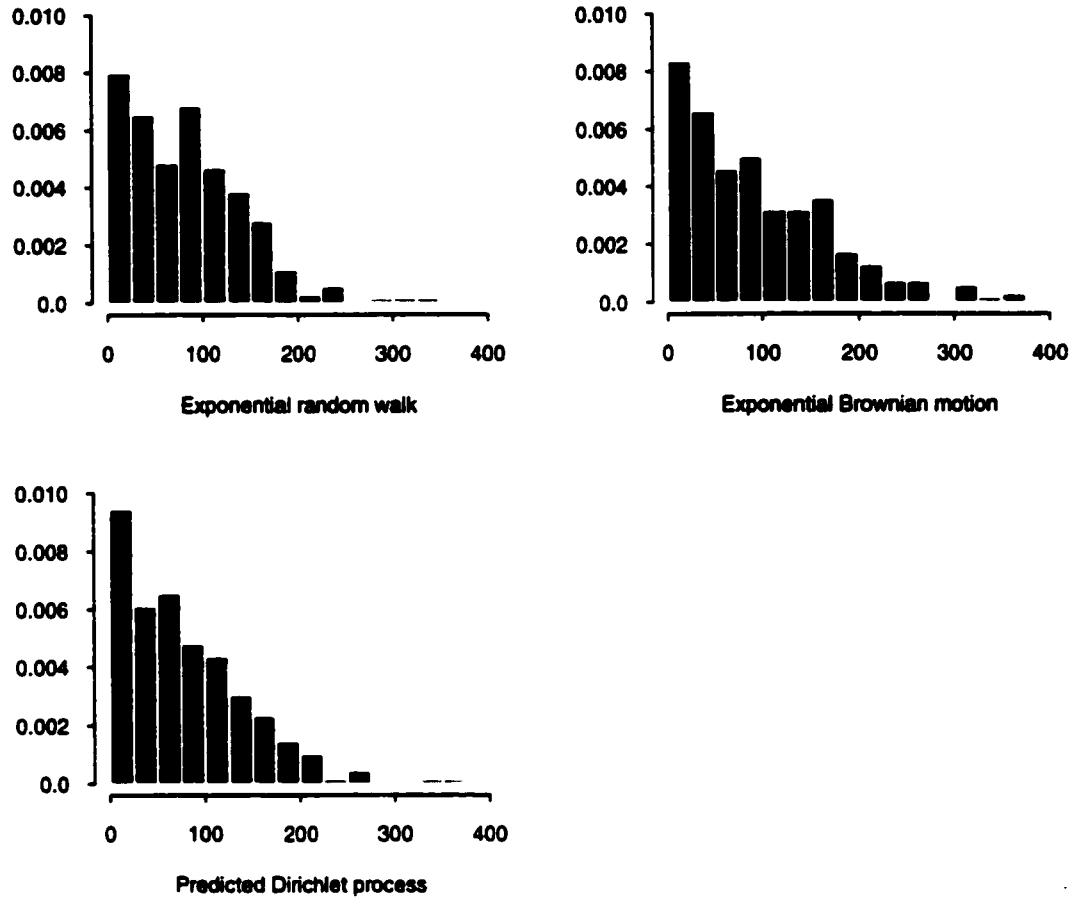

Figure 4.39: Empirical distributions for 1,000 simulations of a European put $\hat{p}_{120}$, with expiration date $T = 132$, exercise price $K = 1,200$, and underlying stock based on an exponential random walk model with chi-square residuals. Zero values were suppressed in the figures: 719 for the exponential random walk, 722 for the exponential Brownian motion, and 725 for the predicted Dirichlet process.

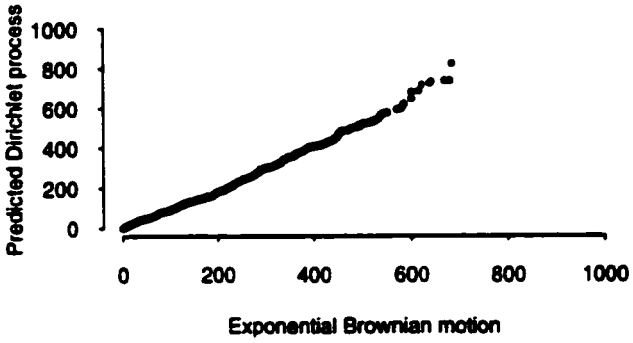

Figure 4.40: Qqplot of $\hat{c}_{120}$ for 1,000 simulations of the exponential Brownian motion and the predicted Dirichlet process procedures, with $T = 132$, $K = 1,200$, and underlying stock based on an exponential random walk model with chi-square residuals.

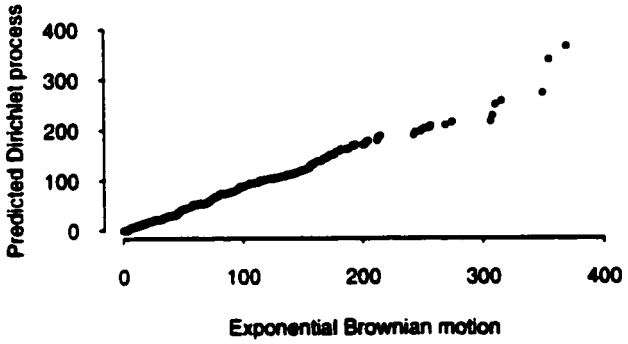

Figure 4.41: Qqplot of $\hat{p}_{120}$ for 1,000 simulations of the exponential Brownian motion and the predicted Dirichlet process procedures, with $T = 132$, $K = 1,200$, and underlying stock based on an exponential random walk model with chi-square residuals.

	$\hat{c}_{120}$		$\hat{p}_{120}$	
Prediction method	Mean	Std.dev.	Mean	Std.dev.
Exponential random walk	142.02	159.14	23.24	48.85
Exponential Brownian motion	145.68	153.27	26.03	58.02
Predicted Dirichlet process	144.12	158.96	21.75	48.76
Black-Scholes formula	145.32	-	23.67	-

Table 4.6: Mean prices and estimated standard deviations for 1,000 simulations of a European call $\hat{c}_{120}$ and a European put $\hat{p}_{120}$, both with expiration date $T = 132$, exercise price $K = 1,200$, and underlying stock based on an exponential random walk model with chi-square residuals.

The pricing of options on an exponential random walk model with chi-square residuals is not a common pricing method. The greater probability of extreme events caused by the skewness of the distribution tends to reduce the accuracy in the same way the heavier tails affected the example with stable residuals.

However, the results in Table 4.6 show that all four methods produced comparable results. The call option prices all lie in the same range, but the put prices are more differentiated. The predicted Dirichlet process put price is inferior to the other prices, while the mean price and the estimated standard deviation of the exponential Brownian motion put are slightly greater. An explanation for this variability may the non-stationarity of the initial data set. As shown in Figures 4.33 and 4.34, the first 60 observations exhibit much lower variability than the following 60 observations.

As in Section 4.2.4, we expected the predicted Dirichlet process and the exponential random walk results to be close from each other and much different from those obtained with exponential Brownian motion or the Black-Scholes formula. This was not achieved in the current example, mostly because the right tails of the exponential random walk and the predicted Dirichlet process histograms shown in Figure 4.35 were not much heavier than that of exponential Brownian motion.

The results obtained for a horizon of 48 months are illustrated in Table 4.7. Once

again, the exponential Brownian motion and the predicted Dirichlet process methods could not capture the variability of the exponential random walk model for the call option.

	$\hat{c}_{120}$		$\hat{p}_{120}$	
Prediction method	Mean	Std.dev.	Mean	Std.dev.
Exponential random walk	200.10	326.77	108.13	147.04
Exponential Brownian motion	172.42	267.09	104.73	147.05
Predicted Dirichlet process	173.29	283.38	115.49	158.99
Black-Scholes formula	177.13	-	105.30	-

Table 4.7: Mean prices and estimated standard deviations for 1,000 simulations of a European call $\hat{c}_{120}$ and a European put $\hat{p}_{120}$, both with expiration date $T = 168$, exercise price $K = 1,500$, and underlying stock based on an exponential random walk model with chi-square residuals.

4.2.6 Discussion

From an option pricing perspective, the results obtained in the previous examples showed that all three simulation methods are equivalent when dealing with an exponential random walk model with normal residuals. For the models with stable or chi-square residuals, the prices obtained using the exponential Brownian motion and the predicted Dirichlet process methods were less variable than those obtained from the exponential random walk. The pricing of options on such exponential random walk models with stable or chi-square residuals is not commonly used, but nevertheless this underestimation of the standard deviation is dangerous for an investor because it increases the possibility of computing wrong option prices.

As for the conditional distribution of the future stock prices, the exponential Brownian motion approach was quite performant for the examples with normal residuals, but not as accurate for the models with stable or chi-square residuals. In these models, the simulations failed to capture the variability of the stock prices, which should

not be surprising since the Brownian motion is based on a normal distribution.

For the predicted Dirichlet process approach, the conditional empirical distributions of the future stock prices are mostly based on the distribution of the initial random sample when the sample size is large enough compared to α. Of course, the simulation of the Dirichlet process is expected to replicate the overall shape of this distribution. Whereas the method showed nice results for the models with normal or chi-square residuals, those obtained using a model with stable residuals were not as conclusive. The low number of extreme observations in the initial random sample made it difficult to produce a distribution with heavy tails.

Nevertheless, the predicted Dirichlet process simulation remains a valid procedure to estimate the conditional distribution of future stock prices. In fact, because of its greater flexibility, the predicted Dirichlet process approach provided superior results compared to the exponential Brownian motion simulation when the residuals were not assumed to be normally distributed.

Chapter 5

Option Pricing for the S&P 500

This chapter presents an application of the predicted Dirichlet process method to the pricing of European options where the underlying asset is a stock index. The application was implemented using 133 monthly closing prices of the Standard & Poor's 500 Total Return Index ($US)[1] for the period extending from December 31st, 1989 to December 31st, 2000. The S&P 500 index measures the aggregate stock return earned by the 500 companies with the largest market capitalization in the United States.

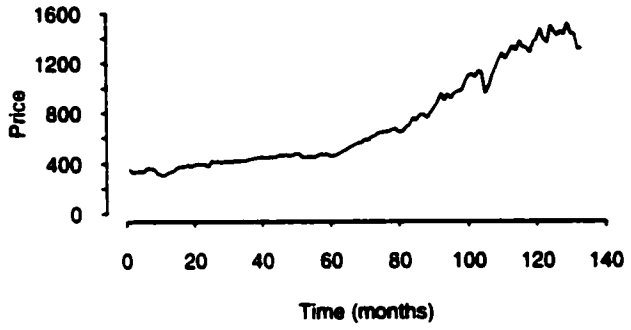

Figure 5.1: Monthly closing prices of the S&P 500 index from December 31st, 1989 to December 31st, 2000.

[1]Data source: Yahoo! Finance, `http://finance.yahoo.com`. The complete data set is provided in Appendix D.

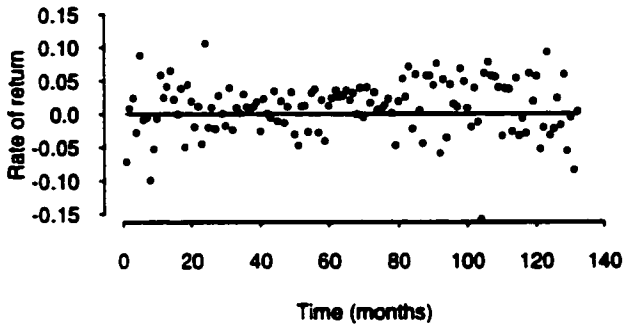

Figure 5.2: Monthly rates of return of the S&P 500 index from December 31st, 1989 to December 31st, 2000.

The simulations presented in this chapter were conducted under the exact same conditions as in Chapter 4, with the only difference that the underlying asset is now a real stock index instead of a fictive data set constructed from an exponential random walk model. Nevertheless, this modification should not impact on the simulations since we demonstrate in Section 5.1 that the S&P 500 index seem to have a random walk structure.

5.1 Random Walk Structure of the S&P 500

Consider the first order time series

$$X_t = \mu + \rho X_{t-1} + \varepsilon_t, \quad \text{for } t = 1, 2, \ldots,$$

where $X_0 = 0$ and $\varepsilon_t \sim N(0, \sigma^2)$. When $\rho = 1$, this time series becomes the random walk model (4.1). Thus, the test for random walk structure is performed by verifying the following hypotheses:

$$H_0 : \rho = 1 \quad \text{vs.} \quad H_1 : \rho \neq 1.$$

This is achieved using the limiting distribution of $n(\hat{\rho} - 1)$ for $\rho = 1$, where

$$\hat{\rho} = \frac{\sum_{t=2}^{n} X_t X_{t-1}}{\sum_{t=2}^{n} X_t^2}$$

is the maximum likelihood estimator of ρ. If the value computed for $n(\hat{\rho}-1)$ is between the lower and upper limits, then we accept H_0 and conclude that the model has a random walk structure. If otherwise $n(\hat{\rho}-1)$ is outside those limits, then we reject H_0 in favour of H_1.

Such a test can be performed on the S&P 500 index by considering that X_t is the cumulative return of the index between times 0 and t. Table 5.1 displays the results obtained using the first n returns of the S&P 500 at a 10% significance level. The critical values of the limiting distribution were taken from Fuller [14].

n	$n(\hat{\rho}-1)$	Lower 5% limit	Upper 5% limit
60	-1.93	-7.74	1.33
120	-2.39	-7.91	1.31
132	-1.63	-7.92	1.31

Table 5.1: Test for the random walk structure using the first n returns of the S&P 500 index at a 10% significance level.

The null hypothesis H_0 is accepted for all three cases since each value of $n(\hat{\rho}-1)$ is found between the upper and lower critical values. Consequently, we do not reject the hypothesis that the S&P 500 has a random walk structure at the 10% significance level.

5.2 Application to Option Pricing

5.2.1 European Option Pricing with $t = 60$ and $T = 72$

The first case we discuss is the pricing at time $t = 60$ of European options expiring at time $T = 72$, conditional on the observed index prices $S_0, \ldots, S_{60}$. This analysis was conducted assuming risk-neutral valuation using the exponential Brownian motion

and the predicted Dirichlet process simulation methodologies described in Section 4.1.

The exponential Brownian motion simulation was performed using process (4.3) with $r = 0.005$. The observations were drawn from a $N(0, \hat{\sigma}^2)$ with $\hat{\sigma}$ equal to the sample standard deviation of $Y_1, \ldots, Y_{60}$, i.e. $\hat{\sigma} = 0.03571384$. For the Dirichlet process sampling, we assumed once again process (4.4) with $\alpha = 6$ and therefore $w_{60} = 1/11$. The predicted index returns were then drawn from the distribution $H \sim N(0, \hat{\sigma}^2)$ with probability $w_{60} = 1/11$, or from the S&P 500 random sample $Y_1, \ldots, Y_{60}$ with probability $1 - w_{60} = 10/11$. When sampling from the random sample, each observation was assigned an equal weight 1/60.

The major difference between this example and those described in Chapter 4 is that the actual distribution of the S&P 500 index returns is unknown. Even if these returns are often modelled using a normal density, the occurrence of extreme events such as the stock market crash of October 19^{th}, 1987 demonstrates that the normal distribution does not always provide an appropriate representation of financial data.

Figure 5.3 shows the empirical distribution of $\hat{S}_{72} \mid S_0, \ldots, S_{60}$ for both the exponential Brownian motion and the predicted Dirichlet process models. Both histograms have a similar shape and appear to be normally distributed around a mean slightly inferior to 500. If the normal shape of the exponential Brownian motion histogram was expected, that of the predicted Dirichlet process method was observed because the distribution of the S&P 500 index must be close to a normal distribution. As we know, the Dirichlet process simulation tends to reproduce the distribution of the initial random sample when the sample size is large enough compared to α.

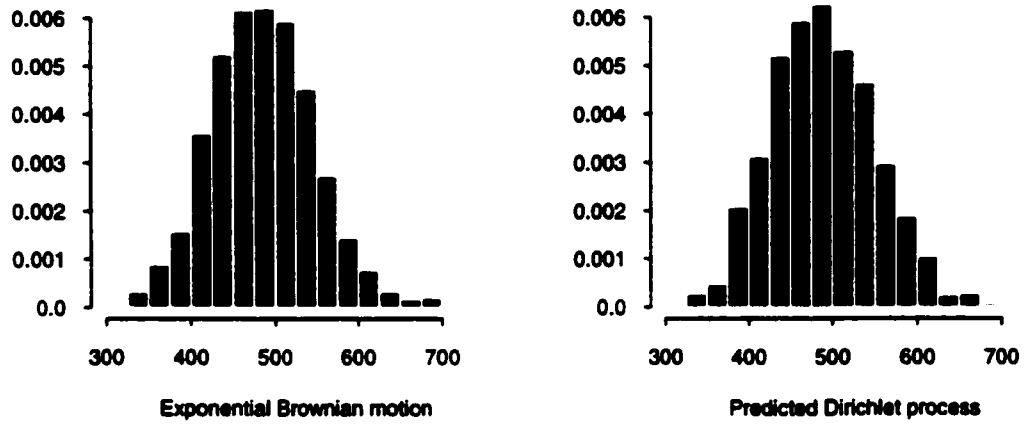

Figure 5.3: Empirical distributions of $\hat{S}_{72} \mid S_0, \ldots, S_{60}$ for 1,000 simulations of the exponential Brownian motion and the predicted Dirichlet process procedures, based on the S&P 500 index.

In Figure 5.4, the straight line formed by the quantiles of both simulations is another sign of the normality of the predicted Dirichlet process results.

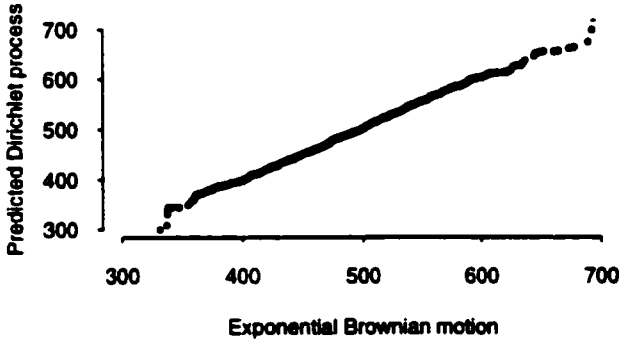

Figure 5.4: Qqplot of $\hat{S}_{72} \mid S_0, \ldots, S_{60}$ for 1,000 simulations of the exponential Brownian motion and the predicted Dirichlet process procedures, based on the S&P 500 index.

The residuals obtained from the simulations are illustrated in Figure 5.5. Because the actual growth of the S&P 500 index was higher than our risk-neutral hypothesis of $r = 0.005$, both simulation methodologies tend to understate the actual price of the index. As mentioned in Section 4.2.1, this fact is not important when pricing derivative products. Under the risk-neutral valuation assumption, only the expected growth rate of the index must be considered. The SSE computed for the exponential Brownian motion simulation was $20,635,302$, while that of the predicted Dirichlet process was $20,102,455$.

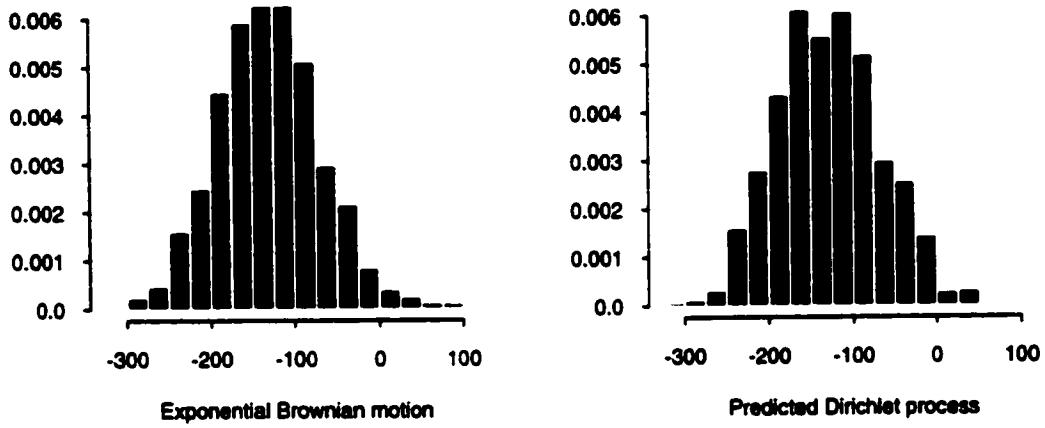

Figure 5.5: Empirical distributions of $\left(\hat{S}_{72} - S_{72}\right) \mid S_0, \ldots, S_{60}$ for $1,000$ simulations of the exponential Brownian motion and the predicted Dirichlet process procedures, based on the S&P 500 index.

Let us now consider the pricing at $t = 60$ of European call and put options with $T = 72$ and $K = 500$. The exponential Brownian motion and the predicted Dirichlet process empirical distributions are displayed in Figures 5.6 and 5.7. Again, these graphs represent the distributions of the non-zero values of the option prices. Figures 5.8 and 5.9 illustrate the qqplots of the option prices, while Table 5.2 contains the mean prices and the estimated standard deviations computed for each method.

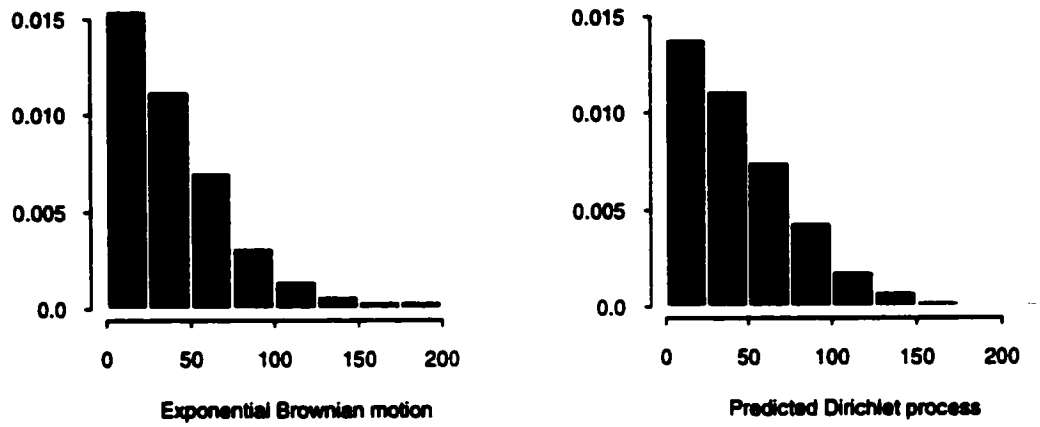

Figure 5.6: Empirical distributions for 1,000 simulations of a European call $\hat{c}_{60}$ on the S&P 500, with $T = 72$ and $K = 500$. Zero values were suppressed in the figures: 599 for the exponential Brownian motion and 587 for the predicted Dirichlet process.

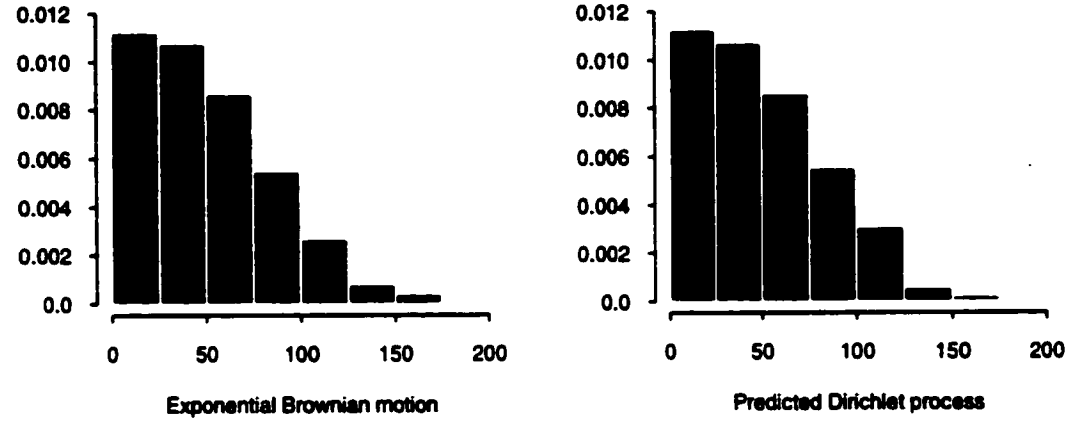

Figure 5.7: Empirical distribution for 1,000 simulations of a European put $\hat{p}_{60}$ on the S&P 500, with $T = 72$ and $K = 500$. Zero values were suppressed in the figures: 401 for the exponential Brownian motion and 413 for the predicted Dirichlet process.

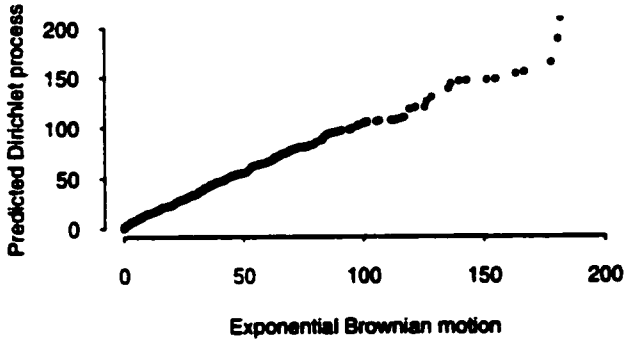

Figure 5.8: Qqplot of $\hat{c}_{60}$ for 1,000 simulations of the exponential Brownian motion and the predicted Dirichlet process procedures, with $T = 72$, $K = 500$, and the S&P 500 index as the underlying asset.

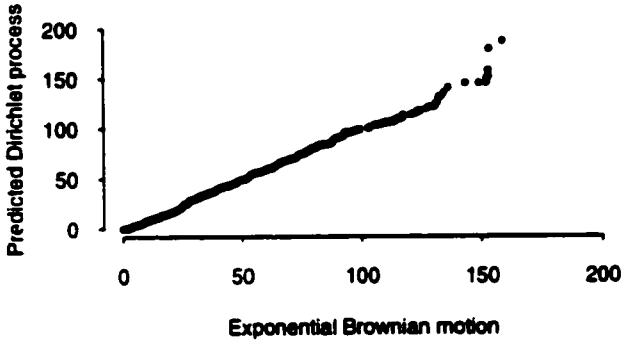

Figure 5.9: Qqplot of $\hat{p}_{60}$ for 1,000 simulations of the exponential Brownian motion and the predicted Dirichlet process procedures, with $T = 72$, $K = 500$, and the S&P 500 index as the underlying asset.

	$\hat{c}_{60}$		$\hat{p}_{60}$	
Prediction method	Mean	Std.dev.	Mean	Std.dev.
Exponential Brownian motion	16.78	30.62	30.14	36.61
Predicted Dirichlet process	18.85	32.46	29.43	36.40
Black-Scholes formula	17.60	-	29.21	-

Table 5.2: Mean prices and estimated standard deviations for 1,000 simulations of a European call $\hat{c}_{60}$ and a European put $\hat{p}_{60}$ on the S&P 500 index, both with expiration date $T = 72$ and exercise price $K = 500$.

As shown in Table 5.2, the predicted Dirichlet process estimates are closer to the Black-Scholes prices than those obtained from exponential Brownian motion. Except for the Dirichlet process call, every other option price underestimated the Black-Scholes prices. The differences are not significant enough to conclude the superiority of one method over the other, but nevertheless the validity of the predicted Dirichlet process method is confirmed by the fact that we know exponential Brownian motion to be an appropriate model for the S&P 500 index. The fact that the estimated standard deviations lie in the same range reinforce this statement.

Note that these conclusions are not particular to this example. Further simulations run across various sample paths of the S&P 500 index showed that the exponential Brownian motion and the predicted Dirichlet process methods are somewhat equivalent.

5.2.2 European Option Pricing with $t = 120$ and $T = 132$

Let us now consider a similar example with a larger history. This case is concerned with the pricing at time $t = 120$ of European call and put options with expiration date $T = 132$ given the historical stock prices $S_0, \ldots, S_{120}$.

Once again, the exponential Brownian motion observations were sampled from a $N(0, \hat{\sigma}^2)$. The sample standard deviation of $Y_1, \ldots, Y_{120}$ was found to be $\hat{\sigma} = 0.03881977$. As for the predicted Dirichlet process observations, they were sampled

from the distribution $H \sim N(0, \hat{\sigma}^2)$ with probability $w_{120} = 1/11$, or from the S&P 500 random sample $Y_1, \ldots, Y_{120}$ with probability $1 - w_{120} = 10/11$. When sampling from the random sample, each observation was assigned an equal weight 1/120. We assumed a risk-free rate $r = 0.005$.

The empirical conditional distribution of $\hat{S}_{132} \mid S_0, \ldots, S_{120}$ is illustrated for both simulation methodologies in Figure 5.10. Note the heavier right tail for the exponential Brownian motion graph, and also the higher peak in the middle of the predicted Dirichlet process histogram. Despite these minor irregularities, both densities appear to have a similar normal shape.

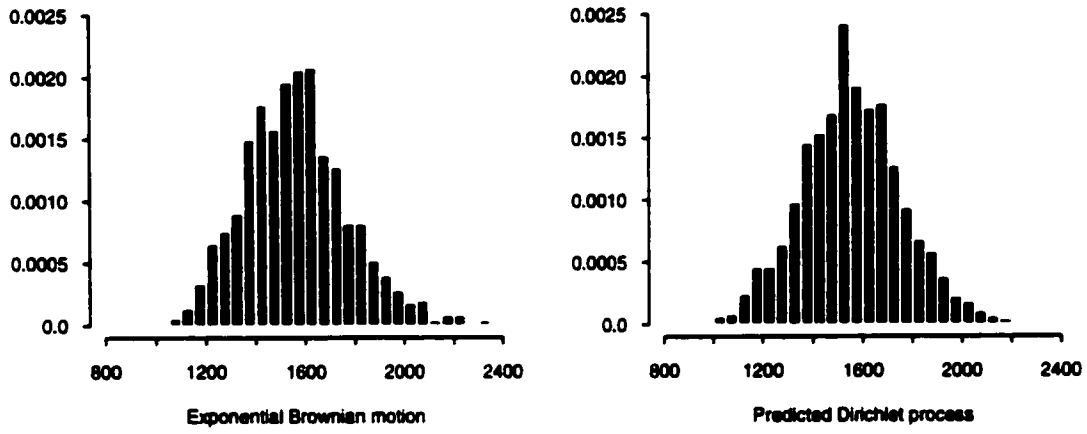

Figure 5.10: Empirical distributions of $\hat{S}_{132} \mid S_0, \ldots, S_{120}$ for 1,000 simulations of the exponential Brownian motion and the predicted Dirichlet process procedures, based on the S&P 500 index.

The plot of the exponential Brownian motion and the predicted Dirichlet process quantiles is illustrated in Figure 5.11. Because this qqplot displays a straight line, we can suppose that both distributions have the same density.

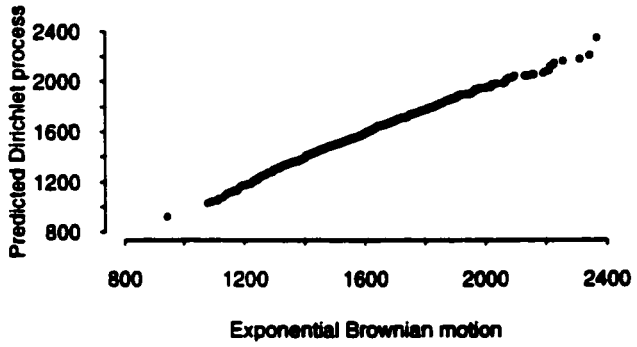

Figure 5.11: Qqplot of $\hat{S}_{132} \mid S_0, \ldots, S_{120}$ for 1,000 simulations of the exponential Brownian motion and the predicted Dirichlet process procedures, based on the S&P 500 index.

Figure 5.12 shows the empirical distribution of the errors. The SSE's computed for this example were 105,604,303 for the exponential Brownian motion simulation versus 97,286,332 for the predicted Dirichlet process. This represents a huge increase compared to the SSE's computed in Section 5.2.1, as both simulation methodologies significantly outgrew the actual value of the S&P 500 index. One of the main reasons for this overestimation is the bear market experienced between $t = 120$ and $T = 132$. Both our simulations models contained a positive drift term of 6% per annum, but the S&P 500 index dropped from 1,469.25 to 1,320.28 during that period.

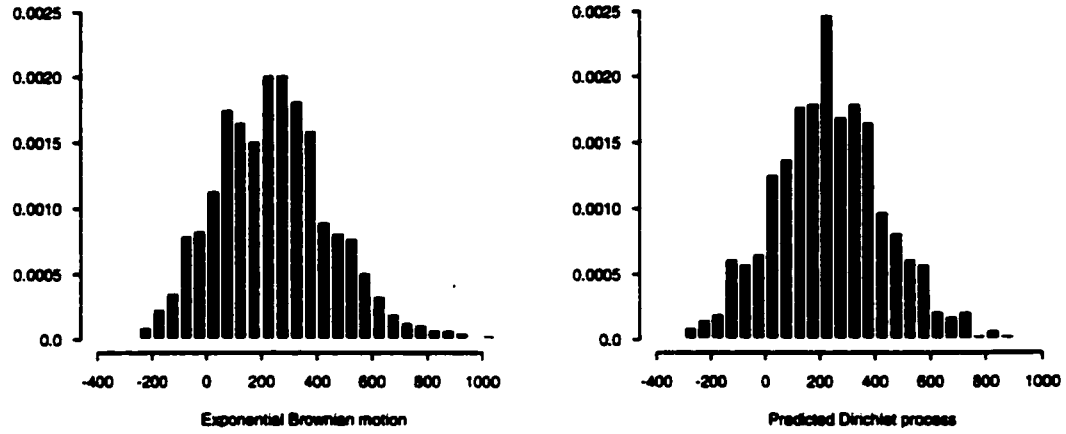

Figure 5.12: Empirical distributions of $\left(\hat{S}_{132} - S_{132}\right) \mid S_0, \ldots, S_{120}$ for 1,000 simulations of the exponential Brownian motion and the predicted Dirichlet process procedures, based on the S&P 500 index.

The results obtained for the pricing of European call and put options with expiration date $T = 132$ and exercise price $K = 1,600$ are displayed in Figures 5.13 to 5.16. Figures 5.13 and 5.14 show the empirical distributions of the prices for the exponential Brownian motion and the predicted Dirichlet process models, while the qqplots are displayed in Figures 5.15 and 5.16. The actual mean prices and their estimated standard deviations are shown in Table 5.3.

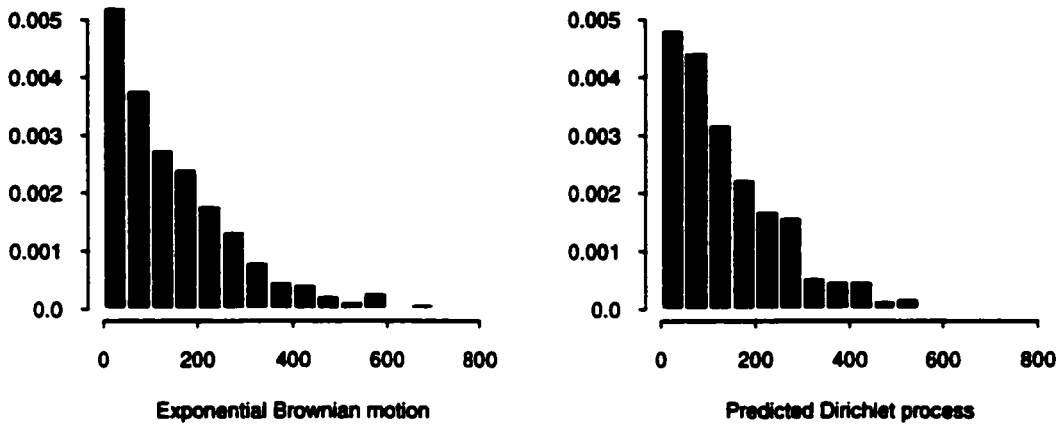

Figure 5.13: Empirical distributions for 1,000 simulations of a European call $\hat{c}_{120}$ on the S&P 500, with $T = 132$ and $K = 1,600$. Zero values were suppressed: 588 for the exponential Brownian motion and 599 for the predicted Dirichlet process.

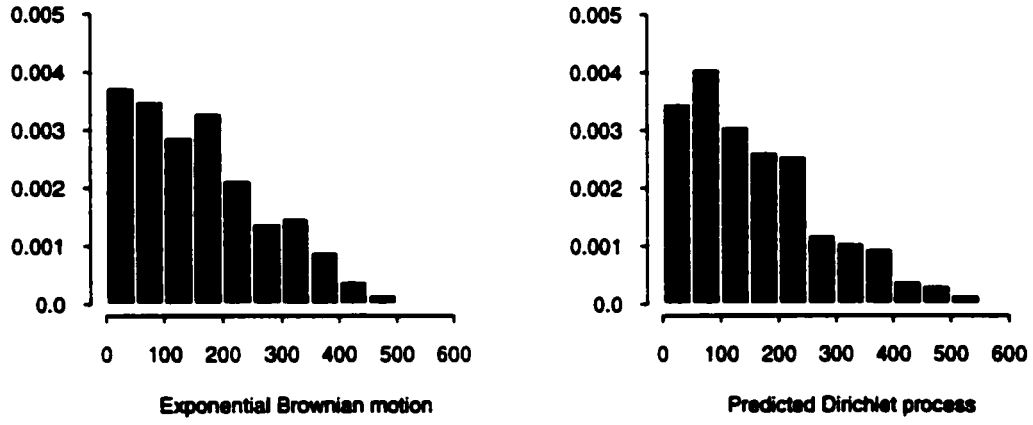

Figure 5.14: Empirical distributions for 1,000 simulations of a European put $\hat{p}_{120}$ on the S&P 500, with $T = 132$ and $K = 1,600$. Zero values were suppressed: 412 for the exponential Brownian motion and 401 for the predicted Dirichlet process.

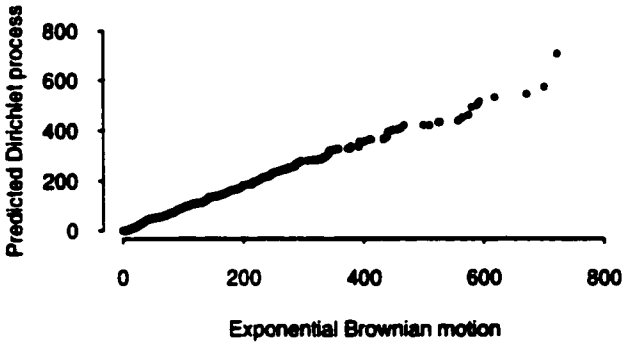

Figure 5.15: Qqplot of $\hat{c}_{120}$ for 1,000 simulations of the exponential Brownian motion and the predicted Dirichlet process procedures, with $T = 132$, $K = 1,600$, and the S&P 500 index as the underlying asset.

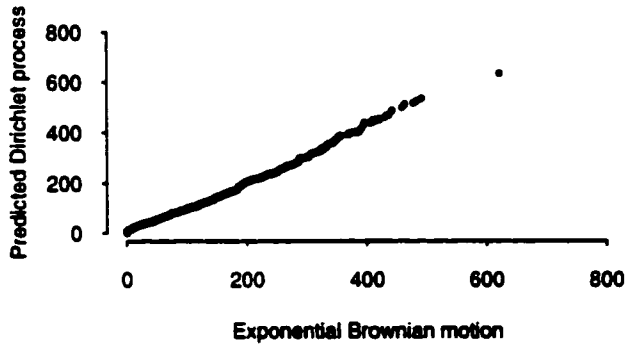

Figure 5.16: Qqplot of $\hat{p}_{120}$ for 1,000 simulations of the exponential Brownian motion and the predicted Dirichlet process procedures, with $T = 132$, $K = 1,600$, and the S&P 500 index as the underlying asset.

	$\hat{c}_{120}$		$\hat{p}_{120}$	
Prediction method	Mean	Std.dev.	Mean	Std.dev.
Exponential Brownian motion	64.06	116.99	96.24	119.16
Predicted Dirichlet process	57.36	103.15	98.84	122.76
Black-Scholes formula	62.38	-	99.96	-

Table 5.3: Mean prices and estimated standard deviations for 1,000 simulations of a European call $\hat{c}_{120}$ and a European put $\hat{p}_{120}$ on the S&P 500 index, both with expiration date $T = 132$ and exercise price $K = 1,600$.

Some of the prices shown in Table 5.3 are somewhat surprising. The exponential Brownian motion simulation produced a decent estimate of the Black-Scholes call price, but not of the put option price. The opposite was observed for the predicted Dirichlet process whose call option price was a much worst estimate than its put option price. This lower call option price and estimated standard deviation may reflect the greater stability of the S&P 500 index prices in the first 60 observations of Figures 5.1 and 5.2. In fact, the estimated standard deviation of the first 60 returns is 0.03571384, while that of the next 60 returns is 0.04061274. This illustrates the necessity on the part of the trader to carefully select data sections with stationary behaviour.

5.2.3 Asian Option Pricing with $t = 120$ and $T = 132$

As mentioned in Section 4.2.3, the Monte Carlo simulation can be used to price various types of exotic options, including Asian options. The results presented in this section were computed using the empirical conditional distributions obtained in Figure 5.10. The following figures display the empirical distributions and qqplots of Asian call and put options whose exercise price is based on the arithmetic average of the stock prices over the life of the option.

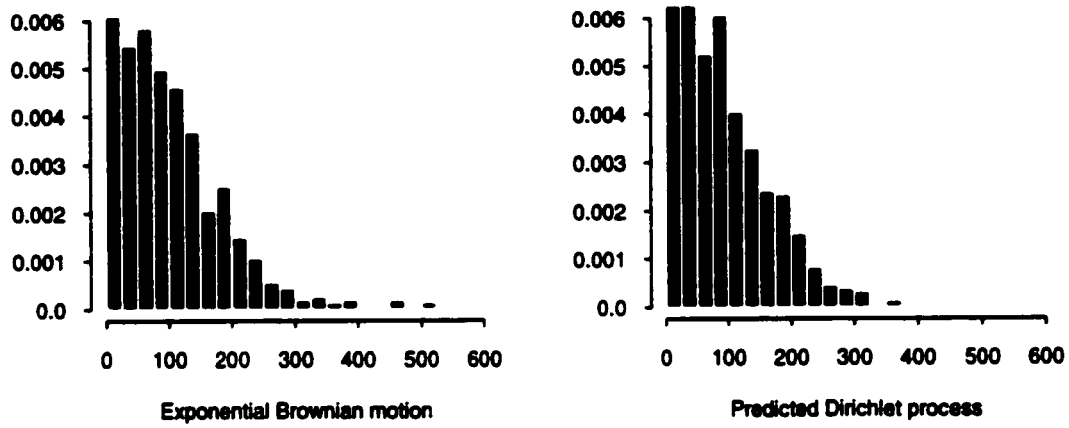

Figure 5.17: Empirical distributions for 1,000 simulations of an Asian call $\hat{c}^A_{120}$ on the S&P 500 index, with $T = 132$ and K based on arithmetic average. Zero values were suppressed: 357 for the Brownian motion and 367 for the Dirichlet process.

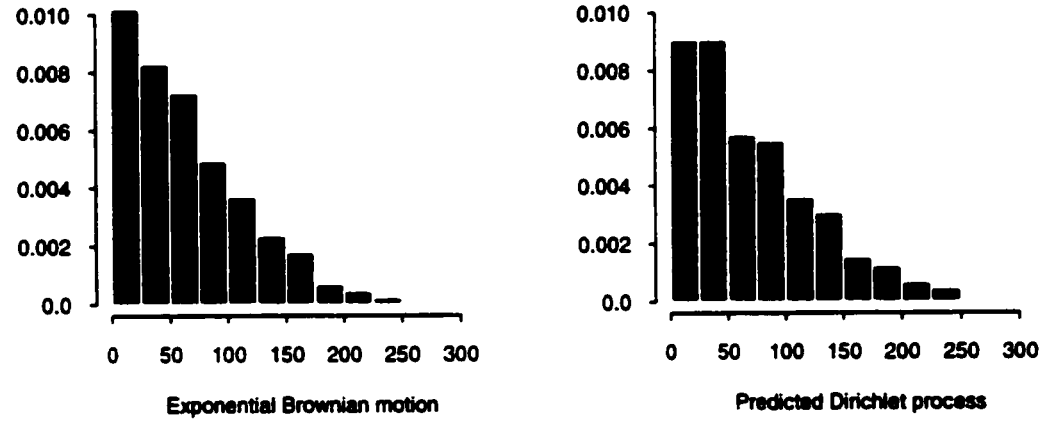

Figure 5.18: Empirical distributions for 1,000 simulations of an Asian put $\hat{p}^A_{120}$ on the S&P 500 index, with $T = 132$ and K based on arithmetic average. Zero values were suppressed: 643 for the Brownian motion and 633 for the Dirichlet process.

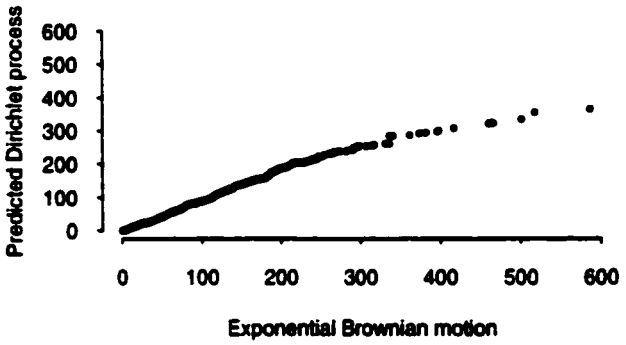

Figure 5.19: Qqplot of $\hat{c}^A_{120}$ for 1,000 simulations of the exponential Brownian motion and the predicted Dirichlet process procedures, with $T = 132$, K equal to the arithmetic average of the stock prices, and the S&P 500 index as the underlying asset.

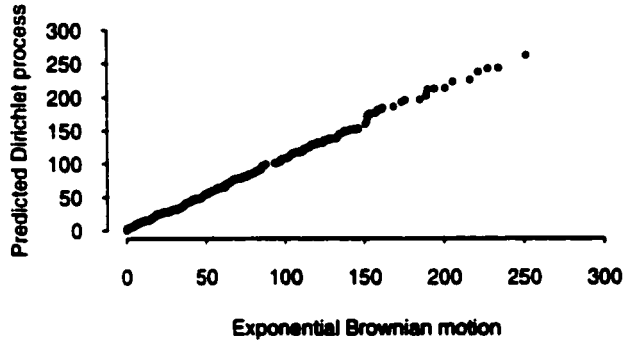

Figure 5.20: Qqplot of $\hat{p}^A_{120}$ for 1,000 simulations of the exponential Brownian motion and the predicted Dirichlet process procedures, with $T = 132$, K equal to the arithmetic average of the stock prices, and the S&P 500 index as the underlying asset.

	$\hat{c}^A_{120}$		$\hat{p}^A_{120}$	
Prediction method	Mean	Std.dev.	Mean	Std.dev.
Exponential Brownian motion	68.01	85.31	23.63	43.85
Predicted Dirichlet process	60.39	72.81	26.01	47.65

Table 5.4: Mean prices and estimated standard deviations for 1,000 simulations of an Asian call $\hat{c}^A_{120}$ and an Asian put $\hat{p}^A_{120}$ on the S&P 500 index, both with expiration date $T = 132$ and exercise price based on an arithmetic average.

The results shown in Table 5.4 illustrate an important discrepancy between the call option prices. The greater price obtained for the exponential Brownian motion simulation is a result of the heavier tail displayed in Figure 5.17. This tail is also illustrated in Figure 5.19 where the plot of the quantiles is clearly concave down. The lower amount of extreme observations obtained in the predicted Dirichlet process simulation may be explained by the non-stationarity of the S&P 500 index over the time period considered. As mentioned in Section 5.2.2, the first 60 observations of the S&P 500 index exhibit a lower variability than the next 60 observations. As for the put option prices and standard deviations, their differences are not quite significant and can be imputed to the randomness of the simulations.

Chapter 6

Discussion and Future Directions

The objective of this thesis was to introduce an alternative methodology for the pricing of equity options, using a Monte Carlo simulation based on the Dirichlet process. If the option pricing results were not always conclusive, the predicted Dirichlet process method nevertheless presented some nice properties.

In fact, the behaviour of the predicted Dirichlet process method was, for practical purposes, comparable to that of the exponential Brownian motion model. Both methods produced above average results for the exponential random walk model with normal residuals, but failed in their attempt of producing accurate option prices for the models with stable or chi-square residuals. However, because the distribution of stock markets is not believed to be as extreme as these distributions, the results obtained for the pricing of options on the S&P 500 index were more than satisfying as to the validity of the predicted Dirichlet process method.

Moreover, the method performed very well in the estimation of the conditional distribution of future stock prices. The better results obtained for the chi-square model demonstrated the increased flexibility of the predicted Dirichlet process model compared to exponential Brownian motion.

This flexibility represents a considerable advantage for the Dirichlet approach as some experts question the validity of the normality assumption used in certain financial models. To many people, the rarity of drawing extreme observations in the tails of a normal distribution is difficult to reconcile with large and sharp movements

in stock markets. The stable distribution has also been criticized because of the high variability that it engenders.

As many believe the tails of the stock markets to be somewhere between those of normal and stable random variables, the predicted Dirichlet process presents a notable alternative to the existing models. The prior guess H in the Dirichlet process simulations is determined from the expert's opinion, but even a wrong choice is not alarming because the shape of the conditional distribution of the future stock prices is mostly explained by the distribution of the initial random sample. When performing this kind of analysis using real stock or index prices, the impact of the normality assumption is not as strong for the predicted Dirichlet process method as it is for other models.

Another advantage of this method is that it considers the entire distribution of the historical returns instead of only considering the sample mean and standard deviation. However, the method also presents some drawbacks, like the complexity of implementation and the lengthy time of computation compared to exponential Brownian motion. The implementation is a one-time problem, but the computation can be frustrating. For the large part, it is due to the important number of beta and normal draws performed in the simulation of the Dirichlet process. To complete $1,000$ simulations on options expiring in twelve periods, the predicted Dirichlet process approach will need to perform over 9 million random draws, while exponential Brownian motion only requires $12,000$ draws. An effective way to reduce the number of observations to be drawn is to increase the value of ϵ in (4.5), but other methods could certainly be explored to speed up the procedure.

As for future directions, the problem of replicating the estimated standard deviations for the stable model should be studied more closely. Also, an interesting route to explore could be to test the option pricing properties of the Pitman-Yor process, which is a generalization of the Dirichlet process.

Appendix A

Review of Some Financial Concepts

A.1 Glossary of Financial Terminology

This glossary is based on Hull [16], Kolb [22], and Reilly and Brown [31]:

American option: An option that can be exercised at any time before or at the expiration date.

Arbitrage: A trading strategy designed to take advantage of two or more securities being wrongly priced relative to each other.

Asian option: An option with an exercise price depending on the arithmetic or the geometric average of the underlying stock price over the life of the option.

Bond: A security issued by a government or a corporation to finance its debt. Bonds generally have a maturity between 1 and 30 years and pay interest periodically.

Call option: An option to buy an underlying asset at a predetermined price before a certain date.

Derivative security (or Derivative product): A financial instrument whose price depends, or is derived from, the price of another asset.

Dividend: A cash payment made to the company's stockholders.

European option: An option that can be exercised only at the expiration date.

Exercise price (or Strike price): The specified price in an option contract.

Exotic option: An option that differs from a European or an American option by the diversity of its payoff structure.

Expiration date (or Maturity): The date at which an option contract expires.

Forward contract: A contract that obligates the holder to buy or sell an underlying security for a predetermined price at a predetermined date. Unlike futures contracts, forward contracts are customized to the needs of the parties involved in the transaction.

Fundamental security: A financial instrument directly issued by a corporation or government in order to raise funds.

Futures contract: A contract that obligates the holder to buy or sell an underlying security for a predetermined price at a predetermined date. Unlike forward contracts, futures contracts are exchange-traded and thus standardized in terms of expiration date and amount of the underlying asset.

Option contract: A contract in which the holder is given the right, but not the obligation, to buy or sell an underlying security at a predetermined price before a certain date. An option to buy is a call; an option to sell is a put.

Option premium (or Option price): Amount paid by the buyer of an option for the right of buying or selling an underlying security at a predetermined price before a certain date. The option premium is paid by the buyer when the option is traded and is kept by the seller whether the option is exercised or not.

Put option: An option to sell an underlying security at a predetermined price before a certain date.

Rate of return (or Return): Percentage of change in the initial investment. In this thesis, returns are defined as $Y_t = \log S_t - \log S_{t-1}$, where S_t represents the price of an asset at time t.

Risk: The uncertainty of an investment.

Risk-free interest rate: The rate of return that can be earned without assuming any risks.

Stock (or Equity): The ownership of a firm.

Stock index: Weighted average of stocks used to compute total returns of an aggregate market or some of its components. Stock indices are often used as benchmarks to judge the performance of individual portfolios. Examples of stock indices include the DJIA 30, the S&P 500, the NASDAQ Composite, and the TSE 300.

Transaction cost: The cost of executing a trade.

Treasury bill: A short-term security issued by the government to finance its debt. Treasury bills pay no interest, but yield the difference between their face value and their discounted purchase price. Their maturity is less than one year.

Treasury bond: A long-term security issued by the government to finance its debt. Treasury bonds have a maturity greater than 10 years and pay interest periodically.

Treasury note: A mid-term security issued by the government to finance its debt. Treasury notes have a maturity between 1 and 10 years and pay interest periodically.

A.2 Time Value of Money

Suppose that a lottery winner has the choice between the following prizes:

$$\begin{aligned} \text{Prize } A &: \text{ Receive \$100 immediately,} \\ \text{Prize } B &: \text{ Receive \$100 in 1 year.} \end{aligned}$$

If the continuous expected interest rate is $i > 0$, then after one year

$$A = \$100e^{i} > \$100 = B,$$

and thus the value of Prize A is greater than that of Prize B.

Formally, the time value of money is defined as the interest rate established in capital markets by comparison of supply of excess income available and demand of excess consumption at a given time.

As a consequence of this concept, any payment made in the future must be discounted using the expected interest rate when calculating the actual price of a financial instrument. In this example, the actual price (or present value) of Prize A would be \$100, and that of Prize B would be $\$100e^{-i}$.

Appendix B

Review of Some Probability Concepts

B.1 Summary of Probability Distributions

This material is based on Casella and Berger [5], Samorodnitsky and Taqqu [34], and Wilks [38].

Beta Distribution $Be(\alpha_1, \alpha_2)$

If $\alpha_1, \alpha_2 > 0$, the beta density function is

$$f(x \mid \alpha_1, \alpha_2) = \frac{\Gamma(\alpha_1 + \alpha_2)}{\Gamma(\alpha_1)\Gamma(\alpha_2)} x^{\alpha_1 - 1}(1-x)^{\alpha_2 - 1}, \quad \text{for } 0 < x < 1.$$

Binomial Distribution $Bin(n, p)$

If $n > 0$ and $0 \leq p \leq 1$, the binomial probability mass function is

$$Pr[X = x \mid n, p] = \binom{n}{x} p^x (1-p)^{n-x} \quad \text{for } x = 0, 1, \ldots .$$

Dirichlet Distribution $Dir(\alpha_1, \ldots, \alpha_{k+1})$

If $\boldsymbol{\alpha} = (\alpha_1, \ldots, \alpha_{k+1}) > 0$, the Dirichlet density function is

$$f(y_1, \ldots, y_k \mid \boldsymbol{\alpha}) = \frac{\Gamma(\alpha_1 + \cdots + \alpha_{k+1})}{\Gamma(\alpha_1) \ldots \Gamma(\alpha_{k+1})} y_1^{\alpha_1 - 1} \ldots y_k^{\alpha_k - 1} (1 - y_1 - \cdots - y_k)^{\alpha_{k+1} - 1},$$

for

$$\mathbf{S} = \left\{ (y_1, \ldots, y_k) : y_j \geq 0, \quad \sum_{j=1}^{k} y_j \leq 1 \right\}.$$

Gamma Distribution $Ga(\alpha, \beta)$

If $\alpha, \beta > 0$, the gamma density function is

$$f(x \mid \alpha, \beta) = \frac{1}{\Gamma(\alpha) \beta^{\alpha}} x^{\alpha - 1} e^{-x/\beta}, \quad \text{for } x > 0.$$

The parameter α is known as the shape parameter, while the parameter β is called the scale parameter.

When $\alpha = 1$, the gamma distribution is called the exponential distribution with parameter β, denoted $Exp(\beta)$. If $\alpha = \beta = 1$, we speak of standard exponential.

When $\alpha = p/2$ and $\beta = 2$, the gamma distribution becomes the chi-square distribution with p degrees of freedom, denoted $\chi^2(p)$.

Normal Distribution $N(\mu, \sigma^2)$

If $-\infty < \mu < \infty$ and $\sigma > 0$, the normal density function is

$$f(x \mid \mu, \sigma^2) = \frac{1}{\sqrt{2\pi\sigma^2}} e^{-\frac{(x-\mu)^2}{2\sigma^2}}, \quad \text{for } -\infty < x < \infty,$$

where μ is the mean and σ is the standard deviation. A $N(0, 1)$ is referred to as a standard normal.

Poisson Distribution $Po(\lambda)$

If $\lambda \geq 0$, the Poisson probability mass function is

$$Pr[X = x \mid \lambda] = \frac{e^{-\lambda} \lambda^x}{x!}, \quad \text{for } x = 0, 1, \ldots,$$

where λ is the rate of the distribution.

Stable Distribution $S_\alpha(\sigma, \beta, \mu)$

Except for a few cases, the density functions of stable random variables are not known in closed form. The characteristic function is

$$\phi(\theta) = \begin{cases} \exp\left\{-\sigma^\alpha |\theta|^\alpha \left(1 - i\beta (\text{sign}\,\theta) \tan\left(\frac{\pi\alpha}{2}\right)\right) + i\mu\theta\right\} & \text{if } \alpha \neq 1, \\ \exp\left\{-\sigma |\theta| \left(1 + i\beta \frac{2}{\pi} (\text{sign}\,\theta) \log|\theta|\right) + i\mu\theta\right\} & \text{if } \alpha = 1, \end{cases}$$

where $0 < \alpha \leq 2$ is the index, $\sigma \geq 0$ is the scale parameter, $|\beta| \leq 1$ is the skewness parameter, and $\mu \in \Re$ is the shift parameter.

When $\alpha = 1$, this characteristic function is that of a Cauchy random variable. When $\alpha = 2$, the stable distribution is equivalent to the normal distribution.

Uniform Distribution $U(a, b)$

If $-\infty < a < b < \infty$, the uniform density function is

$$f(x \mid a, b) = \frac{1}{b-a}, \quad \text{for } a < x < b.$$

B.2 Kolmogorov's Existence Theorem

This section is based on Billingsley [2]. For each k-tuple $(t_1, \ldots, t_k)$ of distinct elements of T, suppose the random vector $(X_{t_1}, \ldots, X_{t_k})$ has over R^k some distribution

$$\mu_{t_1,\ldots,t_k}(H) = Pr\left[(X_{t_1}, \ldots, X_{t_k}) \in H\right],$$

where $H = H_1 \times \cdots \times H_k$ and $H_i \subset \Re^1$. Define the following consistency conditions:

1. $\mu_{t_1,\ldots,t_k}(H_1 \times \cdots \times H_k) = \mu_{t_{\pi 1},\ldots,t_{\pi k}}(H_{\pi 1} \times \cdots \times H_{\pi k})$,
2. $\mu_{t_1,\ldots,t_{k-1}}(H_1 \times \cdots \times H_{k-1}) = \mu_{t_1,\ldots,t_k}(H_1 \times \cdots \times H_{k-1} \times R^1)$.

The existence theorem can be stated in two ways:

Theorem B.1 (Kolmogorov's existence theorem 1) *If $\mu_{t_1,\ldots,t_k}$ are a system of distributions satisfying consistency conditions 1 and 2, then there exists a probability measure P on $\Re^T$ such that the coordinate-variable process $\{Z_t : t \in T\}$ on $(R^T, \Re^T, P)$ has the $\mu_{t_1,\ldots,t_k}$ as its finite-dimensional distributions.*

Theorem B.2 (Kolmogorov's existence theorem 2) *If $\mu_{t_1,\ldots,t_k}$ are a system of distributions satisfying consistency conditions 1 and 2, then there exists on some probability space (Ω, F, P) a stochastic process $\{X_t : t \in T\}$ having the $\mu_{t_1,\ldots,t_k}$ as its finite-dimensional distributions.*

B.3 Infinitely Divisible Characteristic Functions

This result was taken from Rao [30]:

Theorem B.3 (Lévy-Khintchine representation) *A mapping $\phi : \Re \to C$ is an infinitely divisible characteristic function if and only if it can be represented as*

$$\phi(\theta) = \exp\left[i\theta\gamma + \int_{-\infty}^{\infty}\left(e^{i\theta u} - 1 - \frac{i\theta u}{1+u^2}\right)\frac{1+u^2}{u^2}dN(u)\right],$$

where $\gamma \in \Re$ and the Lévy measure N is a bounded non-decreasing function such that $N(-\infty) = 0$.

The proof of this result is rather involved, so we refer the reader to Rao [30] for the complete details.

Appendix C

S-PLUS Programs

This appendix contains the S-PLUS programs used to implement the simulation algorithms described in Section 4.1.

Construction of an Exponential Random Walk Model

Model with Normal Residuals

```
function_func.exprwnorm(size,mu,sigma)
{
z_c(0,rnorm(size-1,0,sigma))
x_rep(0,length(z))
for(i in 2:length(x))
  {
  x[i]_x[i-1]+z[i]+mu
  }
300*exp(x)
}
```

Model with Stable Residuals

```
function_func.exprwstab(size,mu,index,sigma)
{
z_sigma*c(0,rstab(size-1,index,0))
x_rep(0,length(z))
for(i in 2:length(x))
  {
  x[i]_x[i-1]+z[i]+mu
  }
300*exp(x)
}
```

Model with Chi-Square Residuals

```
function_func.exprwchis(size,mu,df,shift,sigma)
{
z_sigma*c(0,rchisq(size-1,df)-shift)
x_rep(0,length(z))
for(i in 2:length(x))
  {
  x[i]_x[i-1]+z[i]+mu
  }
300*exp(x)
}
```

Exponential Random Walk Model Prediction

Model with Normal Residuals

```
function_proj.exprwnorm(randsamp,npast,npred,
         nsim,rate,sigma)
{
spred_matrix(0,nsim,npred)
spred[,1]_(rate-(sigma^2)/2)
          +rnorm(nsim,0,sigma)
if(npred>1){for(j in 2:npred)
  {
  spred[,j]_(rate-(sigma^2)/2)
            +rnorm(nsim,0,sigma)+spred[,j-1]
  }}
spred_randsamp[npast+1]*exp(spred)
spred
}
```

Model with Stable Residuals

```
function_proj.exprwstab(randsamp,npast,npred,
         nsim,rate,index,sigma)
{
spred_matrix(0,nsim,npred)
meansd_func.returnmsd(randsamp[1:(npast+1)])
spred[,1]_(rate-(meansd[2]^2)/2)
          +sigma*rstab(nsim,index,0)
if(npred>1){for(j in 2:npred)
  {
  spred[,j]_(rate-(meansd[2]^2)/2)
            +sigma*rstab(nsim,index,0)
            +spred,[j-1]
  }}
spred_randsamp[npast+1]*exp(spred)
spred
}
```

Model with Chi-Square Residuals

```
function_proj.exprwchis(randsamp,npast,npred,
         nsim,rate,df,shift,sigma)
{
spred_matrix(0,nsim,npred)
meansd_func.returnmsd(randsamp[1:(npast+1)])
spred[,1]_(rate-(meansd[2]^2)/2)
          +sigma*(rchisq(nsim,df)-shift)
if(npred>1){for(j in 2:npred)
  {
  spred[,j]_(rate-(meansd[2]^2)/2)
            +sigma*(rchisq(nsim,df)-shift)
            +spred[,j-1]
  }}
spred_randsamp[npast+1]*exp(spred)
spred
}
```

Exponential Brownian Motion Prediction

```
function_proj.expbm(randsamp,npast,npred,nsim,
          rate,crossval)
{
end_1+(floor(length(randsamp)/npred)
     -floor(npast/npred)-1)*(crossval==T)
spred_matrix(0,nsim*end,npred)
serror_rep(0,nsim*end)
for(i in 1:end)
  {
  rs_randsamp[(npred*(i-1)+1)
      :(npast+npred*(i-1)+1)]
  meansd_func.returnmsd(rs)
  spred[(nsim*(i-1)+1):(nsim*i),1]
   _(rate-(meansd[2]^2)/2)
     +rnorm(nsim,0,meansd[2])
  if(npred>1){for(j in 2:npred)
     {
     spred[(nsim*(i-1)+1):(nsim*i),j]
      _(rate-(meansd[2]^2)/2)
        +rnorm)nsim,0,meansd[2])
        +spred[(nsim*(i-1)+1):(nsim*i),j-1]
     }}
spred[(nsim*(i-1)+1):(nsim*i),]
 _randsamp[npast+npred*(i-1)+1]
   *exp(spred[(nsim*(i-1)+1):(nsim*i),])
serror[(nsim*(i-1)+1):(nsim*i)]
 _spred[(nsim*(i-1)+1):(nsim*i),npred]
   -randsamp[(npast+npred*i+1)]
  }
cbind(spred,serror)
}
```

Predicted Dirichlet Process Method

Predicted Dirichlet Process Method

```
function_proj.dpnorm(randsamp,npast,npred,nsim,
          rate,alpha,crossval)
{
randsamp_na.omit(randsamp)
end_1+(floor(length(randsamp)/npred)
     -floor(npast/npred)-1)*(crossval==T)
spred_matrix(0,nsim*end,npred)
serror_rep(0,nsim*end)
for(i in 1:end)
  {
  rs_randsamp[(npred*(i-1)+1)
      :(npast+npred*(i-1)+1)]
  meansd_func.returnmsd(rs)
  rs_func.dpformatrs(func.returnadj(rs),nsim)
  spred[(nsim*(i-1)+1):(nsim*i),1]
   _(rate-(meansd[2]^2)/2)
     +apply(rs,1,func.dpsim,npast,alpha)
  if(npred>1){for(j in 2:npred)
    {
    spred[(nsim*(i-1)+1):(nsim*i),j]
     _(rate-(meansd[2]^2)/2)
       +apply(rs,1,func.dpsim,npast,alpha)
       +spred[(nsim*(i-1)+1):(nsim*i),j-1]
    }}
spred[(nsim*(i-1)+1):(nsim*i),]
 _randsamp[npast+npred*(i-1)+1]
   *exp(spred[(nsim*(i-1)+1):(nsim*i),])
serror[(nsim*(i-1)+1):(nsim*i)]
 _spred[(nsim*(i-1)+1):(nsim*i),npred]
   -randsamp[(npast+npred*i+1)]
  }
cbind(spred,serror)
}
```

Simulation of $DP\left(\alpha H + \sum_1^t \delta_{Y_i}\right)$

```
function_func.dpsim(randsamp,npast,alpha)
{
product_1
product2_1
j_0
v_0
w_0
mixtw_alpha/(alpha+npast)
probw_c(mixtw,1-mixtw)
while(product2>1e-05)
  {
  j_j+1
  v[j]_rbeta(1,1,alpha+npast)
  w[j]_v[j]*product
  product2_w[j]
  product_product*(1-v[j])
```

```
  }
if(v[j]!=1) {w[j]_product/(1-v[j])}
if(j==1)
  {
  y_sample(c(rnorm(1,0,var(randsamp)^0.5)
     ,sample(randsamp,1,F)),1,F,probw)
  }
else
  {
  draw_sample(c(0,1),j,T,probw)
  draw2_runif(j,0,1)
  z_c(rnorm(j-sum(draw),0,var(randsamp)^0.5)
     ,sample(randsamp,sum(draw),T))
  z_cbind(draw2,z)
  z_z[order(z[,1],z[,2]),1:2]
  y_sample(z[,2],1,F,w)
  }
y
}
```

Other Functions

```
function_func.dpformatrs(randsamp,nsim)
{
rs_t(randsamp)
rs_matrix(rs,length(randsamp),nsim)
rs_t(rs)
rs
}

function_func.returnadj(randsamp)
{
y_rep(0,length(randsamp)-1)
for(i in 1:length(y))
  {
  y[i]_log(randsamp[i+1]/randsamp[i])
  }
y-mean(y)
}

function_func.returnmsd(randsamp)
{
y_rep(0,length(randsamp)-1)
for(i in 1:length(y))
  {
  y[i]_log(randsamp[i+1]/randsamp[i])
  }
c(mean(y),var(y)^0.5)
}
```

Appendix D

Data Sets

This appendix contains the original data sets used for the simulations described in Chapters 4 and 5.

Exponential Random Walk (Normal Residuals)

Time	Price	Time	Price	Time	Price	Time	Price	Time	Price
0	300.00	30	470.91	60	768.00	90	928.73	120	1117.17
1	309.02	31	437.27	61	792.31	91	927.29	121	1115.49
2	317.79	32	421.91	62	781.92	92	951.45	122	1080.60
3	321.09	33	459.97	63	767.59	93	896.92	123	995.47
4	323.70	34	469.39	64	780.75	94	931.71	124	1035.23
5	349.91	35	504.72	65	815.73	95	942.94	125	1019.20
6	364.21	36	516.70	66	829.78	96	937.88	126	992.44
7	370.62	37	550.53	67	839.41	97	888.26	127	1009.54
8	390.53	38	545.91	68	834.15	98	851.90	128	1041.83
9	391.60	39	547.35	69	814.53	99	880.91	129	1067.73
10	394.15	40	595.06	70	772.44	100	878.15	130	1101.00
11	391.95	41	616.56	71	806.06	101	891.82	131	1131.68
12	416.03	42	589.25	72	770.85	102	943.67	132	1085.33
13	417.11	43	589.33	73	807.48	103	1033.66		
14	416.88	44	603.84	74	850.38	104	1022.66		
15	422.51	45	605.22	75	835.60	105	1062.03		
16	403.38	46	585.01	76	825.44	106	1059.71		
17	406.20	47	598.56	77	816.18	107	1046.67		
18	422.35	48	632.68	78	848.09	108	1075.56		
19	452.57	49	654.79	79	906.01	109	1043.16		
20	485.17	50	647.81	80	925.29	110	1089.13		
21	487.88	51	574.58	81	910.63	111	1058.83		
22	497.54	52	621.09	82	958.18	112	979.43		
23	520.53	53	661.66	83	940.47	113	1033.29		
24	530.49	54	652.85	84	976.99	114	1045.12		
25	498.36	55	662.83	85	1049.91	115	1054.42		
26	453.26	56	696.32	86	1038.55	116	1035.69		
27	454.37	57	749.38	87	1018.53	117	1064.45		
28	456.38	58	780.81	88	986.55	118	1094.76		
29	459.84	59	785.45	89	905.41	119	1067.48		

Exponential Random Walk (Stable Residuals)

Time	Price	Time	Price	Time	Price	Time	Price	Time	Price
0	300.00	30	397.46	60	442.10	90	474.62	120	581.60
1	303.02	31	408.92	61	450.66	91	479.51	121	590.73
2	300.09	32	367.21	62	390.88	92	478.85	122	602.28
3	293.37	33	371.19	63	394.15	93	481.53	123	621.21
4	294.80	34	373.64	64	406.29	94	461.78	124	633.41
5	293.59	35	383.63	65	420.65	95	457.27	125	642.47
6	297.70	36	385.18	66	425.84	96	463.19	126	641.47
7	299.12	37	386.11	67	413.23	97	470.83	127	653.87
8	308.09	38	387.70	68	418.00	98	452.65	128	644.86
9	307.48	39	401.89	69	418.66	99	456.39	129	645.68
10	309.41	40	403.41	70	429.17	100	463.54	130	628.40
11	318.43	41	407.74	71	433.35	101	462.08	131	634.75
12	327.31	42	415.07	72	439.02	102	474.96	132	642.09
13	326.62	43	409.89	73	442.35	103	475.76		
14	334.13	44	405.93	74	444.12	104	472.23		
15	337.59	45	409.43	75	445.51	105	468.61		
16	342.76	46	411.00	76	443.42	106	475.86		
17	344.78	47	407.28	77	457.01	107	482.11		
18	351.65	48	412.95	78	467.43	108	480.62		
19	350.04	49	414.79	79	462.77	109	477.56		
20	356.91	50	417.91	80	467.88	110	507.28		
21	350.39	51	430.69	81	485.07	111	497.04		
22	356.09	52	429.57	82	476.63	112	508.48		
23	353.93	53	440.17	83	473.27	113	504.10		
24	356.59	54	442.83	84	476.18	114	497.55		
25	358.61	55	447.05	85	482.79	115	514.41		
26	365.81	56	440.47	86	475.77	116	525.33		
27	379.29	57	425.26	87	475.22	117	564.67		
28	392.43	58	423.48	88	476.44	118	569.65		
29	394.62	59	435.54	89	470.52	119	578.95		

Exponential Random Walk (Chi-Square Residuals)

Time	Price	Time	Price	Time	Price	Time	Price	Time	Price
0	300.00	30	363.69	60	507.69	90	1061.11	120	1251.77
1	300.00	31	350.72	61	499.27	91	1105.89	121	1278.67
2	317.74	32	341.63	62	492.03	92	1134.27	122	1270.30
3	313.90	33	332.01	63	479.43	93	1165.37	123	1234.96
4	324.20	34	325.93	64	472.87	94	1137.06	124	1190.36
5	337.73	35	325.47	65	497.41	95	1142.91	125	1231.42
6	332.42	36	367.19	66	527.61	96	1175.46	126	1236.62
7	346.17	37	368.37	67	526.02	97	1148.24	127	1280.78
8	362.04	38	385.99	68	514.13	98	1168.53	128	1242.57
9	355.72	39	372.11	69	538.03	99	1225.49	129	1235.93
10	376.43	40	389.25	70	590.33	100	1188.41	130	1207.89
11	372.97	41	372.89	71	608.22	101	1154.07	131	1216.07
12	379.12	42	369.19	72	646.13	102	1252.45	132	1198.74
13	376.06	43	371.09	73	657.17	103	1305.98		
14	369.10	44	380.94	74	711.46	104	1342.93		
15	375.70	45	381.43	75	713.36	105	1307.05		
16	394.59	46	368.15	76	691.12	106	1263.02		
17	378.54	47	392.25	77	678.48	107	1345.77		
18	378.69	48	392.40	78	678.27	108	1330.15		
19	370.67	49	393.05	79	657.12	109	1323.08		
20	364.45	50	383.03	80	691.95	110	1267.34		
21	374.61	51	374.68	81	768.30	111	1299.35		
22	376.06	52	400.55	82	792.77	112	1332.10		
23	366.09	53	409.51	83	908.80	113	1301.80		
24	391.96	54	396.70	84	1003.05	114	1301.46		
25	384.53	55	425.34	85	994.34	115	1275.25		
26	379.11	56	503.23	86	949.73	116	1266.11		
27	380.69	57	500.36	87	948.49	117	1270.04		
28	383.65	58	497.69	88	991.33	118	1277.25		
29	370.99	59	522.90	89	1086.55	119	1267.91		

S&P 500 Index

This series represent monthly closing prices of the Standard & Poor's 500 Total Return Index ($US), for the period extending from December 31st, 1989 to December 31st, 2000.[1]

Date	Price	Date	Price	Date	Price	Date	Price
Dec 89	353.40						
Jan 90	329.08	Jan 92	408.78	Jan 94	481.61	Jan 96	636.02
Feb 90	331.89	Feb 92	412.70	Feb 94	467.14	Feb 96	640.43
Mar 90	339.94	Mar 92	403.69	Mar 94	445.77	Mar 96	645.50
Apr 90	330.80	Apr 92	414.95	Apr 94	450.91	Apr 96	654.17
May 90	361.23	May 92	415.35	May 94	456.50	May 96	669.12
Jun 90	358.02	Jun 92	408.14	Jun 94	444.27	Jun 96	670.63
Jul 90	356.15	Jul 92	424.21	Jul 94	458.26	Jul 96	639.95
Aug 90	322.56	Aug 92	414.03	Aug 94	475.49	Aug 96	651.99
Sep 90	306.05	Sep 92	417.80	Sep 94	462.71	Sep 96	687.33
Oct 90	304.00	Oct 92	418.68	Oct 94	472.35	Oct 96	705.27
Nov 90	322.22	Nov 92	431.35	Nov 94	453.69	Nov 96	757.02
Dec 90	330.22	Dec 92	435.71	Dec 94	459.27	Dec 96	740.74
Jan 91	343.93	Jan 93	438.78	Jan 95	470.42	Jan 97	786.16
Feb 91	367.07	Feb 93	443.38	Feb 95	487.39	Feb 97	790.82
Mar 91	375.22	Mar 93	451.67	Mar 95	500.71	Mar 97	757.12
Apr 91	375.34	Apr 93	440.19	Apr 95	514.71	Apr 97	801.34
May 91	389.83	May 93	450.19	May 95	533.40	May 97	848.28
Jun 91	371.16	Jun 93	450.53	Jun 95	544.75	Jun 97	885.14
Jul 91	387.81	Jul 93	448.13	Jul 95	562.06	Jul 97	954.31
Aug 91	395.43	Aug 93	463.56	Aug 95	561.88	Aug 97	899.47
Sep 91	387.86	Sep 93	458.93	Sep 95	584.41	Sep 97	947.28
Oct 91	392.45	Oct 93	467.83	Oct 95	581.50	Oct 97	914.62
Nov 91	375.22	Nov 93	461.79	Nov 95	605.37	Nov 97	955.40
Dec 91	417.09	Dec 93	466.45	Dec 95	615.93	Dec 97	970.43

[1]Data source: Yahoo! Finance, `http://finance.yahoo.com`.

S&P 500 Index (Continued)

Date	Price	Date	Price
Jan 98	980.28	Jan 00	1394.46
Feb 98	1049.34	Feb 00	1366.42
Mar 98	1101.75	Mar 00	1498.58
Apr 98	1111.75	Apr 00	1452.43
May 98	1090.82	May 00	1420.60
Jun 98	1133.84	Jun 00	1454.60
Jul 98	1120.67	Jul 00	1430.83
Aug 98	957.28	Aug 00	1517.68
Sep 98	1017.01	Sep 00	1436.51
Oct 98	1098.67	Oct 00	1429.40
Nov 98	1163.63	Nov 00	1314.95
Dec 98	1229.23	Dec 00	1320.28
Jan 99	1279.64		
Feb 99	1238.33		
Mar 99	1286.37		
Apr 99	1335.18		
May 99	1301.84		
Jun 99	1372.71		
Jul 99	1328.72		
Aug 99	1320.41		
Sep 99	1282.71		
Oct 99	1362.93		
Nov 99	1389.07		
Dec 99	1469.25		

Bibliography

[1] Barone-Adesi, G. and Whaley R.E., (1986). The Valuation of American Call Options and the Expected Ex-Dividend Stock Price Declines. *Journal of Financial Economics*, **17**, 91–112.

[2] Billingsley, P., (1995). *Probability and Measure*, 3rd edition. New York: John Wiley & Sons.

[3] Black, F. and Scholes M., (1973). The Pricing of Options and Corporate Liabilities. *Journal of Political Economy*, **81**, 637–659.

[4] Blackwell, D. and MacQueen, J.B., (1973). Ferguson Distributions Via Pólya Urn Schemes. *Annals of Statistics*, **1**, 353–355.

[5] Casella, G. and Berger, R.L., (1990). *Statistical Inference*. Belmont, CA: Duxbury Press.

[6] Cox, J.C., Ross, S.A., and Rubinstein, M., (1979). Option Pricing: A Simplified Approach. *Journal of Financial Economics*, **7**, 229–264.

[7] Cox, J.C. and Rubinstein, M., (1985). *Options Markets*. Englewood Cliffs, NJ: Prentice Hall.

[8] Fabius, J., (1964). Asymptotic Behavior of Bayes Estimates. *Annals of Mathematical Statistics*, **35**, 846–856.

[9] Fama, E., (1965). The Behavior of Stock Market Prices. *Journal of Business*, **38**, 34–105.

[10] Ferguson, T.S., (1973). A Bayesian Analysis of Some Nonparametric Problems. *Annals of Statistics,* **1**, 209–230.

[11] Ferguson, T.S., (1974). Prior Distributions on Spaces of Probability Measures. *Annals of Statistics,* **2**, 615–629.

[12] Ferguson, T.S. and Klass, M.J., (1972). A Representation of Independent Increment Processes Without Gaussian Components. *Annals of Mathematical Statistics,* **43**, 1634–1643.

[13] Freedman, D.A., (1963). On the Asymptotic Behavior of Bayes' Estimates in the Discrete Case. *Annals of Mathematical Statistics,* **34**, 1386–1403.

[14] Fuller, W.A., (1996). *Introduction to Statistical Time Series,* 2nd edition. New York: John Wiley & Sons.

[15] Geske, R., (1979). A Note on an Analytical Valuation Formula for Unprotected American Call Options on Stocks with Known Dividends. *Journal of Financial Economics,* **7**, 375–380.

[16] Hull, J.C., (2000). *Options, Futures, and Other Derivatives,* 4th edition. Upper Saddle River, NJ: Prentice Hall.

[17] Ishwaran, H. and Zarepour, M., (2000). Exact and Approximate Sum-Representations for the Dirichlet Process. Unpublished note, University of Ottawa.

[18] Ishwaran, H. and Zarepour, M., (2000). Markov Chain Monte Carlo Approximate Dirichlet and Beta Two-Parameter Process Hierarchical Models. *Biometrika,* **87**, 371–390.

[19] Itô, K., (1951). On Stochastic Differential Equations. *Memoirs, American Mathematical Society,* **4**, 1–51.

[20] Johnson, H.E., (1983). An Analytic Approximation for the American Put Price. *Journal of Financial and Quantitative Analysis,* **18**, 143–151.

[21] Karlin, S. and Taylor, H.M., (1975). *A First Course in Stochastic Processes.* New York: Academic Press.

[22] Kolb, R.W., (1997). *Futures, Options, and Swaps,* 2nd edition. Malden, MA: Blackwell Publishers.

[23] Mandelbrot, B.B., (1962). Sur certains prix spéculatifs: Faits empiriques et modèle basé sur les processus stables de Paul Lévy. *Comptes rendus,* **254**, 3968–3970.

[24] Mandelbrot, B.B., (1963). New Methods in Statistical Economics. *Journal of Political Economy,* **71**, 421–440.

[25] Mandelbrot, B.B., (1963). The Variation of Certain Speculative Prices. *Journal of Business,* **36**, 394–419.

[26] Mandelbrot, B.B., (1967). The Variation of Some Other Speculative Prices. *Journal of Business,* **40**, 393–413.

[27] Merton, R.C., (1973). Theory of Rational Option Pricing. *Bell Journal of Economics and Management Science,* **4**, 141–183.

[28] Mittnik, S. and Rachev, S.T., (1993). Modeling Asset Returns with Alternative Stable Distributions. *Econometric Reviews,* **12**, 261–330.

[29] Muliere, P. and Tardella, L., (1998). Approximating Distributions of Random Functionals of Ferguson-Dirichlet Priors. *Canadian Journal of Statistics,* **26**, 283–297.

[30] Rao, M.M., (1984). *Probability Theory with Applications.* Orlando: Academic Press.

[31] Reilly, F.K. and Brown, K.C., (1997). *Investment Analysis and Portfolio Management,* 5th edition. Fort Worth, TX: Dryden Press.

[32] Rendleman, R.J. and Bartter, B.J., (1979). Two-State Option Pricing. *Journal of Finance,* **34**, 1093–1110.

[33] Roll, R., (1977). An Analytic Valuation Formula for Unprotected American Call Options on Stocks with Known Dividends. *Journal of Financial Economics*, **5**, 251–258.

[34] Samorodnitsky, G. and Taqqu, M.S., (1994). *Stable Non-Gaussian Random Processes*. New York: Chapman & Hall.

[35] Sethuraman, J., (1994). A Constructive Definition of Dirichlet Priors. *Statistica Sinica*, **4**, 639–650.

[36] Stoll, H.R., (1969). The Relationship Between Put and Call Option Prices. *Journal of Finance*, **24**, 801–824.

[37] Whaley, R.E., (1981). On the Valuation of American Call Options on Stocks with Known Dividends. *Journal of Financial Economics*, **9**, 207–212.

[38] Wilks, S.S., (1962). *Mathematical Statistics*. New York: John Wiley & Sons.